PB-219 394

ION-SELECTIVE ELECTROCHEMICAL SENSORS

Isaac Trachtenberg

Texas Instruments, Incorporated

Prepared for:
Office of Saline Water

March 1973

SELECTED WATER RESOURCES ABSTRACTS INPUT TRANSACTION FORM	844	W

ION-SELECTIVE ELECTROCHEMICAL SENSORS

March 1973

Trachtenberg, Isaac

Texas Instruments Incorporated
Dallas, Texas 75222

OSW R & D Progress Report No. 844

14-01-0001-1737

Office of Saline Water

104 Pages, 26 Figures, 18 Tables, 24 References

Ion-selective electrochemical sensors can provide a means for rapidly determining and continuously monitoring the concentration of a variety of ionic species in aqueous solutions, particularly saline and brackish waters. The development of novel ion-selective sensors was the goal of this research program. Specifically, the program goal was to develop inexpensive, chemically durable, and highly selective electrochemical sensors which would provide rapid and specific response to Fe^{+3}, Cu^{+2}, Ca^{+2}, Mg^{+2}, Na^{+}, K^{+}, and $SO_4^{=}$ in saline and brackish water. The primary approach taken in this program was to investigate the use of nonoxide materials, both crystalline and amorphous, which, when fabricated into sensors, gave selective response to the specific ions of interest. The research program had four major parts: sensor material preparation; material characterization, including resistivity; sensor preparation and evaluation for ion selectivity; and sensor mechanism studies.

17a. Descriptors

*Desalination, *Electrodes, *Water Purification
*Calcium, *Magnesium, *Sulfate, *Iron, *Copper

17b. Identifiers

*Ion Selective Electrodes, *Nonoxide Glasses

17c. COWRR Field & Group 03A

18. Availability NTIS

19. Security Class. (Report)

20. Security Class.

21. No. of Pages 104

22. Price

Send To:

WATER RESOURCES SCIENTIFIC INFORMATION CENTER
U.S. DEPARTMENT OF THE INTERIOR
WASHINGTON, D. C. 20240

Dr. Raymond J. Horowitz | Office of Saline Water

PB 219 394

ION-SELECTIVE ELECTROCHEMICAL SENSORS

United States Department of the Interior

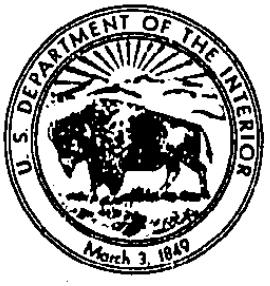

Office of Saline Water . Research and Development Progress Report No. 844
Int-OSW-RDPR-73-844

113

RESEARCH AND DEVELOPMENT PROGRESS REPORT NO. 844 March 1973
Int-OSW-RDPR-73-844

ION-SELECTIVE ELECTROCHEMICAL SENSORS

By Isaac Trachtenberg, Texas Instruments, Inc., Dallas, Texas, for Office of Saline Water, J. W. O'Meara, Director; W. Sherman Gillam, Assistant Director, Research; Sidney Johnson, Chief, Applied Science Division

Contract No. 14-01-00001-1737

UNITED STATES DEPARTMENT OF THE INTERIOR . Rogers C. B. Morton, Secretary
James R. Smith, Assistant Secretary for Water and Power Resources

As the Nation's principal conservation agency, the Department of the Interior has basic responsibilities for water, fish, wildlife, mineral, land, park, and recreational resources. Indian Territorial affairs are other major concerns of America's "Department of Natural Resources".

The Department works to assure the wisest choice in managing all our resources so each will make its full contribution to a better United States—now and in the future.

FOREWORD

This is one of a continuing series of reports designed to present accounts of progress in saline water conversion and the economics of its application. Such data are expected to contribute to the long-range development of economical processes applicable to low-cost demineralization of sea and other saline water.

Except for minor editing, the data herein are as contained in a report submitted by the contractor. The data and conclusions given in the report are essentially those of the contractor and are not necessarily endorsed by the Department of the Interior.

TABLE OF CONTENTS

TABLE OF CONTENTS
(continued)

LIST OF ILLUSTRATIONS

LIST OF ILLUSTRATIONS
(continued)

LIST OF ILLUSTRATIONS
(continued)

LIST OF TABLES

LIST OF TABLES
(continued)

FINAL REPORT

FOR

ION-SELECTIVE ELECTROCHEMICAL SENSORS

I. INTRODUCTION

Ion-selective electrochemical sensors can provide a means for rapidly determining and continuously monitoring the concentration of a variety of ionic species in aqueous solutions, particularly saline and brackish waters. This is the broad goal of the research program sponsored by the Office of Saline Water under Contract No. 14-01-0001-1737 with Texas Instruments Incorporated. Specifically, the program goal is to develop inexpensive, chemically durable, and highly selective electrochemical sensors which will give rapid and specific response to Fe^{+3}, Cu^{+2}, Ca^{+2}, Mg^{+2}, Na^{+}, K^{+}, and $SO_4^{=}$ in saline and brackish water. The primary approach taken in this program was to investigate the use of nonoxide materials, both crystalline and amorphous, which, when fabricated into sensors, give selective response to the specific ions of interest. The research program had four major parts: sensor material preparation; material characterization, including resistivity; sensor preparation and evaluation for ion selectivity; and sensor mechanism studies. Each of these topics will be discussed in terms of individual sensors.

Ion-selective electrochemical sensors can be combined with other sensors to build up process control systems. These systems will permit better control and automation of such processes as reverse osmosis demineralization of brackish waters, acid mine drainage water demineralization, and monitoring of total copper concentration in the final brine discharge from a distillation desalination process.

Ion-selective electrochemical sensors will provide accurate monitoring of the concentration of individual ionic species in solution on a continuous and real-time basis. The efficiency of the various subsystem elements (pretreatment section, chemical addition, membranes, etc.) can be easily determined and optimized for the current operating conditions. Thus, the quality of incoming and product water could be easily established. In addition, such process control systems can signal changes in raw materials and in environmental and operating conditions. These signals will allow corrective actions to be initiated before the operation has

degraded to the point at which it must be shut down. However, if the changes have been too drastic and cannot be corrected within a reasonable period of time so that continued operation at these levels would result in permanent damage to the systems, the process control system would actually shut the process down to prevent serious damage to expensive components such as the membranes. Inclusion of ion-selective electrochemical sensors in process control systems will provide critical information needed to improve operations at a lower total operating cost.

Much of the work performed on this contract has been published.[1-5] The three previous Intermediate Reports for this contract, U. S. Department of the Interior, Office of Saline Water Research and Developments Progress Reports #496, 619, and 761, contain detailed accounts of all of the work performed prior to the last year of the contract. A paper entitled "Ion-Selective Electrochemical Sensors- Fe^{+3}, Cu^{+2}" was published in The Journal of Electrochemical Society.[4] It summarizes the early work on the Fe^{+3} sensor. A second manuscript[5] entitled "Potentiometric Titration of Sulfate Using an Ion-Selective Iron Electrode" was published in Analytical Chemistry. Currently, at least two more manuscripts[6] are planned for publication in the open literature. Portions of the work reported in the five publications mentioned above are used in this report for purposes of completeness and understanding. All other work and results not previously reported are included here.

In this report each sensor is identified and discussed in terms of the ion to which it responds most selectively. Included in the discussion of each ion are sensor material preparation, resistivity of sensor material, evaluation of materials in ion-selective sensors, and mechanistic studies to provide a better understanding of the way the sensor functions and some of the precautions necessary to ensure its reliable performance. Hence, the sections that follow are devoted to discussions of sensors of each of the following ions: Fe^{+3}, Cu^{+2}, $SO_4^{=}$, and Ca^{+2} plus Mg^{+2}. One section describes preliminary work on other sensors that were not pursued to any great extent in this program. A section is also devoted to describing laboratory work closely related to applications in various demineralization processes. The final section summarizes the results and provides recommendations for future work in this area.

II. Fe^{+3} SENSORS

One of the first groups of materials investigated during this program was the nonoxide containing chalcogenide glasses. Although a number of different materials were investigated and reported,[1-4] the chalcogenide glass that showed the most promise for Fe^{+3} had the composition $Se_{60}Ge_{28}Sb_{12}$ and had been previously designated as TI #1173. If glass 1173 is properly doped with Fe (Fe-1173), the resulting material, when fabricated into sensors,[1] will develop potentials that can be related to the free uncomplexed ferric iron concentrations of aqueous solutions. The electrode exhibits a Nernstian response with a slope of approximately 59 mV/decade change in Fe^{+3} concentration at ambient laboratory temperatures. This effect is of practical interest in monitoring various demineralization processes and has particular application to acid mine drainage water, waste water treatment, and several other process effluents. The response of the sensors is of considerable scientific interest because (a) the electrode potential is independent of the concentration of almost all the common univalent and divalent cations and particularly ferrous iron content of the solution; while (b) the potential response to ferric iron is a nominal 59 mV/decade concentration change, indicative of a one-electron process rather than the expected three-electron process (20 mV/decade).

Repetition of previously reported results[1-4] concerning the Fe^{+3} sensor will be kept to a minimum here, and emphasis will be placed on results not previously reported. The additional information presented here concerns the Fe-1173 sensors only: the preparation, composition, and activation of the Fe-1173 material; the electrochemical performance of this unique material; and the ion-sensing mechanism of the electrode.

A. Experimental

The iron glasses were prepared by fusing the appropriate amount of iron wire at 900 to 1000°C with the glass, $Se_{60}Ge_{28}Sb_{12}$, previously synthesized directly from the pure elements. To form electrodes, discs 1.1 to 1.2 cm diameter and 0.1 to 0.2 cm thick were cut from the melt; gold was then evaporated onto one side of the glass disc; a platinum wire lead made contact to the gold via Silver Micropaint; and the lead side of the glass was isolated from the test solutions by sealing the glass disc into a Plexiglas tube.

Resistivity and potential measurements were made as described previously.[4] Potentiostatic measurements were made with a Wenking Model 6343R potentiostat. All potentials are reported with respect to the commercial Ag/AgCl electrode used as reference. In experiments concerned with the possible influence of chloride ion on the measured potentials, this electrode was replaced with an Orion double-junction Ag/AgCl reference electrode containing a potassium nitrate solution in the outer junction. All measurements were made at ambient room temperature.

Usually, four Fe-1173 electrodes were immersed in the specific solutions under test, to separate out spurious electrode effects from the particular parameter being studied. For simplicity of presentation, only the data from one set will be discussed.

To obtain a reproducible surface, independent of the previous history of the electrode, the sensors were etched periodically in 10% KOH for 30 seconds, rinsed with supporting electrolyte, re-etched, and re-rinsed. The electrodes were then stored in 10^{-3} M Fe^{+3} overnight before use. The significance of these etching and equilibration steps will be discussed.

The supporting electrolytes used in this study were 1 M KCl and 0.1 N $NaClO_4$. Chloride forms weak complexes with ferric iron; perchlorate shows little tendency to complex.[7] The responses in nitrate were discussed previously.[4]

A motor-driven paddle stirrer was used in the experiments concerned with the effect of stirring on response time. Magnetic stirrers were avoided to obviate any possible complications from the heat so produced.

The analytical method for determining the total iron content of the various slices of Fe-1173 glasses was based on dissolution of the sample in aqua regia, followed by measurement with an atomic absorption spectrometer.

B. Results and Discussion

The surface of an electrode prepared as described in Section II.A is visibly heterogeneous, containing islands of one phase embedded in a matrix phase. Portions of this electrode material were ground to a powder, and an x-ray (Fe radiation)

pattern was taken under prolonged exposure. In no case could a detectable pattern be found. It must therefore be concluded that neither phase of the electrode material is crystalline.

The Fe-1173 electrodes are opaque to infrared radiation; the parent 1173 glass is transparent. It must therefore be concluded that neither phase is the original 1173 glass. It was not possible to withdraw separately portions of either phase for chemical analysis.

The homogeneity of the melts prepared as previously described[4] is indicated by the data shown in Table I for the iron contents of slices taken along the length of two melts (slice 1 is the top of the melt). There are significant variations in composition from slice to slice, and it is not possible to infer the composition of slice x from that of slice x ± 1. No trend in iron content could be established from the position of the slice within the melt; crushing and remelting the slices did not improve the homogeneity of melt composition.

It had been shown previously[4] that there was a dependence of resistivity on the iron concentration of the melt. The existence of a critical iron concentration, above which the resistivity decreased from the order of 10^3 ohm cm down to the order of 50 ohm cm, was confirmed with chemical analysis of the individual slices on which the resistivity measurements had been made. This was necessary in view of the compositional variations shown in Table I. As a result of improved analyses, the critical concentration found was 1.3 atom % iron rather than the approximately 2.3% value previously reported.

Table II summarizes the electrochemical performance of four high-resistance electrodes; performance is discussed in terms of the potential-log concentration slopes between the specified concentration limits. All the high-resistance glasses showed less than the expected Nernstian slope to changes in iron concentration at low net ferric iron contents. Table III shows the steady-state Nernstian slopes for 16 low-resistivity (≤ 50 ohm cm) electrodes over the concentration range of 10^{-5} to 10^{-2} M ferric chloride in 1 M KCl, pH 2. All electrodes had iron concentrations of approximately 1.3 atom % Fe. Included in Table III are the standard deviations of slope as calculated from a least-squares fit of the data for each

TABLE I

Iron Content Along the Melts

Weight % Total Iron

Slice No.	Melt 39 (1.0 wt % Fe added)	Melt 23 (1.4 wt % Fe added)
1	0.97	1.27
2	0.91	1.29
3	-	1.27
4	1.02	1.18
5	0.95	1.29
6	0.76	-
7	0.94	1.39
8	0.84	1.30
9	0.82	1.22
10	0.80	-
11	0.76	-
12	0.78	-
13	0.84	-
14	0.84	-

TABLE II

Potential Change vs Fe^{+3} Concentration Change

	Δ Potential (mV)			
Concentration Range:	10^{-5} to 10^{-4}	10^{-4} to 10^{-3}	10^{-3} to 10^{-2}	10^{-2} to 10^{-1}
Electrode Resistivity (ohm-cm)				
540	20.0	26.5	33.5	35.4
10^7	16.7	28.2	45.8	59.0
2×10^3	37.8	57.4	61.0	60.0
4×10^3	28.4	41.2	56.5	60.0

TABLE III

Nernstian Slopes for Low-Resistance
Electrode Response to Fe^{+3}

Electrode	Slope (mV/decade)	Standard Deviation (mV)
30-1	62.1	1.9
30-2	61.3	1.8
30-4	59.3	1.4
30-7	59.9	2.2
30-8	60.3	2.9
30-11	58.3	2.3
32-4	52.5	1.4
32-7	56.2	2.9
32-8	55.2	1.4
32-9	59.5	1.3
32-11	54.9	1.3
32-15	55.5	0.6
46-2	52.1	0.8
46-11	58.2	2.5
49-2	58.6	2.2
49-12	57.3	1.7

electrode. (In this numbering system the first number refers to a particular melt, while the second number refers to a particular slice within the melt.) The average slope is computed as 57.6 mV/decade with a net standard deviation of ± 2.9 mV/decade. This, then, is a measure of the reproducibility with which electrodes can be prepared. No correlation could be found with iron content and performance, except as determined by the resistivity of the glass. Unless otherwise specified, all data discussed below were taken with low-resistance electrodes.

Figure 1 shows the response times of one such electrode to small changes in iron concentration. Steady state was achieved within two to four minutes; response time to increasing iron concentration appeared to be somewhat faster than responses to decreasing concentrations.

Response time increased significantly, however, (a) when the concentration changes were increased to order-of-magnitude increments, and (b) when the ambient ferric iron concentration was decreased below 10^{-4} M ferric iron. With stirring, steady state at 10^{-5} M was achieved within 20 to 30 minutes; without stirring, steady-state responses at 10^{-5} M were always quite long, taking up to 60 minutes to reach steady state (here, steady state is defined as an electrode potential stable to within 0.1 mV/min.). At steady state, the electrode potentials were independent of stirring rate over the range from 0 to 275 rpm. At 10^{-4} M ferric iron, steady state was achieved within 10 to 20 minutes with stirring.

This trend of decreasing response time with increasing iron concentration did not persist above 10^{-3} M; generally, 20 minutes were required to reach steady state, as defined, and stirring had little effect. Response times were the same in perchlorate and in chloride solutions.

During the preliminary studies of electrode behavior, it was often observed that the potential changes measured at and below 10^{-3} M Fe^{+3} were smaller than expected (from a Nernstian slope of about 59 mV per decade) if the electrodes had been first exposed to 10^{-1} or 10^{-2} M ferric iron for prolonged periods of time. Furthermore, the equilibrium potentials themselves were higher than had been observed after the electrodes had first been exposed to 10^{-4} M ferric iron. This effect was found in both chloride and perchlorate solutions. The phenomenon can be illustrated and explained by the following experiment. A thoroughly washed elec-

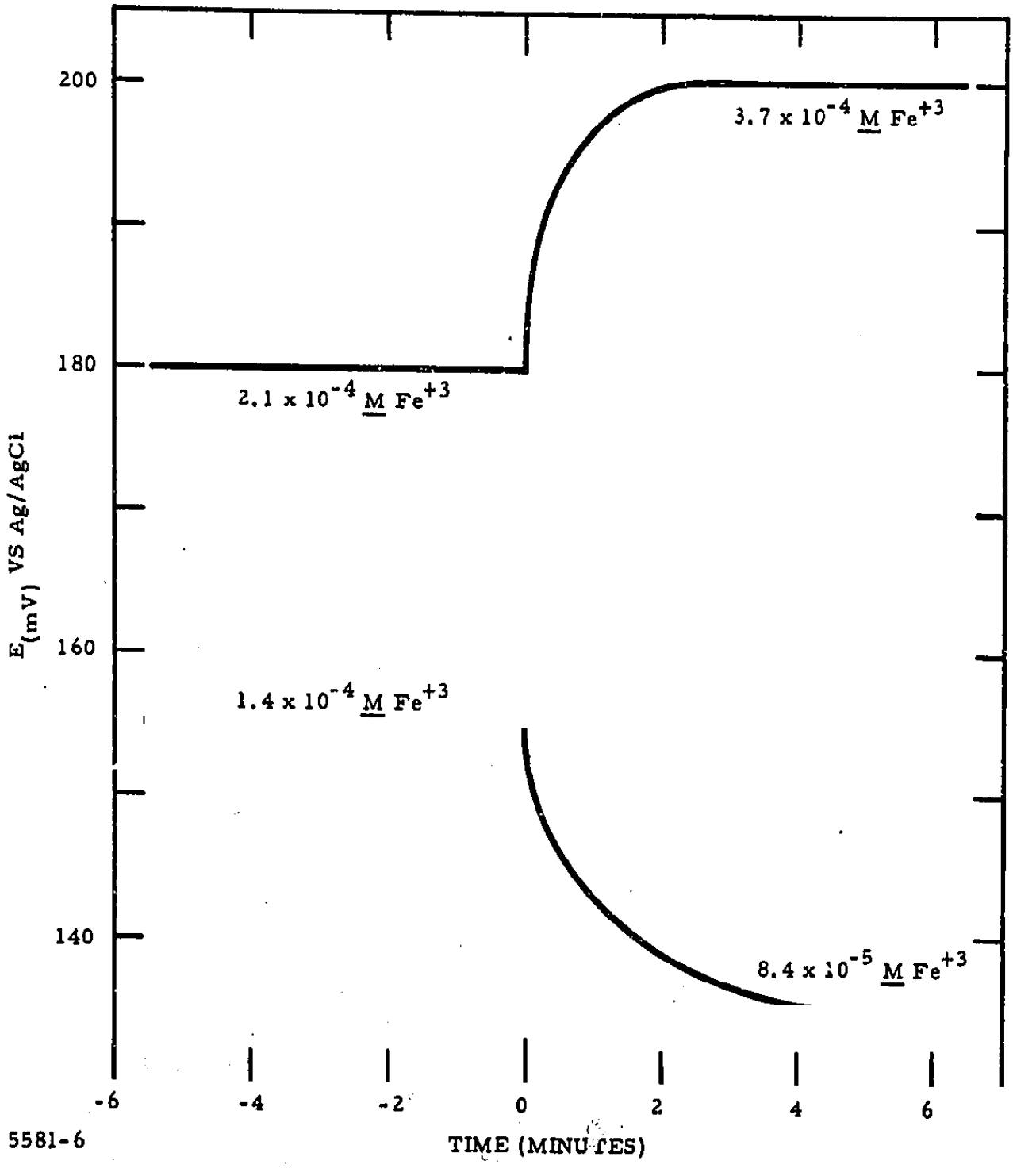

Figure 1 2.39 Mole % Fe^{0}-1173 Glass Electrode Response Times for Changing $[Fe^{+3}]$

trode was equilibrated in 10^{-3} M ferric chloride after exposure for ten minutes to 10^{-1} M Fe^{+3}; a steady potential of +355.7 mV was observed. The electrode was then thoroughly rinsed with supporting electrolyte, and the test solution was replaced with a second sample of the same 10^{-3} M concentration that had not been exposed previously to an Fe-1173 electrode; a steady-state potential of +341.7 mV was recorded. Not only is this potential lower, but it is also what was anticipated from Nernstian behavior and the potential observed at 10^{-2} M ferric iron. Placing the electrode back into the original 10^{-3} M solution restored the potential reading to its original value. This indicates that the potential difference between the two millimolar iron solutions was not an artifact or electrode drift, but was indeed representative of the ferric iron content of the solutions. It would appear, then, that ferric iron was transferred from the surface of the electrode, previously exposed to high iron content solutions, into the first millimolar iron solution.

Thus, when measurements were made to determine the potential of a solution more than an order-of-magnitude different in ferric iron content from the solution previously monitored, the electrodes had to be equilibrated for at least 30 minutes in the test solution and then placed in a fresh portion of the test solution. This provided the most accurate representation of potentials characteristic of the ferric iron content of the particular solution under study.

A more classical source of contamination was also found with a number of the supporting electrolytes used in the study, specifically the presence of a small amount of residual iron impurity in the salt itself. The KCl and $NaClO_4$ electrolytes were analyzed for total soluble iron via an atomic absorption spectrometric method.[5] The 0.1 N $NaClO_4$ solution used contained 1.7×10^{-5} M Fe; the 1 M KCl solution contained 2×10^{-7} M Fe. It was found that the KCl solutions did vary in soluble iron content according to the particular batch of KCl used; most samples contained residual iron in the 10^{-7} M range.

The lower limits-of-detection of the Fe-1173 electrodes were therefore estimated as follows. Equilibrium potentials were first measured for a KCl solution with a known, large concentration of added iron. Sufficient EDTA (at the same pH) was added to complex all iron present; potentials were recorded after

15 minutes. The results of one such experiment in 1 M KCl are shown in Table IV. From a comparison of the potentials at 10^{-5} M Fe^{+3} and those of the KCl + EDTA solution (i.e., no iron), it would appear that the electrodes are sensitive down to approximately 10^{-6} M ferric iron in 1 M KCl.

TABLE IV

Determination of Limit-of-Detection

Solution	Electrode		
	32-5	32-6	32-8
10^{-5} M Fe + KCl	216 mV	235 mV	232 mV
10^{-6} M Fe + KCl	165	203	198
KCl	147	188	184
KCl + EDTA	145	182	180

The same experiment was carried out in perchlorate solution with substantially the same result, i.e., the electrode is capable of measuring soluble ferric iron above a concentration of 10^{-6} M (0.06 ppm).

It was also of interest to note that exposure of the electrode to EDTA did not adversely affect activity; in fact, exposure may well have improved electrode performance. An example of this effect is shown in Table V, which lists the steady state potentials of 10^{-4} Fe, (a) initially, (b) after exposure to 10^{-1} Fe, and (c) after exposure to EDTA. (The significance of the 10^{-1} exposure is discussed below in more detail; suffice it to say that such an exposure has a deactivating effect for subsequent exposure of the electrode to 10^{-4} solutions.) Obviously, there is good agreement between the "initial" and "after EDTA" potentials.

TABLE V

Effect of EDTA on Equilibrium Potentials

Electrode	Potentials (for 10^{-4} M Fe)		
	Initial	After 10^{-1} Fe	After EDTA
5	231.7 mV	223 mV	230 mV
6	210.8	204	211
7	232.6	208.9	230
8	226.6	209.9	227

To generate electrodes which showed these Nernstian responses to varying ferric iron concentrations, it was necessary to activate the sensor surface by exposing a freshly etched electrode to a solution high in ferric iron concentration ($\geq 10^{-3}$ M). This phenomenon is illustrated by the data in Figure 2, which shows the responses of a freshly etched electrode after equilibration overnight in three different iron solutions. In each case, measurements were first made at the 10^{-5} M concentration level, then at successively increasing iron concentrations. Chloride was the supporting electrolyte, but similar results were obtained with perchlorate ion.

Consider first the response of the electrode equilibrated in the 10^{-5} M iron solution: (a) little potential change was observed for solutions of iron concentrations at and below 10^{-4} M; (b) potential readings were abnormally low below 10^{-3} M; (c) the response above 10^{-4} M was super-Nernstian, i.e., greater than $\sim$ 59 mV/decade change in iron concentration. After exposure to 10^{-1} M ferric iron, this electrode showed the normal Nernstian responses as obtained with properly activated electrodes (data not shown in the figure).

Consider next the electrode equilibrated overnight in 10^{-3} M ferric ion. Response was Nernstian, and little hysteresis was observed in potential on increasing and decreasing the iron concentration (data not shown in the figure). Similar behavior was observed after a freshly etched electrode was equilibrated for one hour in 10^{-1} M ferric iron solution.

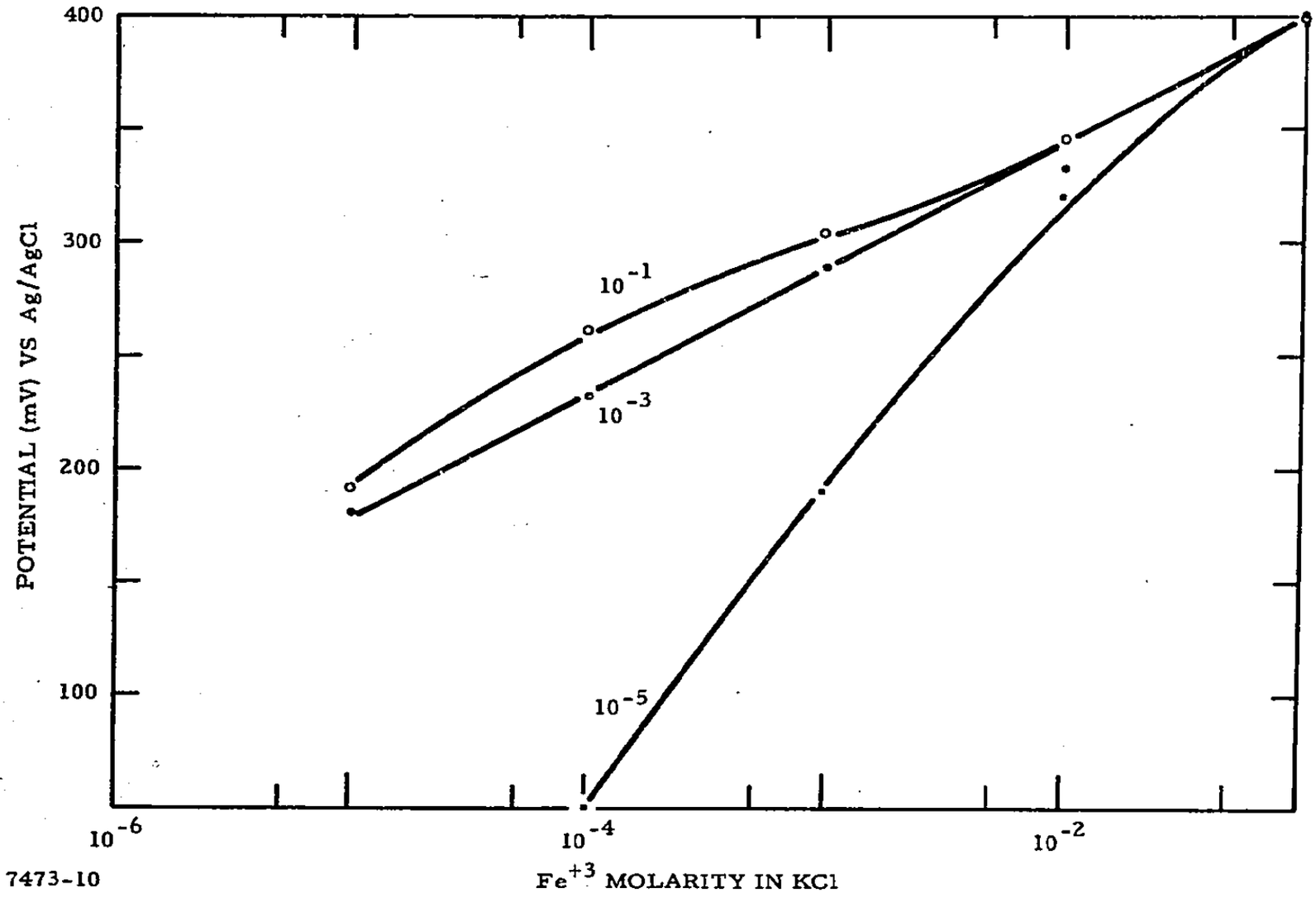

Figure 2 Response After Equilibration Overnight in Three Different Iron Solutions

Finally, consider the plot for the electrode equilibrated overnight in 10^{-1} M ferric iron. The subsequent performance at and above 10^{-3} M is normal; response below 10^{-3} M was less than would be expected from Nernstian behavior. Furthermore, the potentials showed considerable long-term drift. In many cases such treatment with 10^{-1} M ferric iron resulted in electrodes that were completely nonresponsive to changing ferric iron concentration below 10^{-4} M ferric iron.

To confirm that this deactivation involved exposure time as well as ferric iron concentration, an active electrode was exposed to 10^{-3} M ferric iron for 87 hours, rather than overnight as described above. Subsequent measurements of the concentration-potential responses indicated a decrease in sensitivity of the electrode to low concentrations of ferric iron, e.g., a potential change of only 35 mV was observed from 10^{-5} to 10^{-4} M iron and 53 mV from 10^{-4} to 10^{-3}, rather than the previously observed 58 mV/decade. Above 10^{-3} M ferric iron, the response was still Nernstian. This result has obvious implications relative to the use of this sensor for the continuous monitoring of process streams. As with other ion-selective electrodes, best performance is obtained when the electrode is used to measure less than order-of-magnitude changes in concentration around a constant ambient concentration.

To avoid, or at least minimize, such deactivation of the electrode when the sensor is not in use, consideration was given to storing the electrodes in the dry state, without etching and chemical reactivation between applications. Accordingly, a series of four electrodes was activated overnight in 10^{-3} M ferric iron and then operated. After demonstration of the expected sensitivity to ferric iron, the electrodes were washed with supporting electrolyte, washed with distilled water, dried, and left overnight in air. The electrodes were then exposed to solutions of varying iron content, and the steady-state potentials were recorded. The greatest divergence between the two sets of potentials was 20 mV; the average divergence was 10 mV. Two conclusions can be made. First, dry storage does not deactivate the electrode; second, recalibration is a desirable precaution, as with all ion-selective electrodes.

The operational effects discussed above raise significant questions regarding the electrode mechanism for sensing ferric iron concentration. In particular, it

is necessary to rationalize the 58 mV/decade Nernstian slope, i.e., a one-electron process, with the following: (a) the electrode activation phenomenon, (b) the electrode deactivation process, (c) the auto-contamination of the test solutions, and (d) the variation in response times with the magnitude of concentration change and concentration level.

One possible explanation, consistent with previously discussed redox behavior, is that the electrode sees only the oxidation potential of the ferric iron (the reduced half of the equilibrium couple is in the electrode); but to function properly, the electrode surface must first be oxidized, e.g., to a potential approximating that of 10^{-1} M ferric chloride. The auto-contamination effect could indicate that the solubility of the electrode material is potential-dependent. Similarly, the deactivation process could be explained by a competing slow and irreversible oxidation of the surface by ferric iron at potentials equal to or greater than +400 mV vs Ag/AgCl.

The following experiment was carried out in an attempt to evaluate the effect of oxidation potential. (This study was done in replicate, but for simplicity of presentation the data for only one run are discussed.) An electrode was etched, washed with supporting electrolyte, and placed in 1 M KCl, pH 1.7, but with no added iron. The potential of the electrode was set to +400 mV with the potentiostat and held for three hours. This is approximately the potential the electrode would have reached if exposed to 10^{-1} M ferric chloride in 1 M KCl, pH 1.7. A current flow of 2 mA anodic was observed initially, decreasing within 15 minutes to 0.003 mA anodic. This indicates that a chemical oxidation of the electrode surface does take place during the electrode activation step.

After the anodic current had definitely fallen to zero (three hours), the applied potential was removed, and the electrode was exposed to varying concentrations of ferric ion in the same supporting electrolyte, starting with 10^{-5} M and proceeding to higher concentrations in order-of-magnitude increments. The potential-log concentration response obtained in this way was substantially identical to that shown in Figure 2 for the freshly etched electrode exposed to 10^{-5} M ferric chloride. At 10^{-5} M Fe^{+3} the electrode potential was of the order of 150 mV below its equilibrium Nernstian value and only slowly increased toward this poten-

tial (at ~ 5 mV/hour). This rate of approach to equilibrium was much slower than that observed during operation of the chemically activated electrode at this concentration level. Varying the solution Fe^{+3} concentration generated a super-Nernstian response. As concentration increased, the potentials more closely approximated their "true" equilibrium values, and the rate-of-approach to equilibrium increased.

It can thus be concluded that oxidation of the electrode surface occurs during the activation step, but, in itself, is not sufficient to provide an electrode responsive to changing iron concentrations in the supporting electrolyte solution. Exposure to high concentrations of ferric iron is indeed required. Since the phenomenon is observed in perchlorate solution, the important species involved in this process is ferric ion, not a chloride complex.

It had been determined previously that exposure of the electrode to 10^{-1} M ferric iron for three hours, i.e., the time period used in the potentiostatic treatment discussed above, was sufficient to deactivate the electrode response to low concentrations of ferric iron in the solution. However, the potentiostatic treatment did not adversely affect the electrode performance. To further confirm this, a freshly etched and chemically activated electrode was put on the potentiostat at +400 mV for three hours. Subsequent potentiometric response to varying iron content in solution was unchanged, i.e., the electrode was not detectably deactivated. Thus, it can be concluded that electrode deactivation also does not solely involve surface oxidation, i.e., high potential, but that high concentrations of ferric iron are required.

The next point to establish is the nature of the chemical interaction between the ferric iron in solution and the surface of a chemically, or electrochemically, oxidized Fe-1173 electrode. The most likely reaction is that of equilibrium (rather than irreversible) chemisorption of Fe^{+3}. The specificity of such a process would account for the selectivity of the electrode material. The equilibrium exchange of the adsorbed iron with ferric ion in solution would account for the auto-contamination effect, since the electrode is severely shifted from equilibrium by, for example, reducing the solution iron content more than an order of magnitude. Of course, the initial adsorption of ferric iron would be expected to produce a potential change; indeed, after potentiostatic oxidation the addition of ferric

ions subsequently leads to an increase in potential which, as described, is super-Nernstian, i.e., is greater than expected from the effect of concentration change alone.

A series of experiments was carried out in an attempt to elucidate the chemistry involved in this electrode-ferric ion interaction. The specific measurement techniques used were (1) free ferric iron analysis of the equilibration solutions with an activated Fe-1173 electrode, (2) total iron analysis of the equilibration solution via atomic absorption (AA) spectrometric analysis, and (3) Fe^{+3}/Fe^{+2} ratio monitoring via a platinum screen electrode.

Accordingly, an electrode was freshly etched and placed in a 10^{-5} M $FeCl_3$ solution (pH 1.7, 1 M KCl), which was equilibrated with the active Fe-1173 electrode. The potential of the active electrode decreased by 7.8 mV in 60 minutes. AA analysis indicated no change in total iron content. These results are rationalized by noting that a freshly etched electrode is in a reduced state (at approximately -400 mV) and is thus capable of reducing ferric ion to ferrous ion. Potentiostating such an electrode at +400 mV resulted in an anodic current flow, as described previously.

The test electrode was therefore re-etched, potentiostated at +400 mV for 2.5 hours, and then exposed to 10^{-5} M ferric chloride solution. The active Fe-1173 electrode again indicated a decrease in ferric iron content; but the potential change was much smaller, i.e., of the order of a millivolt. The platinum screen electrode indicated a decrease in potential of 4.6 mV. Thus, there is a change in the composition of the equilibrating electrolyte, but it is small. AA analysis of the solution showed no change in the total iron content. However, the changes indicated by the electrodes are at the limit of reproducibility of the AA analytical method. Complicating matters, however, was the observation that in no case during the replicate AA analysis of replicate solutions was there a lower concentration of total iron in the equilibration solution than in the original electrolyte. In fact, in most cases there was a small increase.

Nevertheless, it is possible to conclude that very little, if any, reduced species come off the electrode during the activation step. The potential change

noted for the platinum electrode, if due solely to ferrous iron or a similar reduced species, would be of the order of 10^{-7} M (0.006 ppm Fe). The same conclusion applies to a chemically activated electrode during ferric iron sensing. The platinum electrode was placed in a 10^{-5} M ferric chloride solution until steady state was achieved. An active Fe-1173 electrode was placed in this solution, and no change in potential of the platinum electrode was observed.

These observations are consistent, primarily with the adsorption of ferric iron onto the electrode surface during the activation step. The quantities involved are proportional to solution ferric iron concentration and hence are small at low ambient concentrations of ferric iron. (At higher concentrations there would be the problem of detecting small differences between large numbers.)

The available data make it impossible to exclude completely the desorption or dissolution of material from the electrode surface which would form a stable complex ion with Fe^{+3} and thereby reduce the electrode potentials of the monitoring electrodes as described. Such a mechanism would be consistent with the AA results on total iron content of the solutions. However, (a) such dissolution would have to take place only in the presence of ferric iron (or the process would have been completed during the potentiostating step), (b) such dissolution could not expose a fresh Fe-1173 surface (or steady state would not have resulted), and (c) the Fe^{+3} complex would have to have a low equilibrium constant (log K of the order of 2 or 3) or the changes in ferric iron concentration would be greater than those observed. This, in turn, would imply a solubility product not strongly influenced by the Fe^{+3} concentration and condition (a) would not apply.

Thus, the most likely interaction is adsorption of ferric iron on the fresh electrode surface.

If the deactivation process proceeds via an irreversible, slow adsorption of ferric iron species, which may or may not be potential-dependent, then it would be expected that if the potential of the electrode were reduced, it would be possible to displace ferric iron from the electrode surface, or it would be possible to reduce this adsorbed ferric iron to ferrous iron. Since ferrous iron does not evoke an electrode response, it can be assumed that it is not adsorbed onto the

electrode. In both cases, soluble iron should appear in the supporting electrolyte. Accordingly, a deactivated electrode was potentiostated at +120 mV for ten minutes in 1 M KCl, pH 1.7, containing no added iron. Current flow was cathodic, but less than 0.001 mA. The solution was then analyzed for soluble iron via a more sensitive atomic absorption spectrometric method[8]; 0.34 mg/lit (6×10^{-6} M) iron was found. Although small, the value is nevertheless real, i.e., in excess of the residual iron content found in the particular KCl solution used in this experiment. This is evidence in support of deactivation via irreversible, but slow, adsorption of ferric iron onto the electrode surface. It is consistent with such a mechanism that inactive electrodes always read high, i.e., give potentials in excess of those expected from equilibrium with the solution being measured. Such would be the case for an electrode with an excess of iron on the surface.

We are therefore left with the following conclusions regarding the activation and sensing mechanism of Fe-1173 electrodes. A properly activated electrode will show Nernstian responses to solutions varying in ferric iron content with a slope of approximately 58 mV per decade concentration change, i.e., a one-electron change process. However, for the electrode to function properly, a freshly etched surface must first be exposed to ferric iron solution of moderately high concentration, of the order of 10^{-3} M or higher. During this step, the electrode surface is oxidized, and then a chemical interaction takes place between the electrode and ferric iron in the solution. It is this modified surface that is involved in the sensing of ferric iron content of solutions. The sensing mechanism does not involve the injection of reduced species into the electrolyte. This interaction of the electrode with ferric iron in solution is most likely one of specific adsorption, although the quantity of ferric iron so involved is low, at least at low ambient iron concentrations. The operational effects discussed imply that the subsequent ferric ion sensing mechanism involves the exchange of ferric ions in solution with the electrode surface.

Electrode deactivation is rationalized in terms of a slow, irreversible adsorption of ferric iron taking place simultaneously with the faster adsorption process that forms the basis of the sensing mechanism. In any event, the involvement of ferric iron in the deactivation process is strongly indicated. The rate of deactivation is proportional to the average Fe^{+3} concentration seen by the electrode, thus further supporting the idea of dry storage to prevent deactivation.

The remaining problem is to account, at least qualitatively, for the one-electron Nernstian slope with such a mechanism. Obviously, the electrode mechanism is more complex than that originally proposed, i.e., a redox couple, Fe^{+3}/M^{+2}, where M^{+2} is contained in the electrode surface. There is little doubt that the electrode responds to oxidizing agents such as Ce^{+4} and peroxides.[4] However, there may well be more than one mechanism, depending on the species involved; work in progress is consistent with such a conclusion. To be consistent with the information discussed above relative to Fe^{+3} sensing, it is necessary to postulate a surface adsorption or chelation which involves a potential-determining ion exchange with Fe^{+3} in solution. The overall process of generating an active surface and sensing ferric iron may be represented as follows:

$$\text{Fe-1173} + Fe^{+3}\ (sol) \rightarrow \text{oxidized Fe-1173} + Fe^{+2}\ (sol)$$

$$\text{Fe-1173}\ (ox) + Fe^{+3} \rightarrow M^{*}$$

$$M^{*} + Fe^{+3}\ (sol) \rightleftharpoons M^{*}\ Fe.$$

The freshly etched Fe-1173, on exposure to ferric iron in solution, is first oxidized. This surface then interacts chemically with further ferric iron to form the active centers (M^{*}) involved with the subsequent ferric iron sensing. (This process is inferred from the extremely slow approach of the oxidized electrode to true equilibrium when it is exposed to low concentrations of ferric ion in solution.) The active site (M^{*}) now establishes its potential via fast, reversible adsorption-desorption equilibrium with Fe^{+3} in solution and that adsorbed on the surface. Since this is a one-for-one process, a Nernstian slope of 58 mV/decade results. At the same time, a much slower irreversible adsorption deactivation process takes place which is dependent on the concentration of ferric ion in solution.

C. Summary

Properly prepared, activated, and operated Fe-1173 electrodes show Nernstian responses to changing ferric ion concentration between 10^{-5} and approximately 10^{-1} M Fe^{+3}, with a nominal slope of 58 mV/decade ferric iron concentration. This slope is reproducible from electrode to electrode within ± 3 mV(1 σ level). The same slopes were found in chloride and perchlorate media. Ferrous ion is not seen by the electrode.

As presently prepared, slices of sensor material taken from a given melt can vary ± 10% in total iron content. Fe-1173 glasses containing less than 0.9% (at.) are higher in resistivity ($\geq 10^{+3}$ ohm cm). Electrodes of this material, while they respond to changes in ferric iron content in solution, are less sensitive to low ($\leq 10^{-4}$ M) concentrations of Fe^{+3}. Low resistivity ($< 10^{3}$ ohm cm and preferably $< 10^{2}$ ohm cm) material results in electrodes that are sensitive to concentrations as low as 10^{-6} M Fe^{+3} (0.06 ppm) in chloride and perchlorate solutions.

Electrode response time decreases with decreasing increment of concentration change, with increasing ambient concentration of ferric iron, and with stirring. Exposure of the electrodes to strong chelating agents such as EDTA does not adversely affect subsequent electrode response.

To develop an active sensor for monitoring ferric ion concentration, the electrode surface must be etched in a caustic and exposed to high ($\geq 10^{-3}$ M) concentration of ferric iron. This activation process involves the oxidation of the surface as well as further chemical reaction with ferric iron. The activation process is different from the sensing process in that the latter involves a fast, reversible exchange between solution ferric ions and adsorbed ferric ions. A slow chemical deactivation of the surface takes place which involves, at least in part, the irreversible adsorption of ferric ion. Electrode life can be prolonged by dry storage, and deactivated electrodes are readily reactivated by etching and exposure to ferric ion.

III. Cu^{+2}

Earlier investigations[1,4] demonstrated that the Fe-1173 would indeed respond to Cu^{+2} in the absence of Fe^{+3}. However, the selectivity of this sensor was poor for Cu^{+2} over Fe^{+3}. The mechanistic studies of the Fe^{+3} sensor suggested that the use of oxy-chalcogenide glass could result in a family of sensors for different ions. This first attempt was directed to a specific Cu^{+2} sensor and involved the formation of a $CuO\text{-}As_2S_3$ glass. The material exhibited low resistivity and was sensitive to Cu^{+2} in a variety of electrolytes. Work continued using not only CuO, but also Cu, Cu_2S, and CuS as additives to the As_2S_3. All materials systems responded. Attempts to make sensors for ions other than Cu^{+2} with this chalcogenide system were discussed in O.S.W. progress report # 761.[3]

As in previous sections of this report, earlier work previously reported[1-3] will not be repeated unless it is necessary for clarity. Emphasis will be placed on results obtained since the last report.

This section discusses the preparation, performance, properties and sensing mechanism of a Cu^{+2}-sensitive chalcogenide glass electrode prepared from copper metal and preformed arsenic trisulfide (As_2S_3). Applications of these electrodes will be discussed in Section VII of this report.

A. Experimental

Pure arsenic trisulfide was prepared by heating the elements (6-9's pure) in a sealed quartz ampoule at 525°C for about 90 hours. The resulting glass was deep red and, in 50-mil slices, was transparent. The infrared spectrum of arsenic trisulfide is well known and agrees with that for the material prepared as described. Glasses prepared from commercial arsenic trisulfide were often opaque to the infrared and led to erratic copper sensors. Both effects were ascribed to residual metal impurities in the starting materials.

To prepare the sensor, the crushed glass was mixed with the appropriate amount of copper metal, cupric oxide, or cupric sulfide; then the material was

placed in a quartz ampoule which was evacuated, sealed, and placed in a furnace for 70 hours at 700°C. The temperature was then reduced to 400°C for one hour, and the ampoule was air-quenched to room temperature.

Electrodes were formed in the manner described previously.[4] Most of the measurements were taken with ohmic contact made directly to the sensor glass slice. Entirely equivalent data were obtained when the membrane configuration was used, i.e., when the glass slice was used to separate the solution being studied from an internal solution of constant composition; electrical contact was made via a commercial reference electrode placed in the internal solution.

Potentials were also measured as described.[4] An Orion Ag/AgCl reference electrode was used in the double-junction mode to minimize contamination of some test solutions with halide ion. Standard copper solutions were prepared by dissolving the appropriate copper salt in the following supporting electrolytes: (1) 1 M KCl, pH 2; (2) 3 M KCl, pH 2; (3) 1 M KCl + 1 M HCl; (4) 1 M NaBr, pH 2; (5) 0.1 M KNO_3, pH 2; (6) 1 M sodium acetate, pH 4; (7) 0.1 M sodium acetate + 0.9 M $NaNO_3$, pH 4; (8) 1 M KSCN, pH 2. No attempt was made to remove residual copper contamination from the supporting electrolytes; it was not necessary to deaerate the solutions.

The test solutions were not thermostated; the temperature coefficient remains to be determined. In general, three test electrodes were monitored simultaneously to sort out spurious electrode effects and spurious solution effects. For simplicity of presentation, the data from only one electrode in each set are presented here.

Unless otherwise specified, all measurements were taken in solutions stirred with a paddle stirrer (275 rpm). The consequences of stirring will be discussed.

To obtain a reproducible surface before each series of measurements, the electrodes were etched with 10% KOH, rinsed with the appropriate electrolyte, re-etched and re-rinsed. The electrode was then equilibrated in 10^{-1} M cupric ion solution for one hour before use. The chemistry involved in this important activation step will be discussed.

Comparison measurements were also taken with commercially available copper-sensitive electrodes, i.e., the Coleman Copper Ion-Sensitive Electrode No. 3-804, and the Orion model 94-29A. The purpose here was not to criticize or evaluate commercial electrodes per se, but to determine if significant differences in performance existed relative to the copper - arsenic trisulfide electrodes.

B. Results and Discussion

Visual observation of the glasses indicated a heterogeneous multiphase system with crystalline material distributed randomly throughout an amorphous matrix. The crystalline phases formed from glasses spiked with copper metal, cupric oxide, and cupric sulfide were studied by metallographic and x-ray diffraction techniques.

Semi-quantitative microprobe analysis of these phases indicated they were copper-rich. Distance-concentration profiles taken across a precipitate indicated that its arsenic content was below that of the adjacent matrix phase, but that its sulfur content was about equivalent to that of the matrix phase. The strongest lines in all x-ray diffraction patterns were those ascribable to "sinnerite," a recently reported mineral.[9,10] In no case was it possible to confirm the presence of copper metal, cupric sulfide, cuprous sulfide, or the oxides, even when the initial source of copper was cupric sulfide or cupric oxide.

Sinnerite is reported to exist in two crystalline modifications, cubic $Cu_6As_4S_9$ ($3\ Cu_2S \cdot 2\ As_2S_3$) and triclinic $Cu_{6.3}As_4S_9$. Both modifications were found in the melt containing 0.25 mole fraction added copper. At lower concentrations of copper, one or more of the other phase was found, rather than both. To some extent this could be correlated with the preparative conditions, according to the following argument. The initial precipitate which forms on quenching the melt is the cubic phase and is metastable at room temperature. On standing, copper slowly diffuses through the glass, forming the more stable triclinic distorted material near the $Cu_{6.3}As_4S_9$ composition. Indeed, the triclinic lines were visible primarily in the diffraction patterns of the oldest samples and in the slow-cooled samples. The optical micrographs were consistent with such a crystal growth mechanism, in that a long (> 18 hour) reaction time at 550°C gave needle-like dendritic growth, while the slow-cooled sample gave large crystals.

Resistivity measurements (dc) were taken as described previously,[4] i.e., with 0.1 to 0.2 cm thick slices onto which gold had been evaporated. As shown in Table VI, resistivity decreased with increasing additions of copper. The same effect was obtained regardless of the form of the initially added copper. This is consistent with the x-ray data that the crystalline and conductive material formed in the melt is independent of the starting copper compound.

TABLE VI

Resistivities of Copper - Arsenic Trisulfide Glasses

Mole Fraction Copper	Resistivity (Ω cm)	
	CuO Added	Cu Added
0.05	3×10^{8} to 6×10^{10}	---
0.10	3×10^{6} to 3×10^{8}	2×10^{7} to 4.3×10^{7}
0.15	4×10^{3} to 1×10^{6}	4.1×10 to 4×10^{4}
0.20	1×10^{2} to 8×10^{3}	4×10^{2} to 3×10^{3}
0.25	46 to 50	64 to 69
0.30	--	36 to 37

The primary conclusion to be drawn from the data of Table VI is that the conductivity of the high copper-content glasses is sufficient in itself for stable electrochemical operation and that the addition of conductive binders is not necessary.

The spread in the data represents the spread in resistivities for different slices taken from the same melt. Obviously, the slices are also heterogeneous along the length of the melt as well as along the surface of a slice. Note, however, that this variation in resistivity decreases as the copper content of the melt is increased above mole fraction 0.2, as would be expected if the conductivity were due primarily to the crystalline phase.

A rigorous correlation of electrode performance with electrode composition or physical properties was not attempted. It was generally observed, however, that electrodes containing a mole fraction of copper at or less than 0.2 were less sensitive and shorter-lived than electrodes containing larger amounts of copper. Unless otherwise noted, all data presented in this discussion were taken with electrodes containing 0.25 mole percent copper.

The first series of electrochemical measurements described are those taken with 0.1 M KNO_3 as the supporting electrolyte. Complex ion formation is minimal,[7] and soluble cuprous species are unstable.

Figure 3 shows the potential-concentration relationships for an electrode operated in the following manner. The electrode was first etched and then placed directly into 10^{-6} M cupric nitrate, followed by solutions of increasing copper ion concentration. Exposure times were ten minutes each; potentials were steady to within 2 mV/min. After exposure to 10^{-2} M Cu^{+2}, the electrode was exposed to decreasing concentrations of copper (in order-of-magnitude changes) to 10^{-6} M, and then to increasing concentrations to 10^{-1} M. After thirty minutes at this concentration, the copper content was decreased incrementally to 10^{-6} M and increased incrementally to 10^{-1} M.

The slope of the first of these potential-concentration curves is super-Nernstian, i.e., with a slope greater than 30 mV/decade; the return to lower concentrations gave a slope of less than 30 mV/decade. On subsequently increasing concentration, Nernstian behavior was observed from 10^{-4} to 10^{-2} M; the potential at 10^{-2} M showed a slow but real drift to more positive values; the potential change between 10^{-2} and 10^{-1} was 60 mV. The next cycle between 10^{-1} and 10^{-6} M Cu^{+2} showed no hysteresis of the type described and showed Nernstian behavior from 10^{-2} and 10^{-5} M copper. Such measurements form the basis for the activation procedure described, i.e., to obtain a stable, reproducible, and reversible sensor, the freshly etched electrode must first be exposed to high concentrations of cupric ion.

The time for activation in 10^{-1} M cupric nitrate was evaluated by measuring the potential-concentration dependencies after the electrodes were etched and

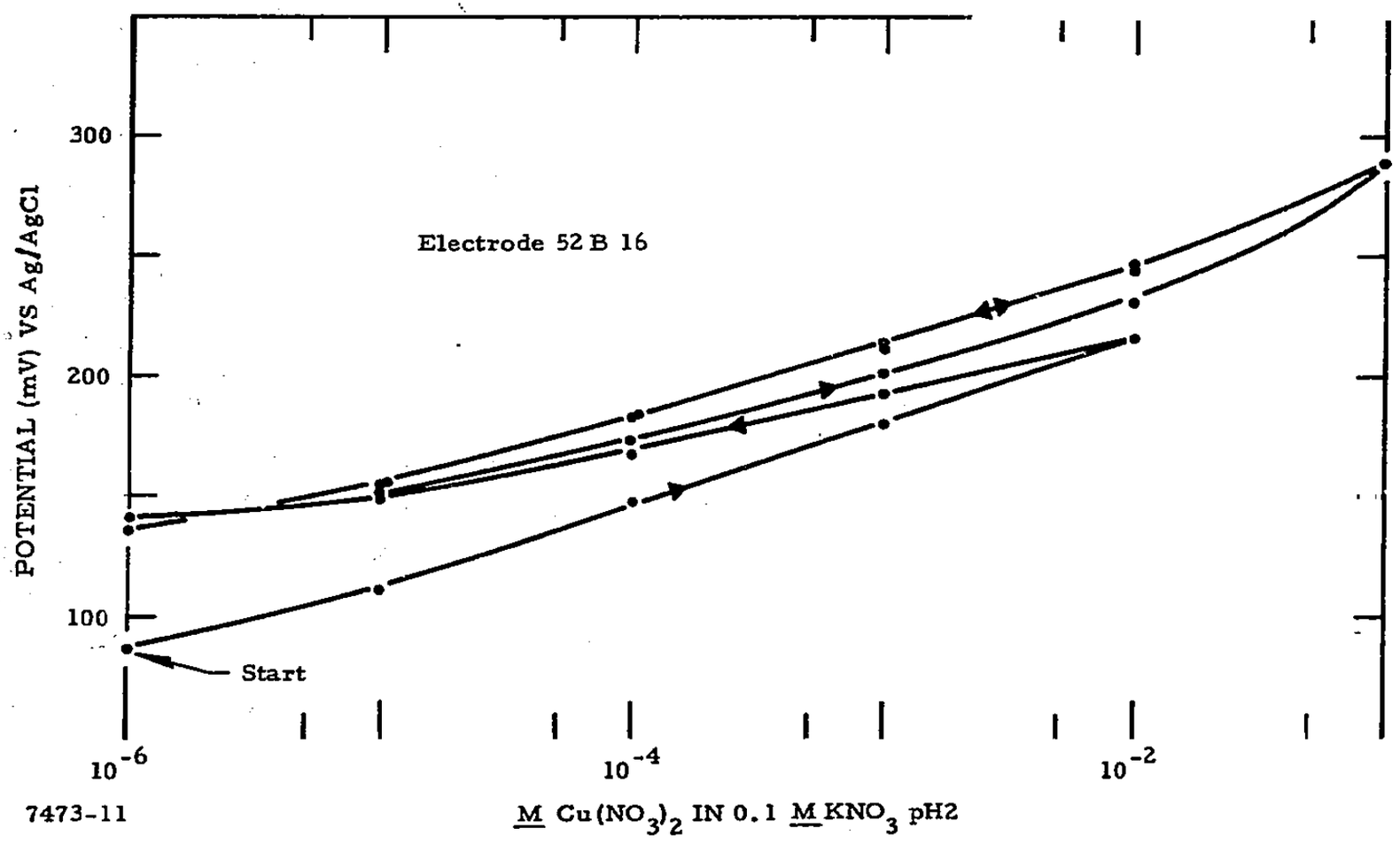

Figure 3 Performance of a Freshly Etched, Not Activated Electrode

equilibrated separately for periods of 45 minutes, one hour, 2.5 hours, and overnight. There was little difference in the slopes of the response curves and the sensitivity, although, as exposure time was increased, the slopes were always displaced to higher potentials. There was also considerable hysteresis after the electrode had been equilibrated in 10^{-1} M cupric nitrate for more than 2.5 hours, between the first exposures of the electrode from 10^{-1} to 10^{-6} M cupric nitrate relative to subsequent cycles in concentration between these limits.

Figure 4 shows the concentration-potential relationships determined in nitrate solutions for a properly activated electrode. Included for comparison are the performances of the commercial electrodes. Below 10^{-2} M copper, the Orion electrode and the copper-arsenic sulfide electrodes were essentially identical in performance, with Nernstian slopes of 31 and 27 mV/decade, respectively. Above 10^{-2} M copper, the copper - arsenic trisulfide electrode showed a slight super-Nernstian response. Below 10^{-4} M copper, this particular Coleman electrode showed little sensitivity to changing copper ion concentration; above 10^{-4} M copper the two commercial electrodes were essentially identical in response.

Response times for all electrodes were good, e.g., at 10^{-5} M copper, steady state was achieved within one to three minutes; here, steady state is defined as a potential that is stable to less than one millivolt drift in three minutes.

The three electrodes showed little dependence on stirring. For example, two minutes after stirring of the 10^{-2} M copper solution was terminated, the potentials of the Cu-As_2S_3, Orion, and Coleman electrodes decreased by 1.9, 1.8, and 0.2 mV respectively.

The effect of pH on sensor response is shown in Figure 5. In the absence of Cu^{+2}, the electrode is pH-sensitive, probably due to some adsorption or reaction of the surface with hydroxyl ion. However, in the presence of cupric ion, the electrode response is independent of pH until cupric hydroxide begins to precipitate. Even as this takes place, the electrode potential follows the remaining copper in solution until the detection limit of the electrode is reached. The data shown were for an electrode prepared from CuO; identical results were obtained for an electrode prepared from copper metal, as would be expected in view of the x-ray studies described above.

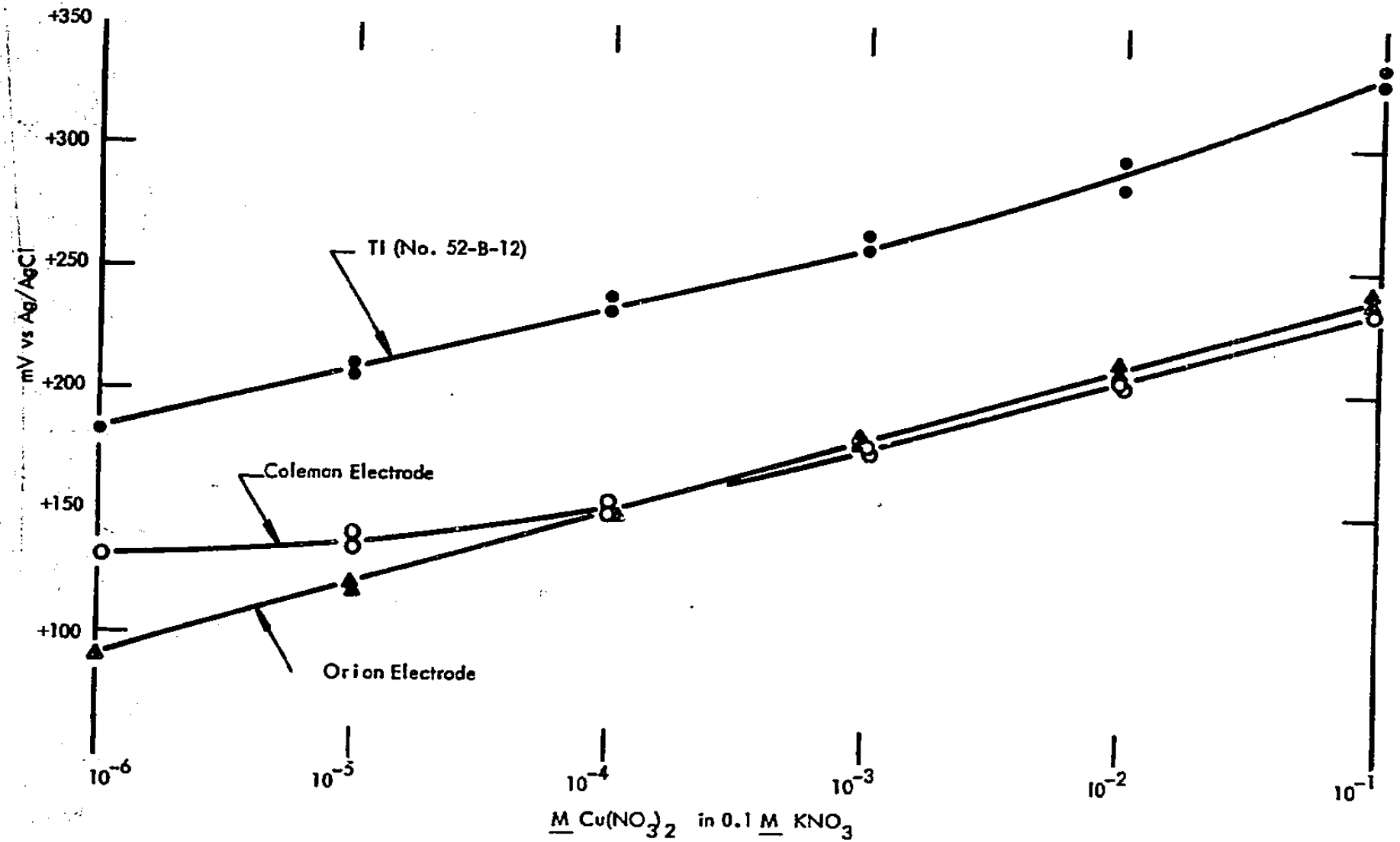

Figure 4 Steady-State Responses of a TI Electrode and Two Commercial Electrodes to Varying Copper Ion Concentrations in a Supporting Electrolyte of 0.1 M KNO_3

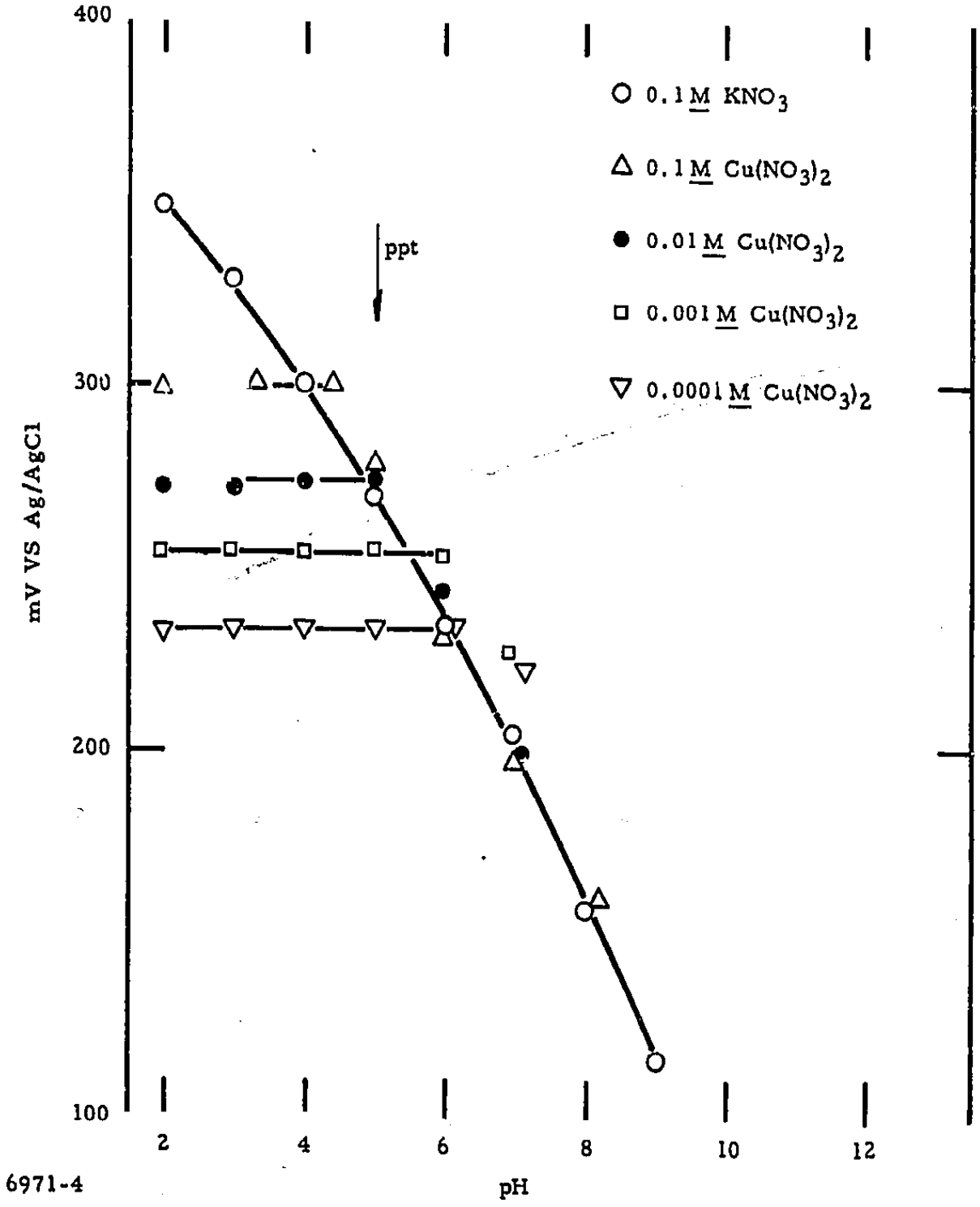

Figure 5 Response of a $(CuO)_{0.15}(As_2S_3)_{0.85}$ Membrane Sensor to Varying $[Cu^{+2}]$ and pH. All solutions 0.1 M KNO_3.

Responses of the Cu-As_2S_3 electrodes in the acetate solutions are summarized in Figure 6. Included for comparison is a response curve for the electrode in 0.1 M nitrate. Prior to each run the electrode was etched and activated to remove possible complications from prior history.

At and below 10^{-3} M added copper the slopes of the curves were basically identical with slopes of approximately 30 mV/decade. The curves did shift to lower potentials with increasing acetate concentration at a fixed added concentration of copper. Qualitatively this is consistent with the argument that the electrode responds to uncomplexed cupric ion which decreases in concentration as acetate increases.[7] The tailing off of the response curve in 1 M acetate is also consistent with this explanation. The slight non-Nernstian increase in potential at the high copper ion concentrations is due to exceeding the complexing capacity of the 0.1 M acetate electrolyte. A rigorous calculation of the shifts in potential with changing acetate concentration was not done, due to the arbitrary shifts in E_o of the electrodes by virtue of the re-etching procedure followed between each series of concentration measurements.

An attempt was made to operate the electrodes in solutions of thiocyanate, which forms a different distribution of complex ions with cupric copper. Unfortunately, the solutions were unstable with time; potential changes of the order of 65 mV were observed between 10^{-3} and 10^{-4} M copper for freshly prepared thiocyanate solutions.

Halide-containing solutions were considered next. Not only do a variety of cupric-containing complex ions exist, but cuprous species are also stable in high concentrations.

Copper - arsenic trisulfide electrodes operated in these solutions also required a similar activation step before stable Nernstian response could be obtained. There was little difference between electrodes equilibrated for one hour and those equilibrated for five hours. Electrodes equilibrated overnight in 10^{-1} M cupric chloride solutions (1 M KCl, pH 2) were less sensitive to changes in cupric ion concentration at and below 10^{-5} M. After the 40-hour exposure, all electrodes showed a significant loss in activity below 10^{-4} M copper, i.e., a lowering in sensitivity to changes in cupric ion concentration.

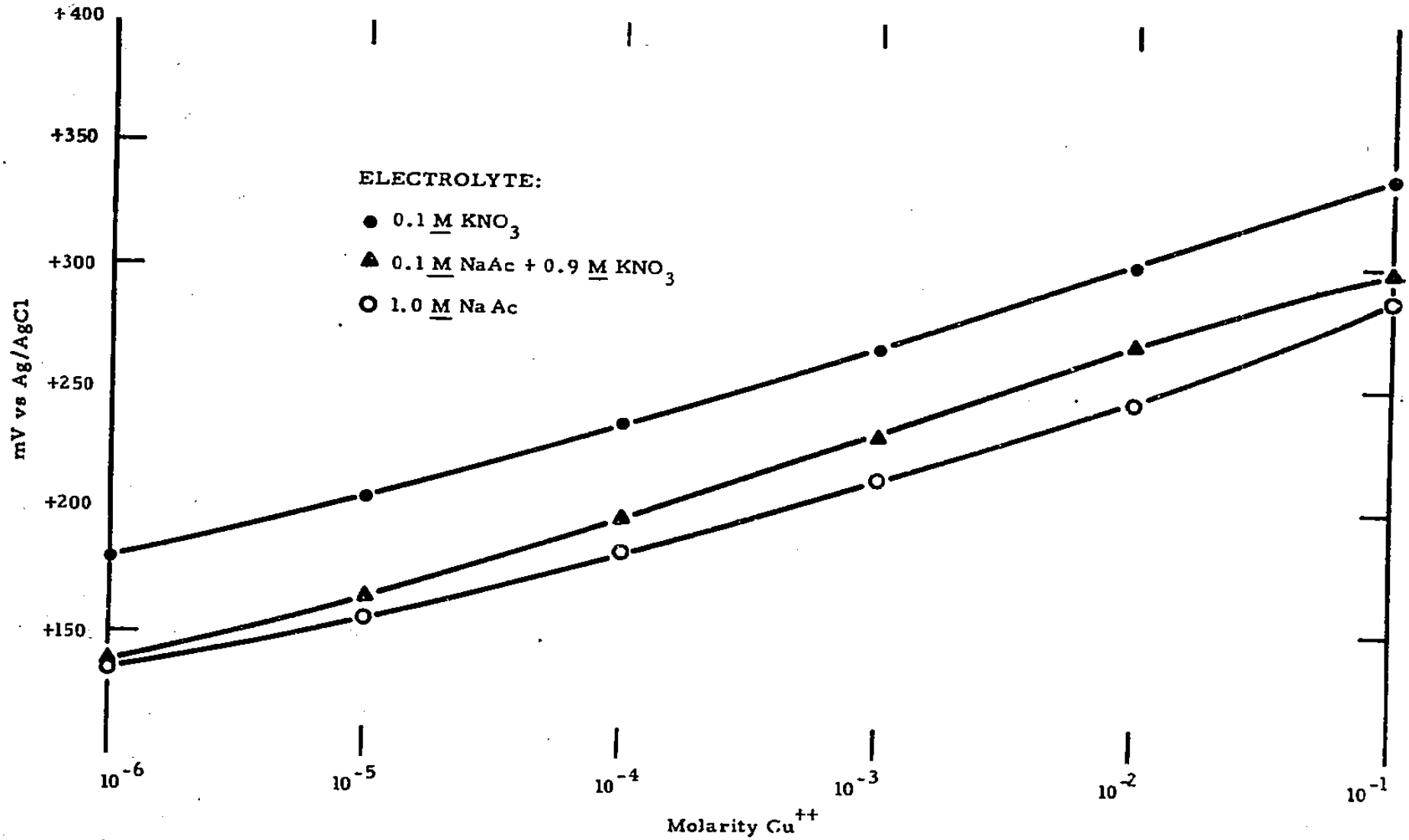

Figure 6 Responses for a Cu-As_2S_3 Electrode in Nitrate Solution, in 0.1 M Sodium Acetate Solution, and in 1.0 M Sodium Acetate Solutions

Figure 7 shows the steady-state responses to varying cupric ion concentrations in 1 M KCl for a copper - arsenic trisulfide electrode and, for comparison, for an Orion and a Coleman electrode. The copper - arsenic trisulfide electrode showed Nernstian behavior over the range of 10^{-5} to 10^{-2} M copper, but with a slope of 49 ± 2 mV/decade, rather than 30 mV/decade. The Nernstian slope for the Coleman electrode was 55 mV/decade from 10^{-4} to 10^{-1} M cupric ion; the potentials oscillated ±2 mV at steady state. The Orion electrode demonstrated a saturation effect at high copper concentrations in this high chloride ion containing solution. This was predicted by the operations manual supplied with the electrode and is apparently due to the reaction[11]: $Ag_2S + Cu^{+2} + 2\ Cl^- = 2\ AgCl + CuS$. Between 10^{-6} and 10^{-4} M copper, the potential change of the Orion electrode was 50 mV per decade rather than 30 mV as predicted by the operations manual. Experiments with other Orion electrodes gave slopes in the 45 to 50 mV range. Thus, the performance of these electrodes at high chloride ion concentrations is more complicated than predicted from the standard solubility product mechanism.

Unlike their performances in nitrate solutions, all electrodes showed a stirring dependence when operated in 1 M KCl and 1 M NaBr solutions. For example, the copper - arsenic trisulfide electrodes generally showed a drop in potential of 30 mV after stirring was stopped in the 10^{-1} M copper chloride solution; smaller changes were observed at the lower copper-containing solutions, e.g., 15 mV at 10^{-4} M cupric ion. This stirring dependence also varied from electrode to electrode, in the best case being only 10 mV/2 minutes at 10^{-1} M cupric chloride and 3.3 mV/2 minutes at 10^{-3} M. However, these electrodes were less sensitive to changes in cupric ion concentration at low levels of copper (i.e., 10^{-5} M, not 10^{-1} M). A tentative explanation for this stirring dependence is given below. No correlation of potential with stirring rate was made.

The Coleman electrode showed a stirring effect of the same magnitude, but in the opposite direction; i.e., the potential increased after the stirring was shut off. One of a set of three Orion electrodes was very stable to stirring. A potential increase of 2 mV in two minutes was found at 10^{-5} M cupric chloride. However, two other electrodes showed stirring dependencies similar to those found with the Coleman electrode.

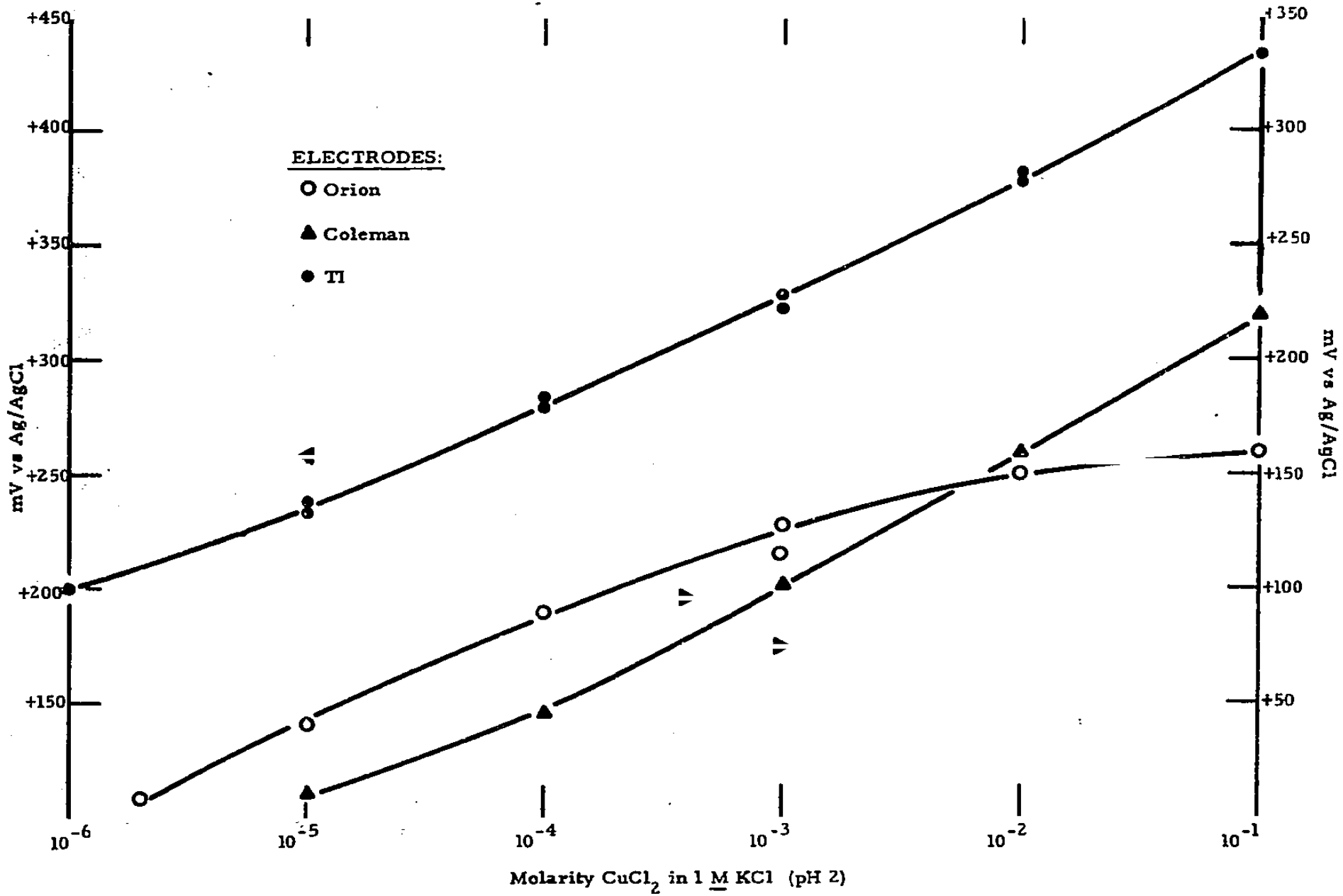

Figure 7 Steady-State Responses for a TI Electrode to Varying Copper Ion Concentrations in a Supporting Electrolyte of 1.0 M KCl (pH 2). The arrows indicate the appropriate potential scales.

The Cu-As_2S_3 electrodes were also run in a supporting electrolyte of 1 M KCl + 1 M HCl to permit direct comparison with data published for pure cupric sulfide electrodes.[12] The Cu-As_2S_3 electrode generated a Nernstian response of 47 mV/decade; the CuS electrode described in Reference 12 had responded with a slope of 29 mV/decade for changing cupric ion concentrations in the same supporting electrolyte.

Since the slopes observed in 1 M chloride were approximately double those observed in nitrate and in acetate, a study was made on the effect of chloride ion concentration on electrode response. Accordingly, electrodes were exposed to varying copper concentrations in supporting electrolytes of 3 M KCl, 1 M KCl and 0.1 M KCl + 0.9 M KNO_3; pH was maintained at 2 in all cases.

Within the accuracy of the experiments, the Nernstian slopes in the 3 M and the 1 M KCl were identical. In all cases the slope for the 0.1 M KCl solution was lower, approximately 40 mV/decade. The actual potentials measured in the 3 M KCl were about 50 mV higher than those measured in 1 M KCl. The differences in slope in relation to the 0.1 M KCl solution were maintained over the concentration range of 10^{-1} to 10^{-5} M cupric chloride. It was not possible to correlate these slopes with the variations in concentration of uncomplexed Cu^{+2} or $CuCl^{+}$.

An evaluation was made of the electrode properties in bromide solution, which has a different distribution of complex ions with cupric copper[13] and in which cuprous copper is still stable.[13] The electrodes were etched, stored overnight in cupric nitrate solution, and exposed to varying cupric ion concentrations in 1 M NaBr and in 1 M KCl. In all cases the potential-concentration slope appeared to be slightly higher in bromide than in chloride, by about 2 mV; however, this is well within the accuracy of the data, so it can only be safely concluded that the Nernstian responses in bromide and in chloride are essentially the same. In all cases the actual potentials of the bromide solutions were higher than those in the chloride solutions. The consistency of these results from electrode to electrode prohibits explanations in terms of vagaries in the electrode surfaces. Stirring dependencies were also observed in bromide electrolytes; again, these were slightly greater than in chloride solutions of the same added copper concentration. According to Reference 7, the copper-bromide complexes are weaker than

the copper-chloride complexes, so that at any given total added copper the available cupric ion concentration will be greater in bromide and could, at least in part, account for the differences observed, assuming that the electrode responds only to uncomplexed cupric ion.

The response of the copper - arsenic trisulfide electrode to other soluble ionic species was evaluated. Univalent ions such as Na^+, K^+, and H^+ do not give a response in the presence of cupric ion other than via ionic strength effects. Some interference results when excessive amounts of ferric ion are present. This is illustrated in Figure 8. Each plot represents the response of a $Cu\text{-}As_2S_3$ electrode immersed in solutions of constant ferric ion concentration, but with varying cupric ion concentrations. These curves indicate that the ferric ion must be at least ten times greater than the cupric ion concentration before significant interference is observed. Tests with other electrodes of approximately the same composition indicated that the ferric ion content must be at least 100 times the cupric ion concentration to cause a significant interference.

The response of the sensor to other ions is shown in Figure 9. A 10^{-3} M cupric nitrate solution was used as test. Varying amounts of calcium, nickel, and ferrous ion were added. The results indicate no interference due to either calcium or nickel. The effect of ferrous ion suggests a titration curve whereby cupric ion is reduced and ferric ion is generated. There are also no interferences from Pb^{+2}, Mn^{+2}, or Zn^{+2}. Interference was found with silver ion.

The sensitivity, selectivity, and performance properties previously described are all satisfactory for the use of the copper - arsenic trisulfide glass electrodes as cupric ion sensors. It is also apparent that the behavior characteristics of these electrodes are not consistent with the usual solubility product type of ion-sensing formalism. A series of experiments was carried out in an attempt to clarify the mechanism operating for the copper - arsenic trisulfide electrodes.

The first feature considered, then, is the electrode-activating mechanism, i.e., the mechanism by which a freshly etched electrode surface must first be exposed to high concentrations of cupric ion before stable Nernstian responses can be obtained. Exposures of the electrode to 10^{-1} M Cu^{+2} solutions obviously presents the electrode with a high concentration of cupric ion, but it also presents the

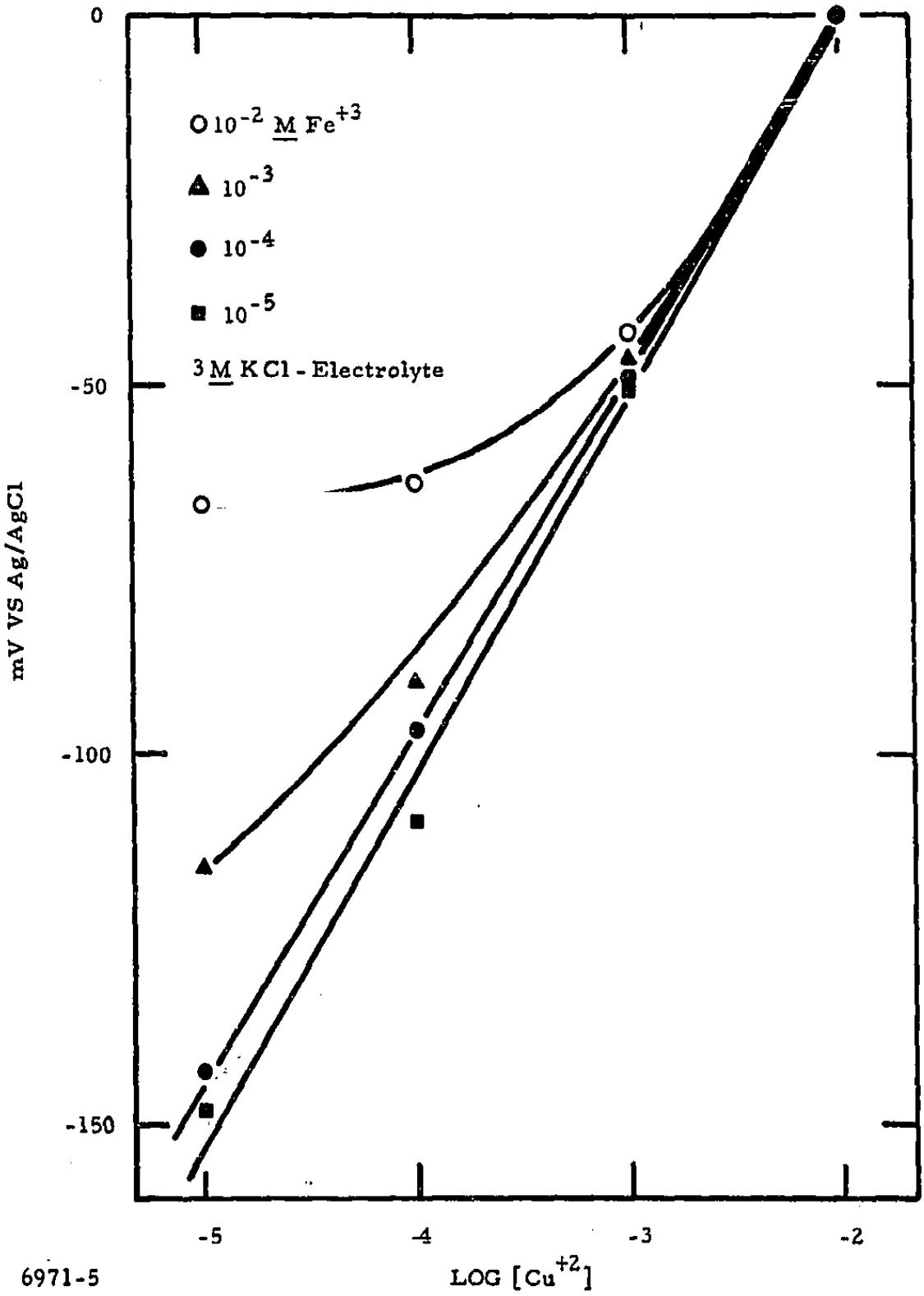

Figure 8 Response of $(CuO)_{0.15}(As_2S_3)_{0.85}$ Membrane Sensors to $[Cu^{+2}]$ in the Presence of Varying $[Fe^{+3}]$ Concentrations

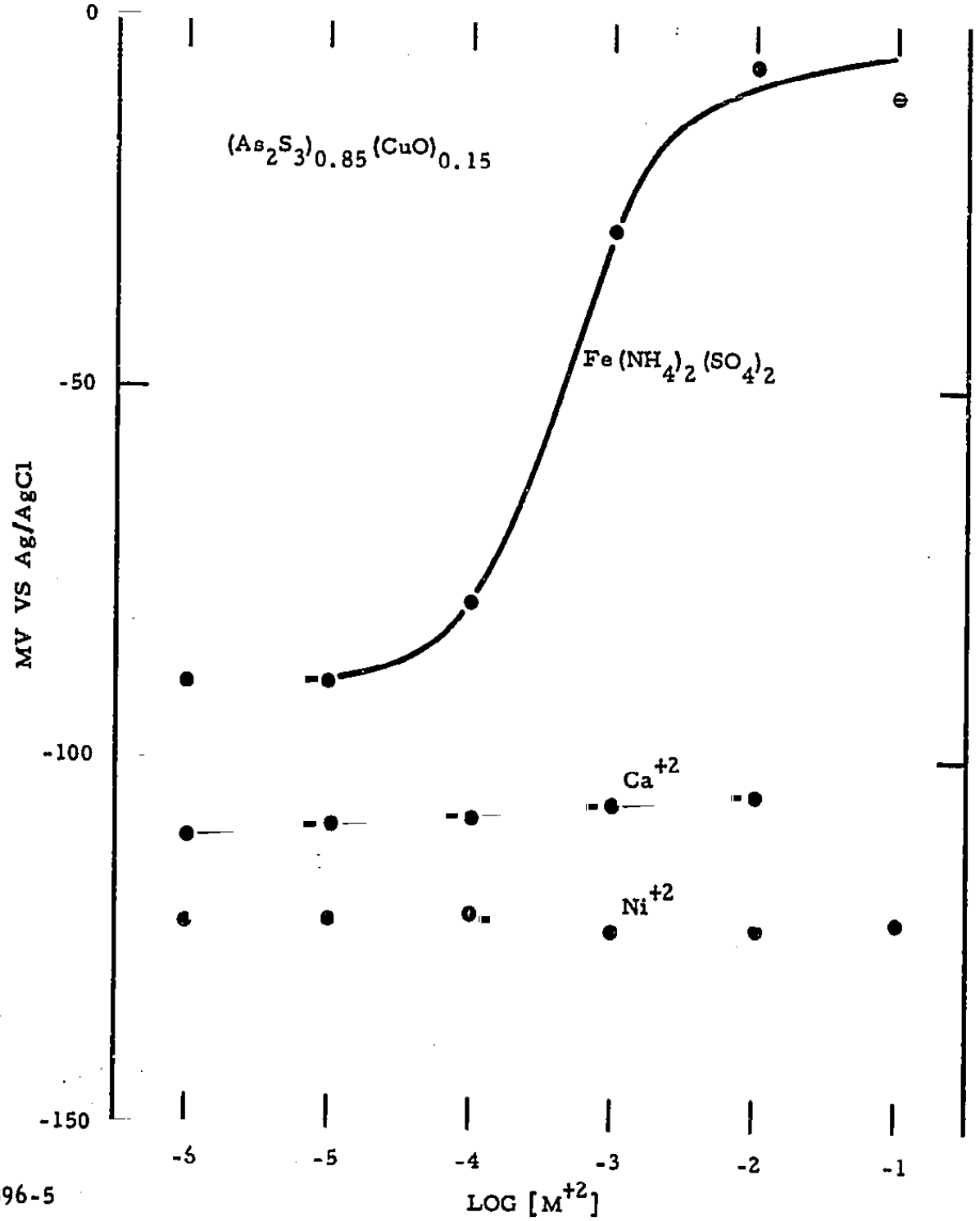

Figure 9 Response of Membrane Sensor 23-126 to Varying Concentrations of Indicated Ions in 10^{-3} $Cu(NO_3)_2$

electrode with a high positive potential, which might oxidize the electrode surface.

To determine the relative importance of these two factors, the following experiment was carried out. Electrodes were freshly etched and then potentiostated at the potential of 10^{-1} M $CuCl_2$, but in the absence of cupric ion. All other components of the solution were identical to those used in the chemical activation procedure, i.e., 1 M KCl, pH 2. An anodic current, independent of stirring, was observed, so that chemical oxidation must take place during the activation procedure. After the anodic current had decreased to zero (less than 1 μA) the electrode was exposed to 10^{-6} M cupric chloride and to incrementally increasing copper concentrations in the usual manner used to test the electrodes. The nature of the response was similar to that shown in Figure 3, i.e., super-Nernstian responses until high cupric ion concentrations were reached. Thus, a high potential alone is not sufficient to activate the electrode surface.

It is not difficult to understand a chemical oxidation-activation mechanism occurring in chloride solution where cuprous ion, the necessary soluble reaction product, is chemically stable. However, the same chemical activation process takes place in nitrate solution where cuprous ion is unstable according to the reaction:

$$2\ Cu^{+} \rightarrow Cu + Cu^{+2} \quad .$$

The equilibrium constant[15] for the concentration of cuprous ion according to the above disproportionation reaction is 2.5×10^{-4} M in 10^{-1} M cupric chloride. In the solutions used, approximately 2.5 amp sec of charge would pass before this concentration was exceeded and copper metal was formed. Since this is in excess of the total charge passed during the potentiostatic oxidation of the electrode, it is possible, even in nitrate solution, for the cupric ion to oxidize the electrode and produce cuprous ion in solution.

The potentiostatically oxidized surface still demonstrated super-Nernstian behavior, which is indicative of more than a one or two electron process; that is, it indicates further interaction of the electrode surface with cupric ion in solution to generate the copper-sensing surface. This chemical interaction between cupric ion and the electrode surface could take a variety of forms, such as com-

pound formation to generate the active sites, or irreversible reaction with strongly adsorbing sites, or both. In any event, this final surface then comes into reversible equilibrium with the cupric ion content of the electrolytes, providing Nernstian slopes.

A fundamental difference in this sensing mechanism must rest between halide solutions and nitrate solutions, since the Nernstian slopes in halides are a nominal 50 mV/decade and a nominal 30 mV/decade in nitrate. Furthermore, there is some dependence of slope on the halide concentration. A major difference in the chemistry of these solutions is the increased stability of cuprous ion in halide electrolytes.

The response of the electrode to cuprous ion was therefore considered. Electrodes were etched and activated as described. Activity was confirmed by exposure to solutions of varying cupric ion concentration in 1 M KCl. The electrodes were then washed with supporting electrolyte and exposed to solutions of cuprous chloride in the same electrolyte. Electrode potential readings were somewhat erratic, but were always less than that expected from 10^{-6} M cupric chloride. It must therefore be concluded, particularly when considering the difficulties in preventing cuprous chloride from air-oxidizing to cupric chloride, that the response of the electrode to Cu^{+} species is minor. Copper powder had been included in the nitrogen-purged solutions to remove cupric ion[12]; some corrosion took place, and eventually, the solubility product of CuCl was exceeded.

This, then, precludes any "solubility product sensing mechanism" involving the participation of sulfide ion in solution. Cuprous sulfide, like silver sulfide, is highly insoluble and should have given rise to a potential shift equivalent to a high cupric ion concentration (low sulfide ion).

The electrode was then washed with supporting electrolyte and exposed to 10^{-4} M $CuCl_2$ in 1 M KCl. Increments of cuprous chloride were added to determine whether the electrode responds to the cupric/cuprous couple. As potentials were recorded, there was some drift upward as, apparently, the cuprous ion was slowly oxidized by air. The data obtained are shown in Table VII. Similar results were obtained when the starting cupric ion concentration was 10^{-3} M.

TABLE VII

Potential Response vs Cuprous Chloride Concentration
(Original solution: 100 ml of 10^{-4} Cu^{+2} in 1 M KCl)

Molar Ratio (Cu^{+2}/Cu^{+})	Electrode Potential (mV)
∞ / 1	287.8
100/ 1	278.9
10/ 1	248.1
0.9/ 1	230.8

Obviously, cuprous copper suppressed the potential normally generated by a fixed amount of cupric ion. The depression increased as cuprous ion concentration increased, but not in a well-defined manner and not to the extent expected from the cuprous/cupric couple (59 mV/decade).

This depression may afford a pragmatic explanation for the stirring dependencies observed with the copper - arsenic trisulfide electrodes in halide solution. It can be argued that a reduced material, presumably cuprous ion, dissolves slowly off the electrode surface and reacts with cupric ion, thus depressing the amount of cupric ion in the vicinity of the electrode and hence depressing the electrode potential. If cupric ion dissolved off, the electrode potential would have increased. When stirring takes place, the cuprous copper is swept away from the electrode vicinity, and the potential takes on a value more characteristic of the cupric ion in solution. The amounts of cuprous ion are sufficiently small, however, to prevent any easily detectable increase in total copper ion concentration in the test solution. Consistent with this dissolution mechanism is the observation that the electrodes that demonstrated the most pronounced stirring dependence were also the most pitted after prolonged use.

It is necessary, in using this explanation, to account for the chemistry of a reaction between cuprous and cupric copper in solution. It has been shown

by optical absorption spectroscopy[14] that a weak, but well-defined, complex exists in solution between cuprous and cupric chlorides in the range of chloride concentration used in the electrode studies. Thus, cuprous copper may well dissolve off the electrode, complex the cupric copper in the vicinity of the electrode, and thus lower the available concentration of cupric copper at the electrode surface. As a result, potential falls.

More direct evidence for cuprous ion dissolution from electrodes in halide solution was obtained as follows. A copper - arsenic trisulfide electrode was etched, activated in 10^{-1} M cupric nitrate, and transferred to a deaerated solution of 10^{-3} M cupric chloride. A platinum screen electrode was then placed about the copper electrode. In the absence of the copper electrode, the potential of the platinum electrode was relatively stable at about +430 mV. The potentials of both electrodes (vs an Orion double-junction reference electrode) after insertion of the copper electrode are shown in Figure 10. The potentials of the platinum electrode were well poised; i.e., they showed no oscillations and continuously drifted to more negative values. The drift rate at steady state (after 60 minutes) was 4.3 mV/hr. Thus, a reduced species, presumably cuprous ion, is indeed dissolving off the electrode surface. The solution was then changed to 10^{-5} M cupric chloride. The final drift rate of the platinum electrode was 1.8 mV/hour. Therefore, the cuprous ion dissolution rate is approximately proportional to the cupric ion concentration.

This proportionality was checked by direct chemical analysis of the solution. Since the copper concentration changes involved are small and hence difficult to detect in the presence of the higher ambient concentrations, analysis was made for arsenic. The results are shown in Table VIII.

There can be little doubt that the electrodes are more soluble in chloride than in nitrate, and that the solubility is higher in the presence of high cupric ion concentrations. All this is consistent with the stirring dependencies discussed previously.

The next question is whether this soluble, reduced material (presumably cuprous ion) is involved in the cupric ion sensing mechanism, or whether this

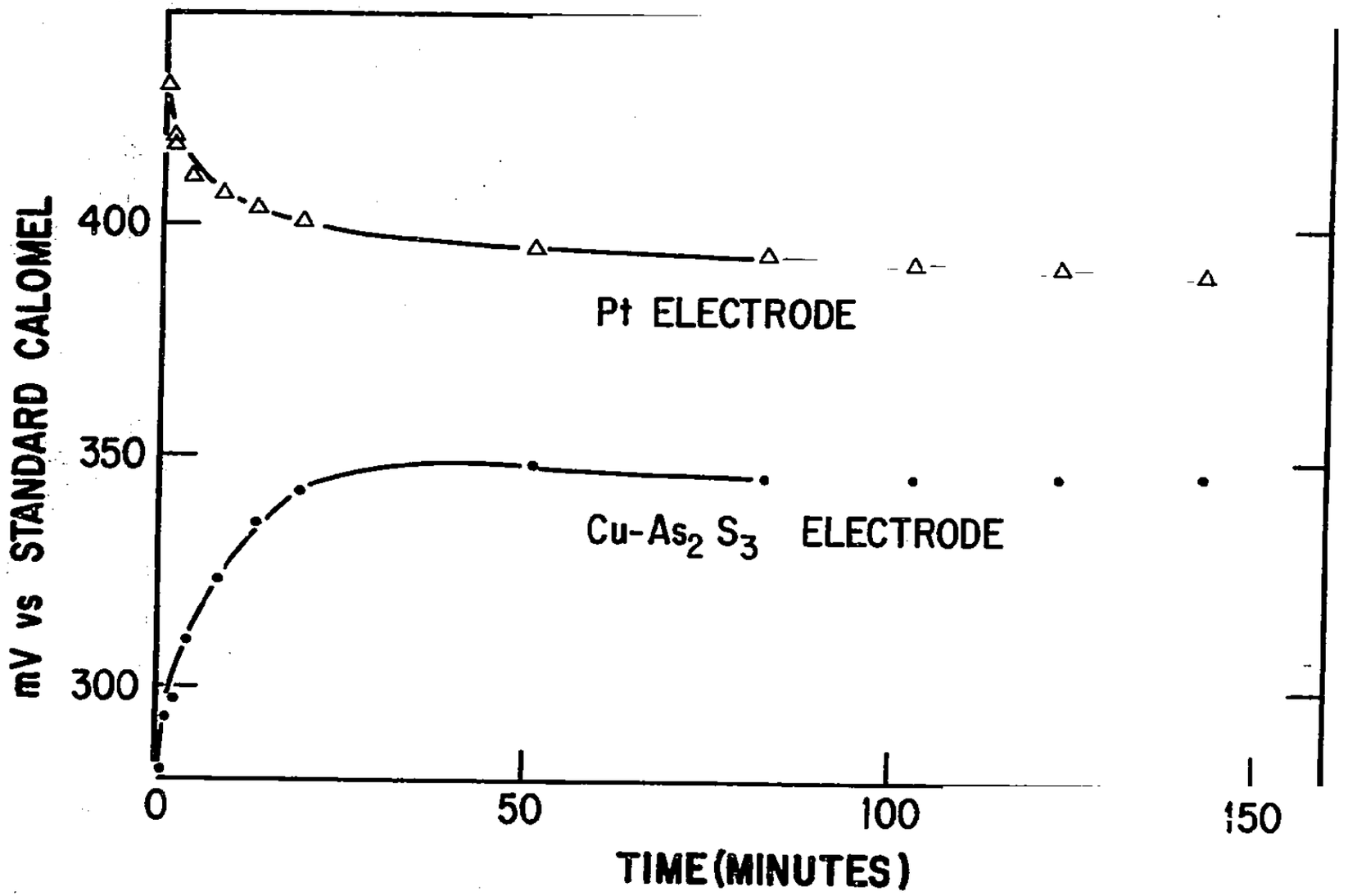

Figure 10 Time Response of $Cu\text{-}As_2S_3$ and Pt Electrodes in 10^{-3} M Cu^{+2} 1 M KCl After Equilibration in 10^{-1} M Cu^{+2} 10^{-1} M KNO_3

TABLE VIII

Arsenic Contents of Equilibration Solutions

Solution	Arsenic Concentration (ppb)
10^{-1} M KNO_3	< 10
10^{-1} M KNO_3 + 10^{-2} M Cu^{+2}	< 10
1 M KCl	35
1 M KCl + 10^{-4} M Cu^{+2}	35
1 M KCl + 10^{-2} M Cu^{+2}	65

dissolution reaction is merely incidental. Freshly etched electrodes were potentiostated at increasingly positive potentials (in 1 M NaBr, pH 2) to oxidize the electrode surfaces more completely, then equilibrated in 10^{-1} M cupric nitrate and exposed to solutions of 1 M NaBr, pH 2, varying in cupric ion content. The results are shown in Figure 11. The responses of a chemically activated electrode are included for comparison.

The behavior of the chemically activated electrode and the electrode potentiostated at +600 mv are essentially identical. The effect of higher potentials is obvious: as potential is made more positive, the subsequent sensitivity of the electrode to changes in copper concentration below 10^{-4} M decreases. It was also observed that electrodes exposed to +1200 mV would oscillate ±4 mV when subsequently equilibrated with copper halide solutions. The stirring dependences decreased when increasing potential was applied to the electrode. Note, however, that sensitivity to low levels of copper concentration decreases at the same time. This is similar to observations made earlier that electrodes with lower stirring dependencies also had lower sensitivities. Application of high potential to such electrodes completely deactivated them. It is thus apparent that the reduced material is involved in the potential sensing mechanism.

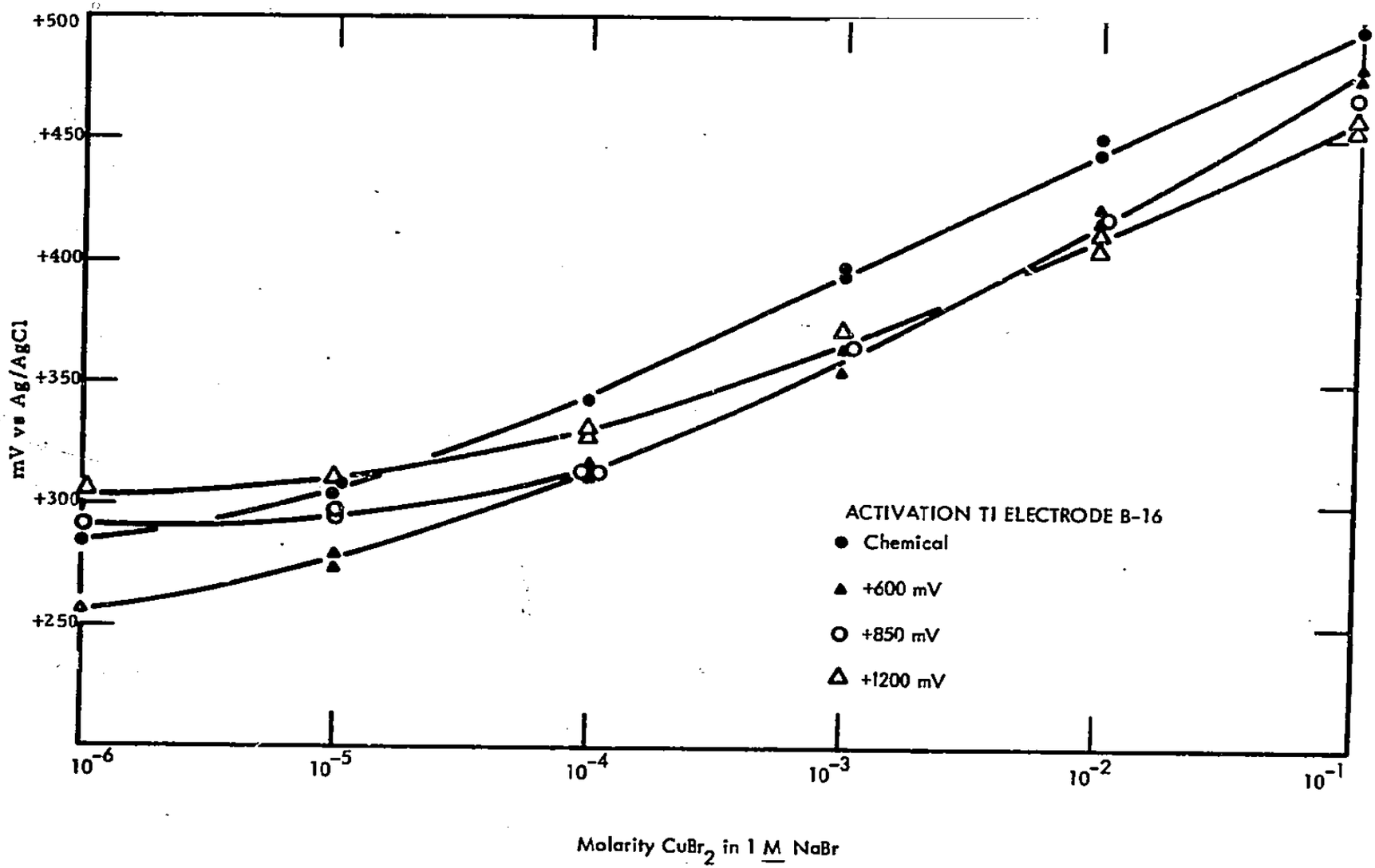

Figure 11 Typical Steady-State Responses of a Cu-As_2S_3 Electrode to Varying $CuBr_2$ Concentrations After Chemical and Potentiostatic Activation

As indicated previously, the electrode is at least a two-phase system, crystalline sinnerite embedded in an amorphous phase. The participation of the amorphous phase in the sensing process was evaluated by comparing the performances of pure sinnerite electrodes with those of $Cu_{0.25}(As_2S_3)_{0.75}$ electrodes.

Accordingly, samples of sinnerite material were compounded by mixing Cu_2S and As_2S_3 in a mole ratio of 3:2. The mixture was placed in an ampoule, evacuated, sealed, and heated to 700°C for one hour. The temperature was then lowered to 500°C for one hour and finally raised to 550°C and maintained at this temperature for 90 hours. The resulting sample was air-quenched to room temperature. Resistivity as measured on two slices was 3.04 and 3.22 Ω cm, indicating that the sinnerite is indeed a conducting material. Three sinnerite electrodes were prepared from this material.

The electrodes were etched, stored overnight in 10^{-3} M cupric nitrate, and exposed to cupric nitrate solutions over the range of 10^{-3} to 10^{-6} M. A Nernstian slope of 30 mV/decade was obtained. The experiment was repeated in 1 M KCL over the range 10^{-1} to 10^{-6} M $CuCl_2$. A Nernstian slope of approximately 55 mV/decade was obtained between 10^{-1} and 10^{-3} M cupric chloride. However, between 10^{-4} M and 10^{-6} M $CuCl_2$ the response was super-Nernstian, of the order of 100 mV/decade. The electrodes also showed a greater stirring dependence at and below 10^{-4} M.

These responses in nitrate (between 10^{-3} and 10^{-6} M) and in chloride solutions (at and above 10^{-3} M $CuCl_2$) are equivalent to those for the two-phase system, so it can be concluded that the amorphous phase is not involved in the potential sensing per se, or that its role is entirely equivalent to that of the sinnerite. This is consistent with the observations that all the copper - arsenic trisulfide electrodes behaved in an equivalent manner, regardless of the initial chemical form of the copper put into the melt. Since the crystalline phase was always sinnerite, the amorphous phase must have differed in composition. If it were involved, then it would have been expected that the electrode behavior would also have differed with the form of the initial copper.

The abnormal behavior of the sinnerite electrodes at low concentrations of cupric chloride was similar in form to that obtained for $Cu_{0.25}(As_2S_3)_{0.75}$ electrodes

exposed to varying Cu^{+2}/Cu^{+} ratios. This performance can be rationalized in terms of the sinnerite electrode depositing abnormally high concentrations of cuprous ion in the vicinity of the electrode and reaching concentration ratios where the cuprous ion exerts a significant effect on observed electrode potential. Furthermore, the pronounced higher stirring dependence for the sinnerite electrodes is what would be expected from the dissolution of greater quantities of cuprous ion.

The conclusions of these semiquantitative mechanistic studies can be summarized by the following formalism. The active electrode material ($Cu_6As_4S_9$) is first oxidized by cupric ion; potentiostated sinnerite developed a high initial anodic current

$$Cu_6As_4S_9 + Cu^{+2} \rightarrow (\text{oxidized surface}) + Cu^{+}. \qquad (1)$$

This oxidized surface then reacts chemically with cupric ion to form the active sites, which come into equilibrium with the cupric ion concentration of the test solutions, i.e.,

$$(\text{oxidized surface}) + Cu^{+2} \rightarrow (\text{active site}) \qquad (2)$$

$$(\text{active site}) + Cu^{+2} \rightleftharpoons (\text{active site})\,(Cu)_{ads} + 2e^{-}. \qquad (3)$$

A second and irreversible process such as reaction (2) is required to account for the super-Nernstian slope observed only initially with oxidized electrodes. It is envisioned that as the sites are formed, they interact with cupric ion according to reaction (3).

It is postulated that this active copper site with adsorbed copper dissolves in halide solution to inject cuprous ion (or some other reduced species which can complex Cu^{+2}) into the electrolyte. The participation of this site is indicated by the inverse proportionality between cupric ion concentration and electrode solubility. Some soluble arsenic, a sulfur-arsenic residue, and some fresh sinnerite surface must also form during this dissolution process.

$$(\text{active site})(Cu)_{ads} + Cl^{-} \rightarrow (CuCl)_{sol} + (As_2S_3)_{residue} + Cu_6As_4S_9. \qquad (4)$$

The involvement of chloride ion in this reaction, due to its stabilizing influence on cuprous ion, accounts for the slight dependence of the Nernstian slope on the chloride ion concentration. The sinnerite so exposed can then proceed through the reactions illustrated by Equations (1) and (2). Since at least one of these

involves electron transfer, a slope greater than 30 mV/decade is obtained. The extent of this reaction is dependent on cupric ion concentration via the participation of the adsorbed copper sites in reaction (4), so that the overall response of the electrode is dependent on cupric ion concentration of the solution. Reaction (4) should lead to an eventual deactivation of the electrode in chloride ion solutions via the accumulation of the residue; this is indeed observed. Furthermore, this deactivation should be less important in nitrate solution due to lower solubility; this is also observed. By the law of mass action it would be expected from Equation (3) that deactivation should take the form of lowering sensitivity to low concentrations of cupric ion; this is also observed.

C. Summary

Fusing arsenic trisulfide with copper, cupric oxide, or cupric sulfide generates an electronically conductive glass which is sensitive to changes in cupric ion concentration over the ranges of at least 10^{-1} to 10^{-6} M copper in molar solutions of chloride, bromide, nitrate, and acetate. Commercially available electrodes do not respond to greater than part-per-million Cu^{+2} when the electrolyte contains greater than about 0.1 M halide (chloride). The electrochemically active component of the Cu-As_2S_3 glass is apparently "sinnerite" ($Cu_6As_4S_9$). Stable, Nernstian responses were obtained only after the electrode surface was etched in caustic and equilibrated with high (> 10^{-3} M) concentrations of cupric ion; excessive oxidation of the surface (> +600 mV vs Ag/AgCl) decreased electrode sensitivity to low levels of copper ion concentration.

In the presence of cupric ions, the electrode response was independent of hydrogen ion concentration from pH 2 to a value at which copper hydroxide precipitation takes place. Even as copper precipitated, the electrode potential followed the remaining copper in solution until the limit of detection of the electrode was reached.

In nitrate and acetate solutions the slopes of the potential-log concentration plots were 29 mV/decade; for the 1, 2, and 3 M chloride and bromide solutions the slopes were 50 mV/decade; the slope in 0.1 M KCl was 40 mV/decade.

The response of the copper - arsenic trisulfide electrodes was independent of stirring in the nitrate and acetate electrolytes. However, in chloride and in

bromide solutions, stirring led to an increase in electrode potential. Stirring dependencies were also found for the commercial electrodes studied, but in the opposite direction.

The copper - arsenic trisulfide electrodes did not respond to cuprous copper, per se, or to the Cu^{+2}/Cu^{+} couple. No interference was found from Ca^{+2}, Pb^{+2}, Zn^{+2}, Ni^{+2}, or Mn^{+2}. Ferric ion, when present in a tenfold excess, interferes; Ag^{+} also interferes.

Qualitative studies of the electrode activation process indicated that direct oxidation of the surface by cupric ion takes place first, followed by two or more chemical reactions between cupric ion in solution and this oxidized surface. It is this final surface configuration that is involved in cupric ion sensing.

In halide solution cuprous ions (or some other reduced species) dissolve off the electrode surface, exposing fresh sinnerite, the original starting surface. This material then proceeds through the activation steps described, leading to a mixed electrode potential. Since the extent of dissolution is proportional to cupric ion concentration, the net electrode response is proportional to cupric ion concentration. Since halide ion is involved in the dissolution process as well, via its stabilizing influence on cuprous ion, there is a dependence of Nernstian slope on halide ion concentration. At high concentrations of cuprous ion in the electrode surface, i.e., for pure sinnerite electrodes, severe departures from Nernstian behavior are observed at low cupric ion concentrations. This is ascribed to complex ion formation in the vicinity of the electrode surface between this cuprous copper, cupric copper, and chloride ion.

IV. $SO_4^=$

A. Introduction

Although ion selective electrodes are available for direct monitoring of the concentrations of many ions in aqueous and nonaqueous solutions, development of an electrode that is responsive directly to sulfate ion has proved difficult. Barium sulfate impregnated membrane electrodes have been suggested,[15] although there is some doubt regarding their eventual practicality[16]; chloride ion, a ubiquitous impurity in most waters, interferes when present above 10^{-3} M.[17] A lead ion selective electrode has been used in the indirect sensing of sulfate via a potentiometric titration of sulfate with $Pb(ClO_4)_2$[18]; dioxane is added to suppress the solubility to lead sulfate. Cu^{+2}, Hg^{+2}, Ag^{+1}, and tenfold excesses of chloride, nitrate, and bicarbonate are reported to interfere.

Previous reports[1-3] during this contract have described various attempts to produce sensors which directly measure $SO_4^=$ concentration, but very limited success has been achieved. However, a successful sensor system based on an indirect sulfate electrode has resulted from this investigation.

The system [fully described in Analytical Chemistry 44, 2373 (1972)] is based on the ferric ion/sulfate complex equilibria and is free of many of the restrictions mentioned above. This discussion of the indirect $SO_4^=$ sensor is presented for completeness of this report.

It has been shown[4] that electrodes formed from Fe-1173 glass ($Ge_{28}Sb_{12}Se_{60}$) have a Nernstian response to ferric iron in nitrate and in dilute chloride solutions, but are non-Nernstian in sulfate solutions, i.e., a medium in which moderately strong iron complex ions are formed (see Table IX). Since the extent of sulfate-iron complex formation depends on total soluble ferric iron, pH, and total sulfate, a relationship should exist between measured potential and sulfate concentration at fixed pH and fixed total soluble iron. Additional evidence to support the contention that this electrode material responds only to free, hydrated Fe^{+3} was obtained by adding oxalate ion to a solution containing Fe^{+3} and observing that the

potential decreases instantly, indicating a sharp reduction of Fe^{+3} concentration.[4] Similarly, in the pH range of 1 to 4 in the absence of Fe^{+3} the electrode shows very little or no response to changing pH; however, in the presence of Fe^{+3}, varying the pH results in considerable variation in potential response, indicating a decrease in Fe^{+3} with an increase in pH. This can also be attributed to complex formation between OH^- and Fe^{+3}.

Table IX

Log Equilibrium Constants[7] for Fe^{+3}, OH^-, and $SO_4^=$ Species

Ion	Constant	Value
$Fe_2(OH)_2^{+4}$	K_{22}	-2.91
$FE(OH)^{+2}$	K_{11}	-3.05
$Fe(OH)_2^+$	K_{12}	-6.31
$FeSO_4^+$	B_1	+2.31
$Fe(SO_4)_2^-$	B_2	+2.62
HSO_4^-	K_{00}	+2.00

Ferric iron also forms complex ions with nitrate and with chloride ions. However, these are substantially weaker than the sulfate complexes; little in the way of strong polynuclear complexes have been reported for ferric iron in sulfate, chloride and nitrate media.[7] Thus, in a solution containing a fixed excess of chloride or nitrate ion, the relative concentration of free ferric ion is independant of the total soluble iron, and there is no significant deviation from linearity of the potential-log concentration plot.

B. Experimental

1. Apparatus

The general properties and preparation of the Fe-1173 glass have been described previously.[4] Potentials (vs a Ag/AgCl reference electrode) were read out on a Hewlett-Packard 3440A digital voltmeter; impedance matching was provided by a Keithley Model 610C electrometer.

2. Reagents

The sulfuric acid stock solution was standardized as 0.4960 M with sodium hydroxide, which, in turn, was standardized against potassium acid phthalate. Sulfate solutions for analysis via the subject method were prepared by dilution with the appropriate electrolyte. pH was adjusted to 2.1 ± 0.1 immediately before titration. The barium chloride titrant was standardized as 0.2054 M with EDTA which, in turn, was standardized against calcium carbonate.

Sample volume was a nominal 100 ml, except for the 476 and 119 ppm sulfate samples, for which the volume was increased to 200 ml. Rapid stirring was maintained with a magnetic stirrer.

3. Procedure

To form the sensor, slices of the glass were cemented to the end of an acrylic tube. After the electrodes were mechanically polished, they were activated by rinsing them with 1 N NaOH, wiping, rinsing with distilled water, and finally exposing them to 10^{-1} M ferric nitrate solution at pH 1.6 for 30 minutes. Electrodes were reactivated in the same manner, about every two weeks. The inner solution between the glass membrane and the Ag/AgCl reference electrode was kept constant at 10^{-3} M $Fe(NO_3)_3$ in 10^{-1} M KNO_3. The sensor electrode-titration cell can thus be represented as follows:

$$Ag|AgCl|x\ M\ SO_4^{=},\ 10^{-3}\ M\ Fe(NO_3)_3|Fe\text{-}1173\ glass|0.1\ M\ KNO_3,\ 10^{-3}\ M\ Fe(NO_3)_3|AgCl|Ag.$$

Computations of the free ferric ion concentration as a function of sulfate concentration and pH were made in terms of the ionic species and equilibrium

constants shown in Table IX. These equilibria were combined with mass balance equations on total iron and total sulfate, and the set of equations was solved on a computer by an iterative procedure. Input consisted of total added iron, total added sulfate, and pH; output consisted of the computed ferric ion concentration plus the concentrations of the species listed in Table IX.

The concentration ranges considered were 10^{-1} to 10^{-6} M Fe and sulfate, pH 0.6 to pH 3. The lower limit for ferric iron is set by the electrode sensitivity; the upper limit is set by the solubility of $Fe(OH)_3$. In spite of the low pH, it had proved necessary to consider the Fe^{+3}/OH^- complexes. HSO_4^- was also considered, since hydrogen ions, in effect, compete with the ferric iron for the free sulfate.

C. Results and Discussion

The first point to be established was whether the Fe-1173 electrode indeed responded solely to uncomplexed ferric ion, or whether some response was also obtained from the ferric iron-sulfate complexes. Figure 12 shows the potential responses for two sensors at fixed sulfate concentration and pH, (a) against total iron present (open points); and (b) against the computed, uncomplexed ferric ion. The potential - total iron plots have average slopes of 71 and 72 mV/decade and show distinct curvature at high iron concentrations. The potential vs free ferric ion plots show no curvature and have slopes of 64.5 ± 2.1 mV (electrode 14-3) and 63.4 ± 1.4 mV (electrode 14-4). These latter slopes closely approximate those observed in nitrate solutions[4] for which complex formation is minor.[7]

Figure 13 compares the computed and observed electrode response for one set of solutions at fixed pH (1.6) and fixed total iron (10^{-3} M Fe), but variable sulfate concentration. The computed electrode potentials were derived from the computed Fe^{+3} concentrations and Figure 12. [A plot directly against log (Fe^{+3}) would have given a curve of the same form.] It is apparent that the measured and computed dependencies of potential on sulfate concentration are essentially identical; the absolute values of potential are of little concern here, being related to vagaries in electrode preparation.

Since the selective response of the Fe-1173 glass to uncomplexed ferric ion in sulfate solutions thus seems fairly reasonable, the electrode was evaluated as a monitor for sulfate ion titration. Calculations indicate that the sulfate-Fe

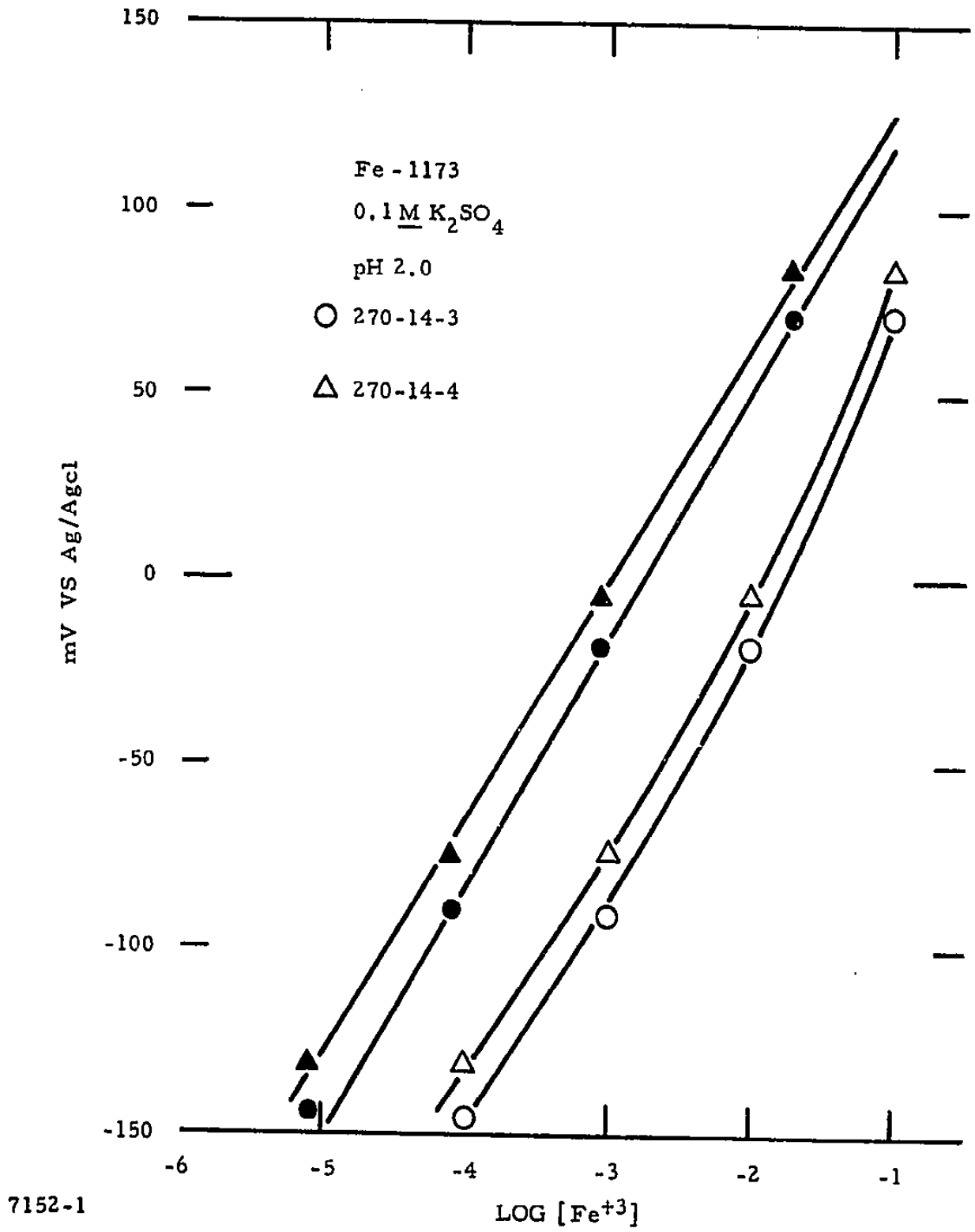

Figure 12 Measured Potentials for Two Electrodes Plotted Against Concentrations of Total Added Iron (Open Points) and Computed Ferric Ion (Closed Points). Sulfate ion concentration was kept constant at 0.1 M.

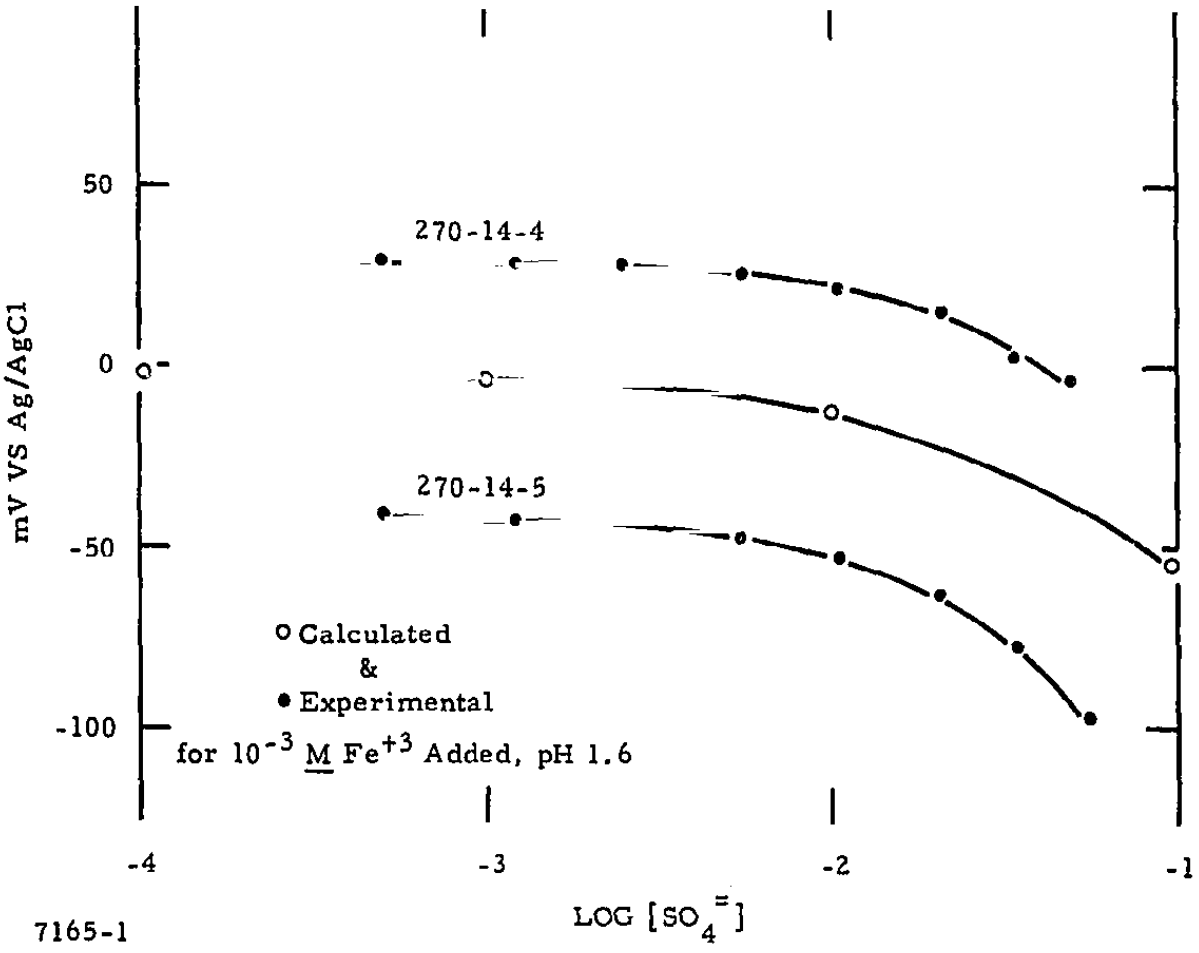

Figure 13 Computed (Open Points) and Experimentally Determined (Closed Points) Dependencies of Electrode Potential on Total Sulfate Concentration. The total added ferric iron content was kept constant at 10^{-3} M.

complexes are too weak to yield a well-defined end point for titrating sulfate directly with iron. However, if a titrant is chosen that will remove sulfate from the complexes, thus releasing ferric ion, a satisfactory titration curve is generated. The end point is defined as the titrant volume at which the potential remains constant. Once sulfate has been completely removed, further additions of titrant change the iron content only by dilution. This resulting change in potential is small (60 mV/decade).

It is seen from Figure 13 that the change in potential generated by such a titration would be the potential difference between that at the initial sulfate concentration and that below 10^{-4} M sulfate. For example, at pH 2.1 with 10^{-3} M Fe added, a 67 mV change would be expected for titrating 10^{-1} M sulfate.

Figure 14 shows the curve predicted by the computer and two sets of experimental points for the titration of 100 ml of 0.06 M sulfate (in 0.1 M KCl, pH 2.1, 10^{-3} M Fe) with 0.213 M $BaCl_2$. These data were normalized by setting the starting potential to zero millivolts. (The absolute potentials have little meaning, as discussed in conjunction with Figure 13.) This plot is essentially a linearized version of Figure 13, since, by definition, volume of titrant is directly proportional to sulfate concentration.

Table X is a comparison of computed potential changes for titration of different sulfate ion concentrations with a set of typical observations. Of particular interest are the values for the 1.25×10^{-3} M $SO_4^=$ (119 ppm) standard. The data given in the table are for 0.1 N NaCl solutions. In distilled water the observed potential changes tended to be slightly higher, e.g., 6.7 to 7.8 mV, which implies a somewhat better limit of detection. This sensitivity effect is most likely the result of a change in equilibrium constant with changes in ionic strength.

An expanded view of the experimental titration end point is shown in Figure 15. There is no difficulty in selecting the end point with ± 0.05 ml; the sensor is stable at the end point to ± 0.1 mV.

The accuracy and reproducibility of this method were evaluated by replicate titrations on known sulfate content solutions over the concentration range 119 to 9520 ppm. Distilled water, 0.1 N NaCl, and 0.1 N $NaClO_4$ were used without complication as diluents for the stock sulfuric acid solution.

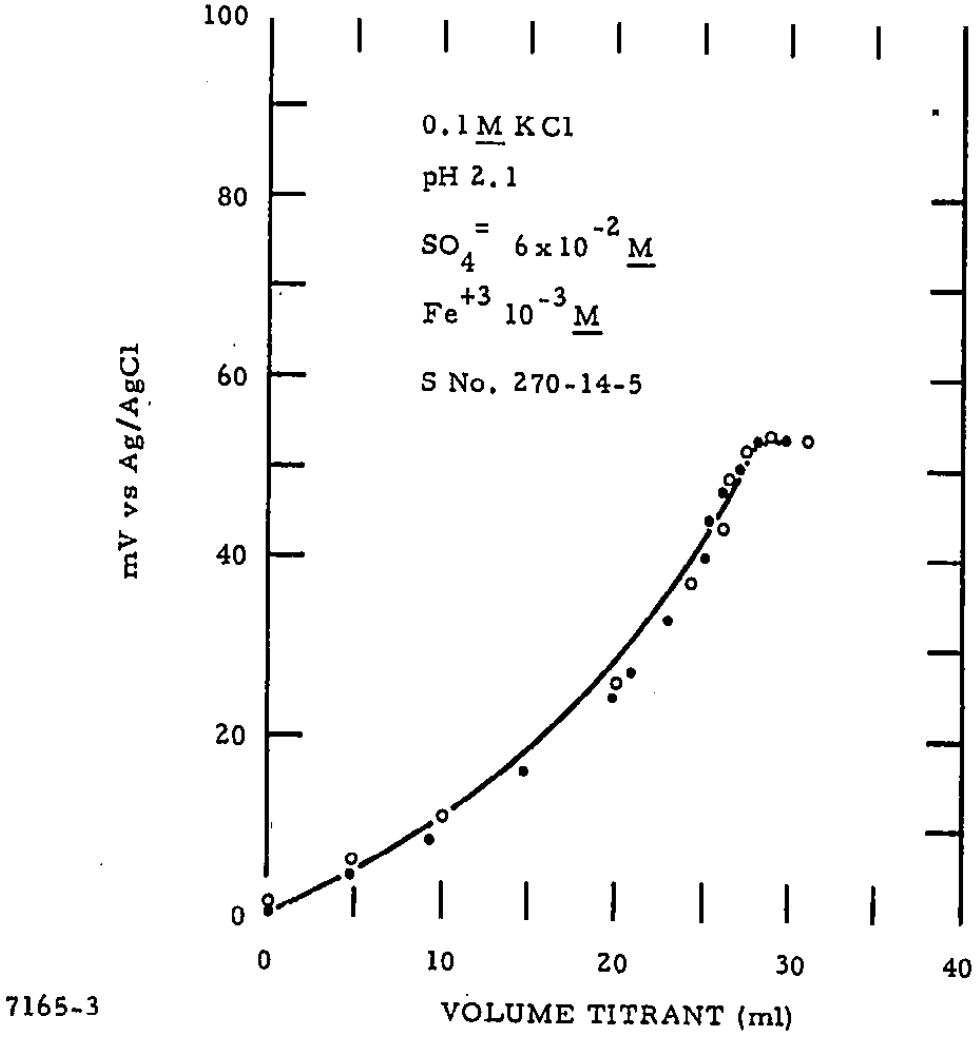

Figure 14 Computer-Simulated Titration Curve (Linear) Together With Two Sets of Experimental Points. The potential at the start of titrations was sub to zero mV.

TABLE X

Potential Changes in Sulfate Titrations

Concentration (Total Sulfate)	Potential Change (mV)	
M	Observed	Computed
6×10^{-2}	56	57
	57	
	49	
3×10^{-2}	40	37
	30	
6×10^{-3}	15.1	15
	14.7	
3×10^{-3}	7.3	8
1.25×10^{-3}	4.7	4
	5.6	
	3.3	

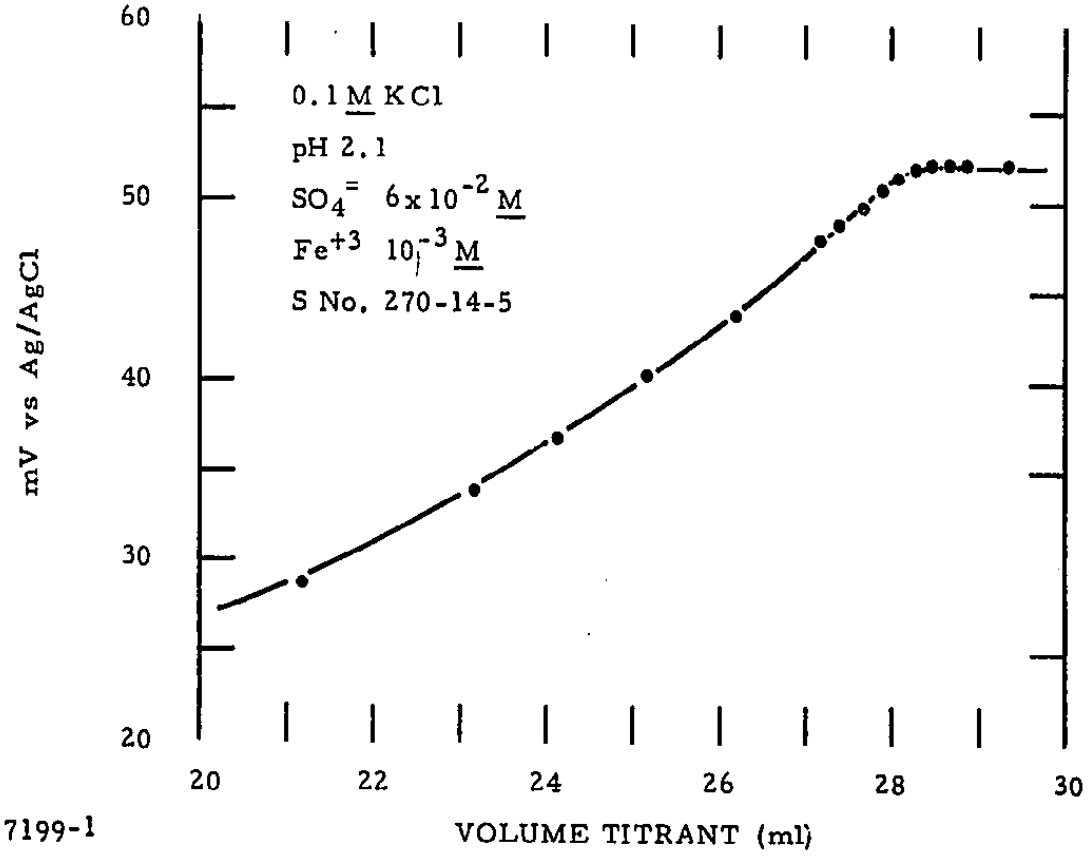

Figure 15 Expanded View of Experimental Titration End Point. Plot shows ml of titrant vs potential of electrode.

An effect of the supporting electrolyte on the reproducibility of the end point was noted when titrations were performed in the presence of 0.1 N KCl. At 9520 ppm sulfate, recovery was 98%; at 4760 ppm, recovery was 96%; at 2380 ppm, recovery was only 94%. Titrations employing barium nitrate titrant and 0.1 N NO_3^- electrolyte were also relatively unsatisfactory. The sensitivity was reduced, and the end point was not as sharp, being definable only to within ± 0.2 ml, rather than within ± 0.1 to ± 0.05 ml.

D. Conclusions

The result shown in Figures 12 and 13 and Table X indicate that (a) the Fe-1173 glass electrode indeed responds selectively to uncomplexed Fe^{+3} in the presence of ferric iron-sulfate and ferric iron-hydroxide complexes, and (b) the equilibrium constants of Table IX adequately describe dilute aqueous solutions of ferric iron and sulfate ion.

With these facts established, it was possible to have some confidence in the computer-determined optimum dependencies of electrode potential on sulfate ion concentration as a function of pH and total added iron. The following conclusions were indicated.

(a) At constant pH and constant total sulfate concentration, the primary effect of changing total soluble iron is Nernstian; i.e., the potential changes are approximately 60 mV/decade.

(b) A second-order change in sensitivity also results from changing iron content; e.g., at pH 2, when the sulfate concentration is changed from 10^{-2} to 10^{-4} M, the potential changes by 21 mV at 10^{-4} M Fe, by 18 mV at 10^{-3} M Fe, and by 12 mV at 10^{-2} M Fe.

(c) The optimum operational region for $SO_4^=$ monitoring is pH 1.7 to pH 2 and 10^{-4} M Fe.

(d) The accessible sulfate concentration range computes as $> 2 \times 10^{-3}$ M ($\sim$ 200 ppm).

(e) This electrode system will yield distinct titration end points if the titrant is chosen so as to remove sulfate ion from solution, liberating uncomplexed Fe^{+3}.

These conclusions were consistent with the limited number of conditions investigated experimentally. Considerations of electrode sensitivity and stability modified item (c) to an optimum added iron concentration of $\sim 5 \times 10^{-4}$ to 10^{-3} M. Titration in dilute salt solution yielded a limit-of-detection of 100 ppm (10^{-3} M), rather than $\sim$ 200 ppm. This again is probably an effect of ionic strength on the equilibrium constants; correction of the calculations would, of course, be possible.

It is to be expected that the method would be subject to many of the same interferences documented for gravimetric measurements of sulfate via $BaSO_4$ precipitation. The stoichiometry of the titration is slightly below theoretical ($\sim$ 1%), except when solutions containing low amounts of salt are titrated. (Note that the "distilled water" solutions high in sulfate also contained comparable quantities of sodium ion from the pH adjustment step.) This discrepancy in stoichiometry is ascribed to coprecipitation of sodium sulfate, a classical problem with barium sulfate based methods.[19] Such an explanation is made more plausible by the poor recoveries observed from electrolytes containing potassium ion. Such solutions are much more notorious for alkali sulfate coprecipitation of ferric iron; this phenomenon is also well documented.

The chemistry of the titration curve is such that the error in defining the end point should be constant and relatively independent of the initial sulfate ion concentration. This feature is borne out by the results shown in Table XI. At low sulfate concentrations about half the error or scatter shown is ascribed to instability or drift in the sensor; at high sulfate concentrations the major portion of the error is ascribed to buret error. These conclusions are based on the following argument.

The drift in sensor reading translates into an error in free ferric ion concentration and hence into an error in the complexing sulfate ion concentration. The sensors used in this work were stable to ± 0.1 mV in the vicinity of the end point. (This stability will vary somewhat with total free Fe^{+3} concentration, i.e., the species being sensed by the electrode.) Thus, with a 60 mV/decade Nernstian relationship of potential to log ferric ion concentration, this error spread of

TABLE XI

Summary of Sulfate Titrations With Average $BaCl_2$ Solution

Sulfate Concentration (ppm)	End Point (ml)	Average Deviation (ml)	% Deviation	% Recovery	Number of Measurements
9, 520	47.8	0.11	0.23	99	12
4, 760	23.85	0.07	0.07	99	15
2, 380	11.9	0.08	0.67	98.7	18
476*	4.85	0.06	1.2	100	7
119*	1.2	0.06	5	99.4	8

*200 CC SAMPLES

0.2 mV translates into 7.5×10^{-6} M Fe at the 10^{-3} M Fe level. The concomitant sulfate ion concentration is computed under the assumption that the $[FeSO_4^+]$ complex is dominant. (This is consistent with the computer calculations.) The sulfate concentration so involved is 3.7×10^{-5} M, or 3.6 ppm.

At the lowest sulfate ion concentration considered in this work (i.e., 119 ppm) the error from sensor drift is ± 2.5%, which is of the order of that found (Table XI) at 4760 ppm. At 4760 ppm the instability scatter error is 0.07%, substantially less than that observed (0.29%). The dominant error, then, must be in delivery of the titrant to the sample. Under the conditions used, the sensor drift error is ~0.02 ml of titrant, leaving about 0.06 ml for buret error, which is reasonable.

We have thus shown that it is possible to monitor $SO_4^=$ in aqueous solution ($> 5 \times 10^{-3}$ M) by merely adding Fe^{+3} in a concentration range of 5×10^{-4} to 1×10^{-3} M, adjusting pH to about 2.1, and reading the potential with an Fe-1173 electrode (Figure 13). These electrodes can also be used to determine sulfate in a titration method by adding a known quantity of Fe^{+3}, adjusting the pH, and determining the number of milliliters of standard $BaCl_2$ titrant required to reach the potential end point. In this titration method the minimum $SO_4^=$ concentration that can be determined in the sample can be as little as 1×10^{-3} M. At this low concentration the relative error was about ± 5%. As the sulfate concentration in the sample is increased, this error becomes smaller, and at 5×10^{-2} M sulfate, the relative error was reduced to about ± 0.3%.

V. Ca^{+2} and Mg^{+2}

Two material approaches have been taken for the development of solid-state sensors for Ca^{+2} and Mg^{+2}; doping of semiconductors such as single crystal n- and p-type silicon, n- and p-type germanium, and polycrstalline silicon; and doping of alkaline earth single crystal salts with either univalent or trivalent ions. Most of these results are detailed in O.S.W. Progress Reports 619 and 761.[2,3] The most promising results were obtained with the doped alkaline earth crystals, and these results are summarized here.

The following discussion is limited to the results obtained in the investigation of CaF_2 doped with 10 mole % NaF, 5 mole % YF_3, and 10 mole % YF_3, as well as Nd_2O_3 doped $CaWO_4$.

A. Material Preparation and Resistivity

The 10 mole % NaF - 90 mole % CaF_2 was prepared from single crystal CaF_2 (Harshaw Chemical Co.) and reagent grade NaF. The weight of a given CaF_2 disc was used as the basis for determining the amount of dopant, in this case NaF, to be added. The doping procedure was carried out via thermal diffusion. The best result for the NaF doping was obtained by placing the weighed disc of single crystal CaF_2 and the proper amount of NaF in a glazed graphite crucible and heating the mixture to 1040°C for 116 hours in a helium atmosphere. The resulting pellet was then placed in a carbonized quartz ampoule, evacuated, sealed, and heated to 1100°C for 210 hours. Although thermal diffusion appeared to be almost complete, the sample did not appear to be homogeneous. The resistivity of this sample was measured and found to be about 10^7 Ω cm.

The CaF_2 used for preparation of YF_3 doped CaF_2 samples was the same as above. The YF_3 was a high purity powder obtained from Dr. S. G. Parker of Texas Instruments. The weight of a given CaF_2 disc was used as the basis for determining the appropriate amount of YF_3 to be added for the desired mole % dopant. The CaF_2 and YF_3 were placed in a glazed graphite crucible with the YF_3 in contact with both sides of the CaF_2 disc. The samples were then heated to 1450°C in a Phillips furnace from

LeMont Scientific. The furnace was held at 1450°C for three to four hours, then allowed to cool slowly to ambient temperature before the sample was removed. A 1450°C temperature was selected because it allowed both CaF_2 and YF_3 to melt, mix, and then form a solid solution on cooling. (The melting point for CaF_2 is close to 1400°C, and that for YF_3 is approximately 1140°C; however, some of the solid solutions of CaF_2-YF_3 have melting points up to 1443°C.) Taking the samples to the molten state shortens preparation time considerably, and the end product is polycrystalline.

The 5% YF_3-CaF_2 was polycrystalline, but not homogeneous. Either YF_3 was not uniformly distributed in the CaF_2 melt at 1450°C, or different solid solutions were formed when the sample was cooled. With the 10% YF_3-CaF_2, however, the polycrystalline product was homogeneous in appearance.

The resistivity of the 5% YF_3 sample could not be measured by the procedure previously described,[1] indicating a value greater than 10^{14} Ω cm. The 10% YF_3 exhibited a resistivity of only 1.5×10^3 Ω cm.

Large crystals of calcium tungstates are readily obtained following a procedure described by Van Uitert, et al.,[20-22] which involves pulling the crystals from a melt. Since these materials tend to lose oxygen at the melting temperature, they can be grown in air or even in an oxygen-rich ambient. The apparatus used to prepare calcium tungstate is shown in Figure 16. The melt is contained in a rhodium crucible approximately 40 mm tall by 40 mm I.D. with a wall thickness of 1.5 mm. The 75 mm diameter, six-turn induction coil and the rhodium susceptor are surrounded by 100 mesh alumina powder to thermally insulate the melt and reduce oxidation of the rhodium. A platinum wire connects the susceptor to ground. Both the seed holder and the thermocouple tubing are made from alumina. A length of split alumina tubing rests on the wall of the susceptor and serves as a heat shield to prevent rapid cooling of the crystal as it is being pulled. Temperature control at the melting point (1540°C) is obtained with an L & N type G controller. A platinum wire with a small loop in the end serves as an effective seed. Approximately 2.5 cm/hour is a typical withdrawal rate at a rotation rate of 10 rpm.

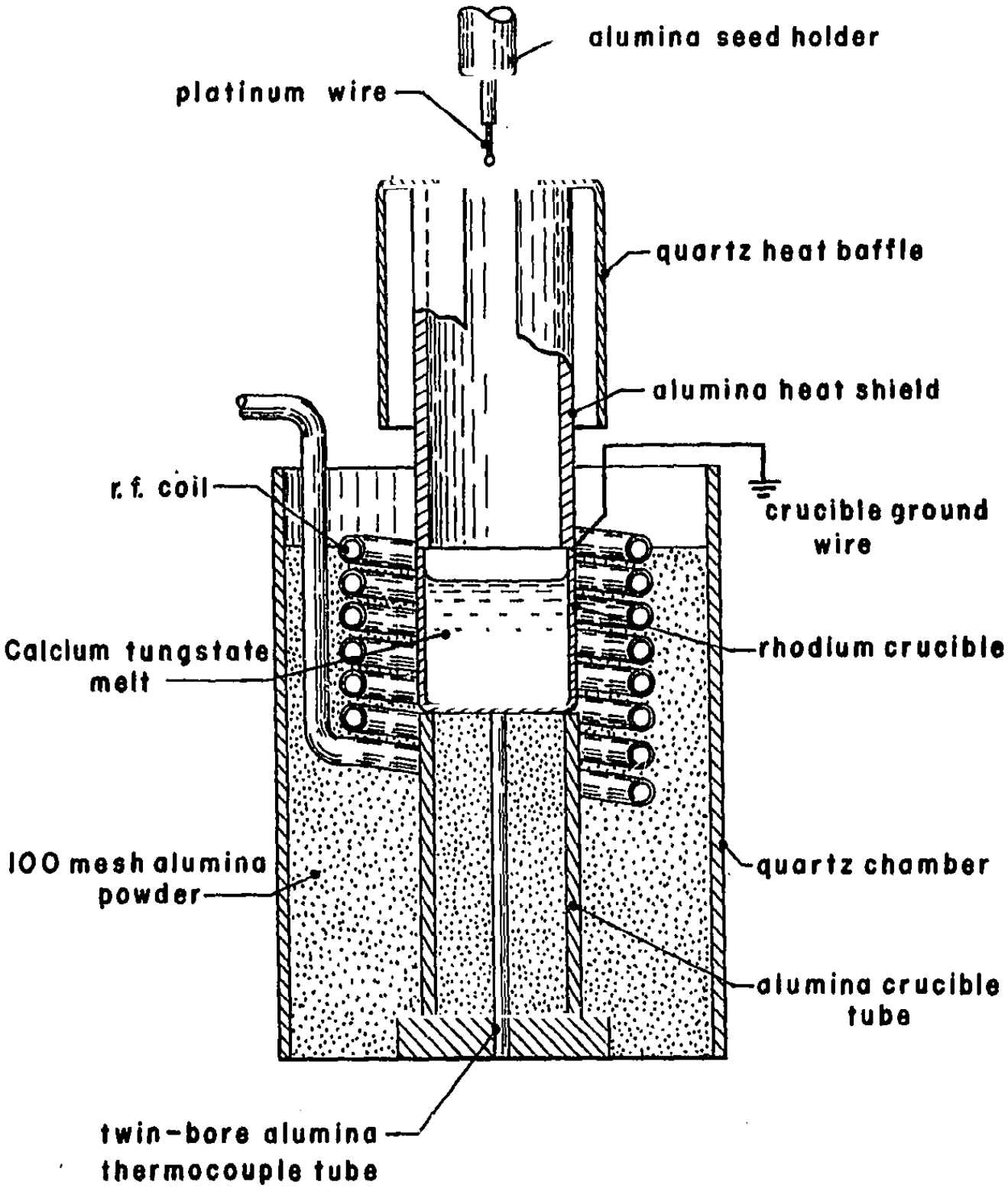

Figure 16 Apparatus for Growth of $CaWO_4$

In the case of $CaWO_4$, approximately 125 g of the reagent grade material was melted in the rhodium crucible together with a weighed amount of 99.9% Nd_2O_3 calculated to achieve 1 mole % neodymium in the resulting crystal. Since $CaWO_4$ crystallizes in the tetragonal scheelite structure, most crystals show a tendency toward fourfold symmetry. Extreme care must be taken in slow-cooling the crystals to prevent excessive cracking. In the absence of a dopant, the crystals are generally colorless and transparent. However, with the Nd_2O_3 the crystal appeared slightly bluish.

Several samples were cut from a crystal of calcium tungstate grown from a melt which contained 1 mole % neodymium added as Nd_2O_3. Although calcium tungstate crystals have a tendency to crack and fracture, the problem appears to be controllable by slow cooling. However, the presence of microcracks cannot be entirely eliminated.

Because the resistivity of these doped $CaWO_4$ slices as-grown was too high, they were heat-treated under vacuum to lower the resistance. The heat treatment was performed in an evaporator by placing the samples in the heating coils and slowly increasing the power. This treatment was carried out for about six hours. The pressure in the evaporator was of the order of 10^{-6} atmosphere. The coil temperature reached a maximum of 1125°C, but the alumina slab supporting the Nd-doped $CaWO_4$ crystals did not exceed 1025°C. The maximum temperatures were maintained for about two hours. Good resistivity data could not be obtained on these samples; however, when they were fabricated into membrane-type sensors they showed good response and stable potentials.

B. Sensor Evaluation

Membrane sensors were prepared from the polycrystalline doped CaF_2 containing 10% NaF, 10% YF_3, and 5% YF_3. All these sensors displayed Nernstian behavior to changes in Ca^{+2} concentration. Typical response curves are shown in Figure 17. In addition, these sensors exhibited reproducible potential responses regardless of the sequence of measurements. Between $< 10^{-4}$ M and 10^{-1} M Ca^{+2}, the slopes of the E-log $[Ca^{+2}]$ curves ranged from 27 mV to 29 mV (theoretical slope $\sim$ 30 mV). The slope of each curve becomes even closer to the theoretical value when activities are used instead of concentrations. A major disadvantage of all of these sensors,

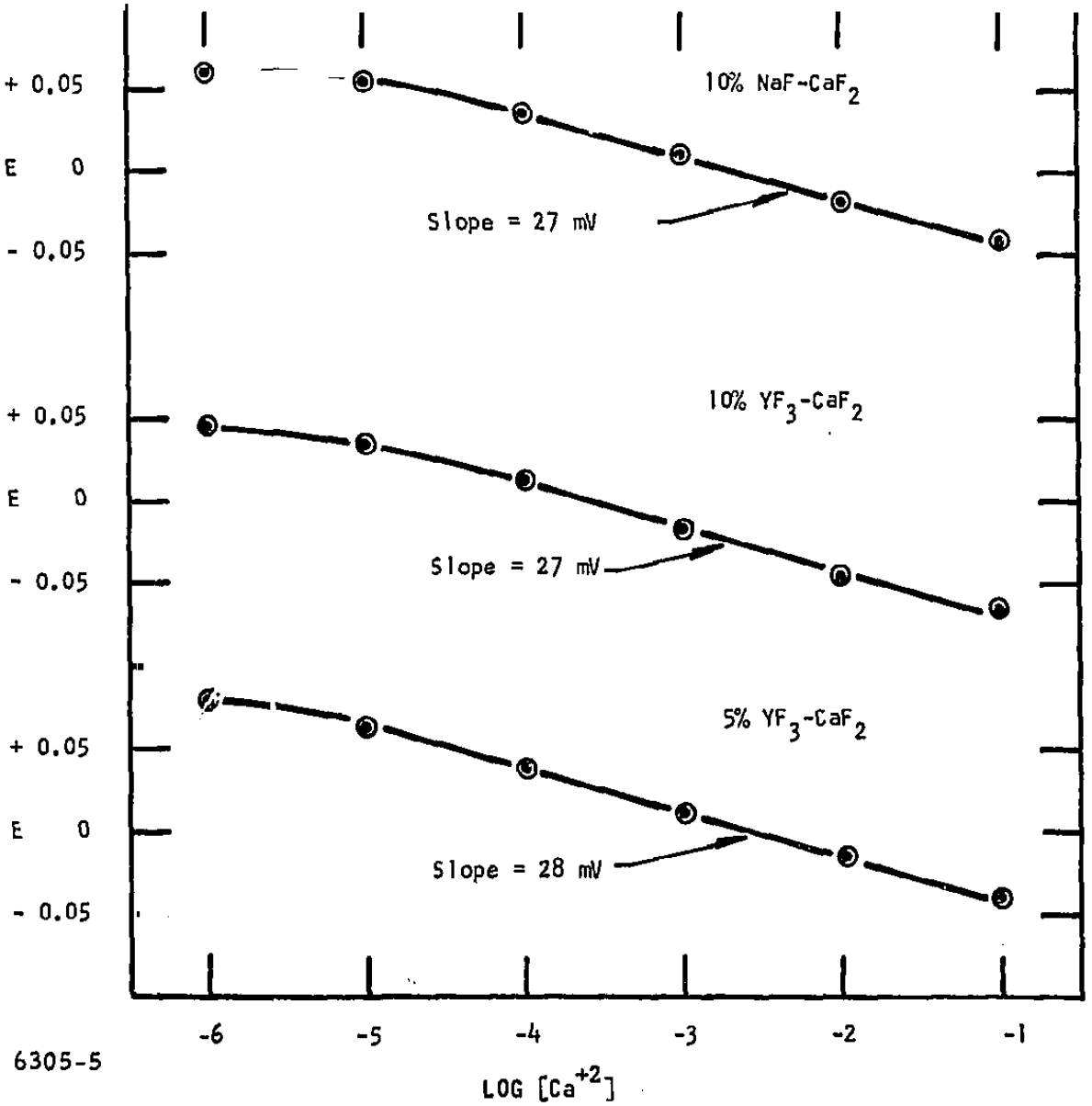

Figure 17 Potential Response of Doped CaF_2 Membrane Sensors to Ca^{+2}. (Monovalent electrolyte was not added to keep ionic strength constant.)

however, was poor selectivity. A small response to Na^+, K^+, and NH_4^+ was measured in the 10^{-3} M to 10^{-1} M range (slope ~ 15 to 17 mV). Whenever one of these monovalent electrolytes was added to the divalent cation test solutions, the response to the divalent cations was inhibited. For instance, with solutions varying in Ca^{+2} concentration from 10^{-6} M to 10^{-1} M and the concentration of KNO_3, $NaClO_4$, or NH_4Cl held constant at 0.1 M, no potential response to Ca^{+2} was measured. When the concentration of monovalent electrolyte was held constant at 10^{-3} M, a linear response to Ca^{+2} was observed from $< 10^{-4}$ M to 10^{-1} M, but the slope was only 23 mV (Figure 18). Apparently the addition of monovalent electrolyte does not affect the limit of detectability for Ca^{+2}, but it does decrease the slope of the E-log $[Ca^{+2}]$ curve. Decreasing the pH produced the same effect, as shown graphically in Figure 19 for the 10% YF_3-CaF_2 sensor. As the pH decreases from pH 6 to pH 3, the ΔE for decade changes in Ca^{+2} concentration decreases. The reversal in E-pH trend as the pH is decreased below 3 may be due to dissolution of the sensor element. The E-pH data clearly show that the pH of the Ca^{+2} solutions must be in the neutral region for Nernstian behavior to be observed.

Considering the ion exchange argument, a potential response to anions such as F^- and $C_2O_4^=$ was expected, but no response was observed. The above observations may be interpreted on the basis of the equation for junction potentials

$$E = E_a + \frac{t_+ - t_-}{t_+ + t_-} \frac{0.059}{Z} \log \frac{a_1}{a_2} \quad , \qquad (5)$$

where E_a is the asymmetry potential; t_+ and t_- are the transport numbers through the membrane for the cation and anion, respectively; and a_1 and a_2 are the activities of the electrolyte on the two sides of the membrane. The Z in Equation (5) represents the charge of the higher valent ion. For the potential responses to Ca^{+2} in $CaCl_2$ or $Ca(NO_3)_2$ solutions, Z = 2, $t_+ = 0$, and $t_- = 1$, which gives the Nernstian slope of ~ 30 mV. It appears that Ca^{+2} is not transported across the membrane ($t_+ = 0$) because of adsorption of the divalent cation by the sensor element. Current is transported through the microcracks or hydrated pores in the sensor material, then, totally by the anion ($t_- = 1$).

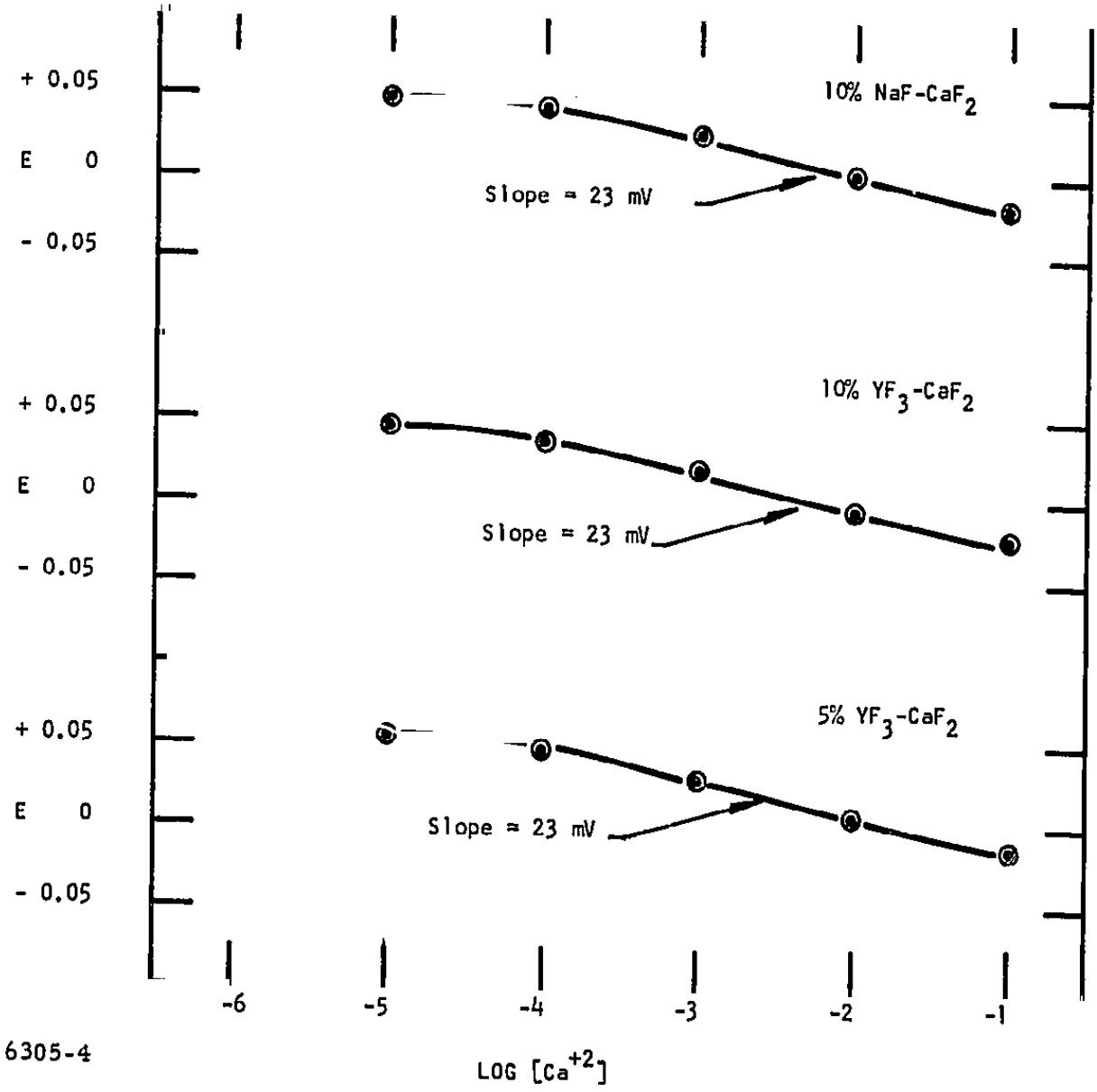

Figure 18 Potential Response of Doped CaF_2 Membrane Sensors to Ca^{+2} When the Concentration of KNO_3 is Held Constant at 10^{-3} M.

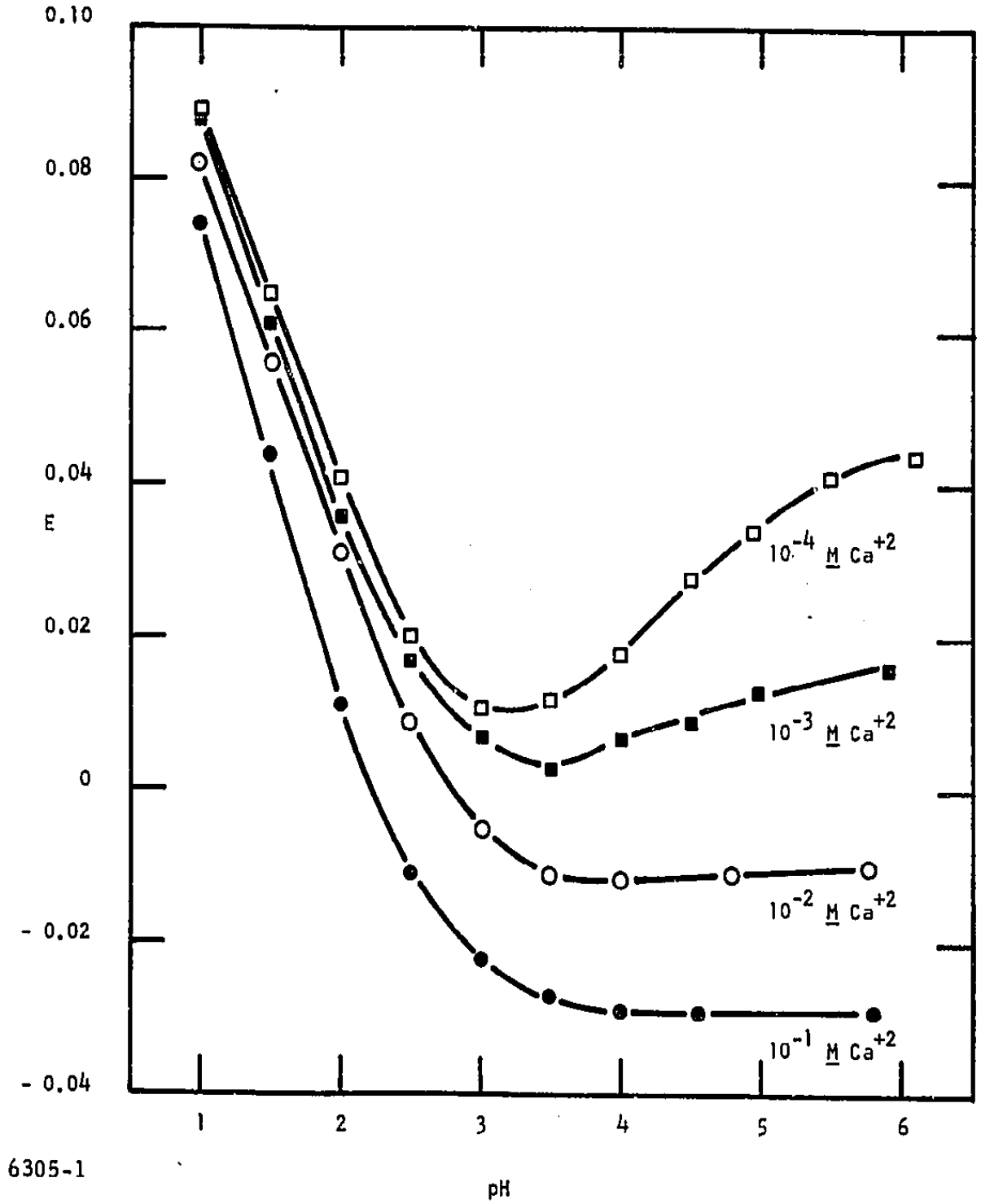

Figure 19 Effect of pH on the Potential Response of the 10% YF_3-CaF_2 Membrane Sensor to Ca^{+2}.

The lack of response to fluoride and oxalate is not understood at present, but it may be related to the charge on the outer layer of the sensor material and its effect in enhancing or inhibiting adsorption.

Numerous additional tests were made with the 10% $NaF-CaF_2$ and 10% YF_3-CaF_2 membrane sensors. In the absence of a background electrolyte, the 10% $NaF-CaF_2$ sensor displayed a Nernstian response to Ca^{+2}, Ba^{+2}, Mg^{+2}, Cd^{+2}, Ni^{+2}, Cu^{+2}, and Mn^{+2} (slope $\sim$ 30 mV) in the 10^{-5} M to 10^{-1} M concentration range. Under the same conditions, the 10% YF_3-CaF_2 displayed a Nernstian response only to the Ca^{+2}, Ba^{+2}, and Mg^{+2}. For the Cd^{+2}, Ni^{+2}, and Mn^{+2} the slopes were $\sim$ 20 mV; the slope for Cu^{+2} was $\sim$ 42 mV. The varying responses of these sensors indicate that the 10% YF_3-CaF_2 membrane sensor shows some degree of selectivity with regard to the transport of the various divalent cations across the membrane. As with the other sensors of this group, the presence of 0.1 M background electrolyte in the test solutions wipes out the response to the normally measurable divalent cation.

In an attempt to obtain the optimum surface conditions at the 10% $NaF-CaF_2$ and 10% YF_3-CaF_2 sensors, the effect of basic and acidic soaks on the sensor performance was evaluated. After the sensor had soaked in pH 10 solution for 16 hours, the sensor response was erratic, and the time to establish equilibrium was long (15 to 20 minutes). In addition, the slope of the E-log $[Ca^{+2}]$ curves was only 20 mV. After a 16-hour soak in pH 2 solution, a Nernstian response was observed, and the potential response was more rapid and reproducible. It was concluded that the acidic soak is beneficial to sensor response, whereas the basic soak is detrimental.

In another experiment, the concentration of Ca^{+2} in the internal reference solution for the 10% $NaF-CaF_2$ and 10% YF_3-CaF_2 membrane sensors was varied from 10^{-3} M to 1.0 M. A slight improvement in response and selectivity of the sensors was observed when the more concentrated internal reference solution was used.

Several sensors have been prepared which respond well to Ca^{+2} and Mg^{+2} when they are the only cations present in the solution. These sensors have

also been evaluated for their selectivity to each of these ions in the presence of the other. In general, these membrane sensors do not distinguish between Ca^{+2} and Mg^{+2} and exhibit only slightly lower responses to the other divalent ions. Typical data for the response of a 10% YF_3-CaF_2 membrane sensor to mixtures of Ca^{+2} and Mg^{+2} are presented in Table XII. These data support a junction potential mechanism. However, it should be pointed out that this mechanism seems to apply only to divalent ions. Therefore, these sensors can be used to monitor brackish waters where the divalent ions are at least 10% of the monovalent ions.

TABLE XII

Response of 10% YF_3-CaF_2 to Ca^{+2} and Mg^{+2}

(Internal solution 0.1 M Ca^{+2})

Potential (volts)	$[Ca^{+2}]$ (moles/liter)	$[Mg^{+2}]$ (moles/liter)
0.027	0.01	0.0001
0.055	0.001	0.001
0.027	0.0001	0.01
0.059	0.001	0.0001
0.060	0.0001	0.001

The Nd-doped $CaWO_4$ sensor material which was vacuum heat-treated was fabricated into a membrane sensor. Its response to changes in Ca^{+2} activity is shown in Figure 20. However, like previous sensors of this type, univalent ions interfered. The interference appears effectively as a short between the two solutions. Conceivably, the univalent ions could transport through the membrane, although they would be hindered. This may be helped by a certain degree of microcracking.

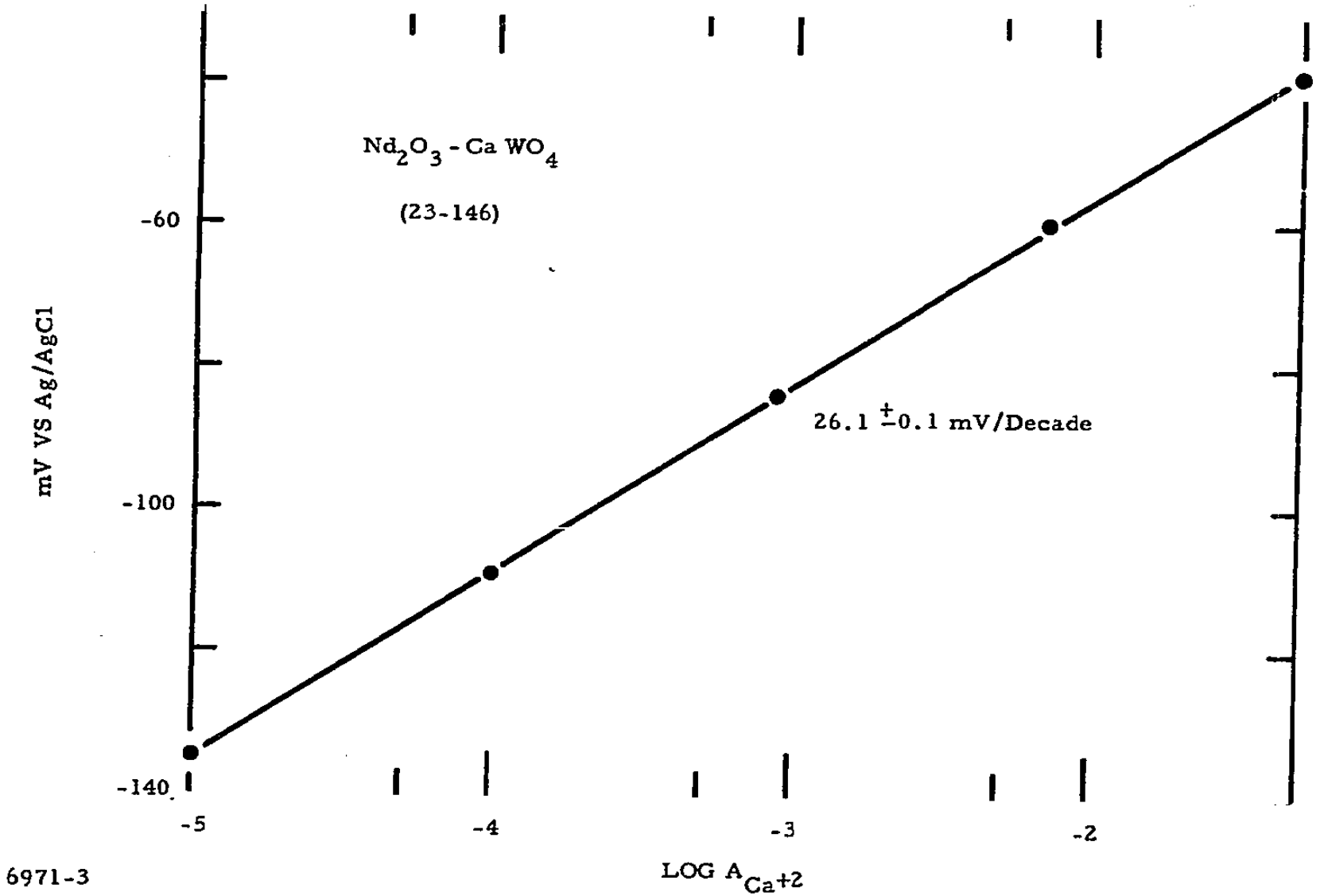

Figure 20 Response of Vacuum Heat-Treated Nd-$CaWO_4$ to Changes in Ca^{+2} Activity

The prospects of obtaining good solid-state sensors for divalent ions with these systems are still good. Crystal preparation (crack-free) and increased conductivity could provide the improvements required for usable sensors.

Usable Ca^{+2} and Mg^{+2} solid-state sensors have been fabricated and tested. While their use is somewhat restricted to solutions containing these ions as a major constituent (> 10%), they still can find use in many applications.

VI. OTHER ION-SELECTIVE SENSORS

During the course of this contract a variety of materials and sensors for ions other than those described in the preceeding sections was investigated.[1-3] Other experiments were performed to obtain information helpful in elucidating the mechanism of the sensors of primary interest. All this work has been reported previously,[1-3] but for completeness and to point the direction for future investigations, some of these results are presented here.

A. Mn^{+2} and Mn^{+3}

Considerable effort was devoted to attempts to produce materials and sensors that would be selectively responsive to Mn^{+2}.[1-3] Both doped semiconductors and amorphous materials were investigated. However, only the limited response obtained to divalent ions with the doped alkaline earth crystals was obtained. This response was poor and nonselective. However, during the course of the work on Mn^{+2}, a sensor was produced which exhibited a good response to Mn^{+3}.

An electrode was fabricated from a material consisting of 4 mole % Mn^{0} - 1173 glass. This sample had a resistivity of about 100 Ω cm. Electrochemical generation of Mn^{+3} was carried out in a solution containing Mn^{+2} in a sulfuric acid - pyrophosphate medium. The $Mn(P_2O_7)^{-2}$ complex is stable (violet color) and does not disproportionate readily. The generation was carried out at a Pt-flag electrode by constant current electrolysis, and the Mn^{+3} produced was directly proportional to the time of the electrolysis. In arriving at the concentration of the test solutions, a 100% current efficiency was assumed for the electrolysis. Although the absolute values of the Mn^{+3} concentrations may be in error, the $\Delta \log [Mn^{+3}]$ should be correct as long as the current efficiency for the electrochemical generation remained constant. Figure 21 shows the potential response of the electrode to Mn^{+3}. In the concentration range 10^{-5} M to 10^{-2} M Mn^{+3}, a linear response was observed and a slope of 99 mV/decade was calculated. A Pt electrode showed a linear response over the same Mn^{+3} concentration range (Mn^{+2} concentration held at 0.1 M) and exhibited a slope of 85 mV/decade.

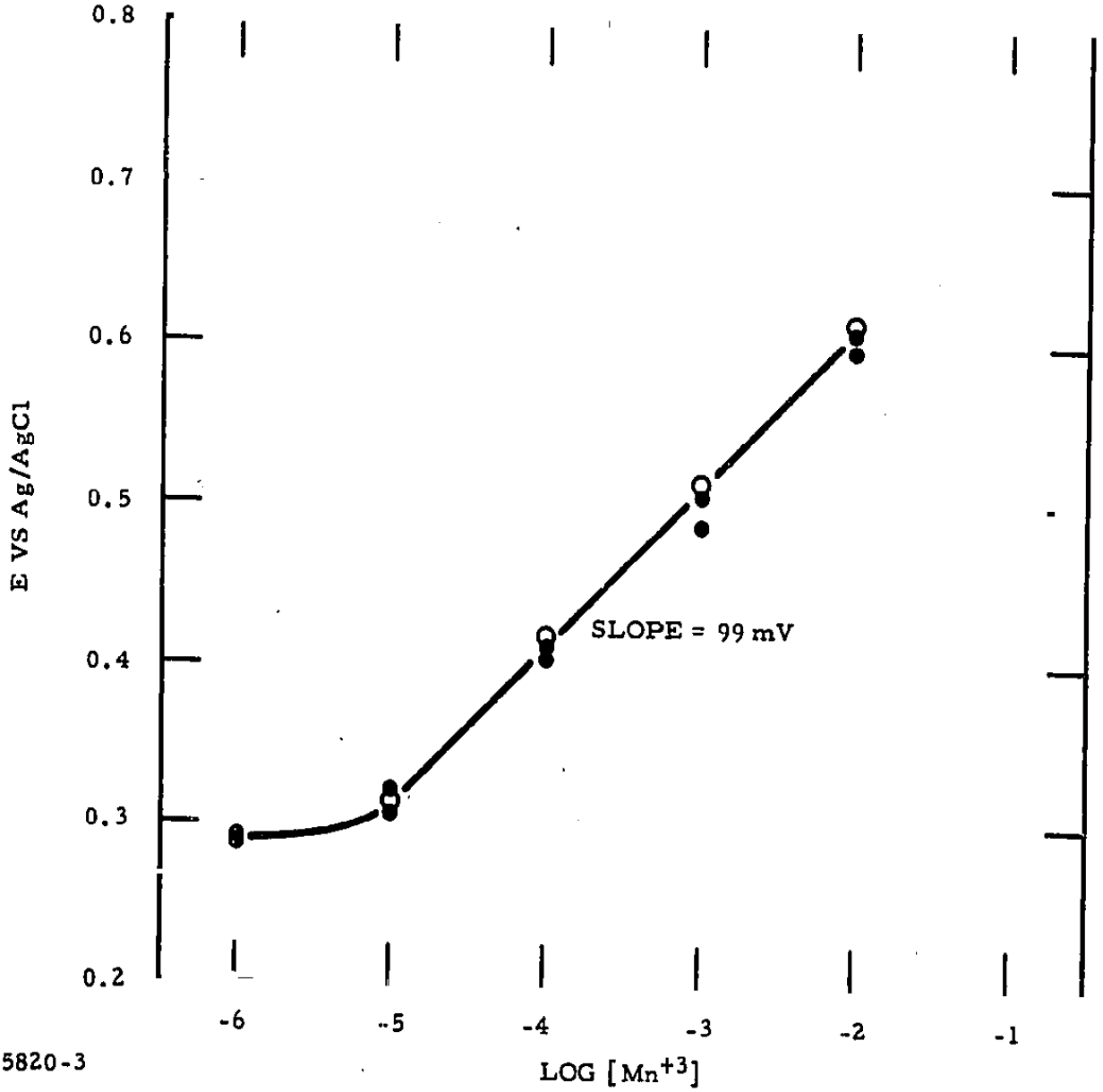

Figure 21 Potential Response of a 4.0 Mole % Mn^0-1173 Glass Electrode to Electrochemically Generated Mn^{+3} in 0.1 M $MnSO_4$, 0.4 M $Na_4P_2O_7$, and 2 M H_2SO_4

These results indicate that the Mn-1173 electrodes may have some sensing application. This work was not pursued further.

B. Cd^{+2} Sensors

In classical electrochemistry the reaction of Cd^{+2} has been used frequently as the demonstration ion for many electrochemical techniques. To obtain information concerning the possible mechanism of doped chalcogenide glass, an investigation of Cd-doped materials and the sensors fabricated from them was undertaken. More details of these investigations are presented in O.S.W. Reports 496 and 619.[1,2]

Membranes and electrodes of 10 mole % CdSe-1173 give reasonably good potential responses to changing Cd^{+2} concentration. The potential response is better when the sequence of measurements is from the dilute solutions to the concentrated ones. Adsorption and/or dissolution rates at the glass interface cause problems when the measurement sequence is reversed. This is shown in Figure 22 for a membrane and an electrode. The theoretical response is 30 mV per decade change in Cd^{+2} concentration, and the response approaches theoretical as the concentration increases. ΔE for a series of solutions is reproducible from one day to the next for a given electrode, but the absolute potential values indicate that the initial conditions existing at the glass interface are not reproducible. Later work has shown that the electrode surfaces need to be etched and activated in Cd^{+2} to obtain more stable responses.

The response to Cd^{+2} did not help determine the mechanism for the potential response to this cation. A clue to the potential mechanism for the Cd^{+2} response was noted while investigating the pH response of the 10% CdSe-1173 membrane. In the absence of Cd^{+2}, a pH response was observed from pH 2 to pH 11 (Figure 23). When Cd^{+2} was present in solution, the pH response was limited to pH's > 8. At pH 8, the Cd^{+2} precipitated and the membrane became sensitive to pH. From pH 2 to pH 8, the Cd^{+2} concentration remained constant and was the potential-determining component of the solution. Since the Cd^{+2} - H^{+} response was competitive rather than additive, the potential mechanism for these two cations appears to be the same. From experiments run in the absence of Cd^{+2}, the slope of the E - pH curve

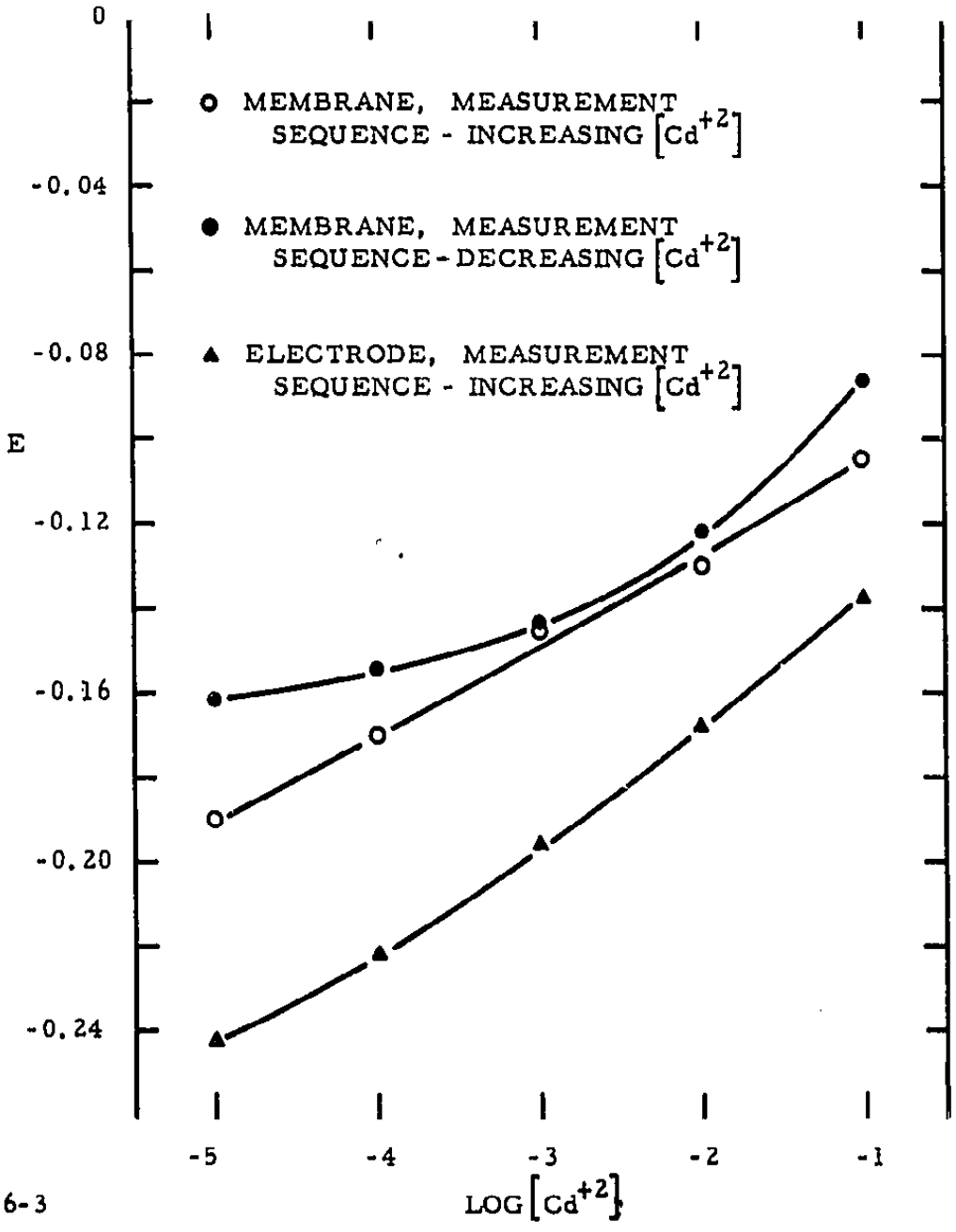

Figure 22 Effect of $[Cd^{+2}]$ and Measurement Sequence on Membrane and Electrode Potentials for 10 Mole % CdSe-1173 Glass. (Total salt concentration held at 0.1 M by addition of KNO_3.)

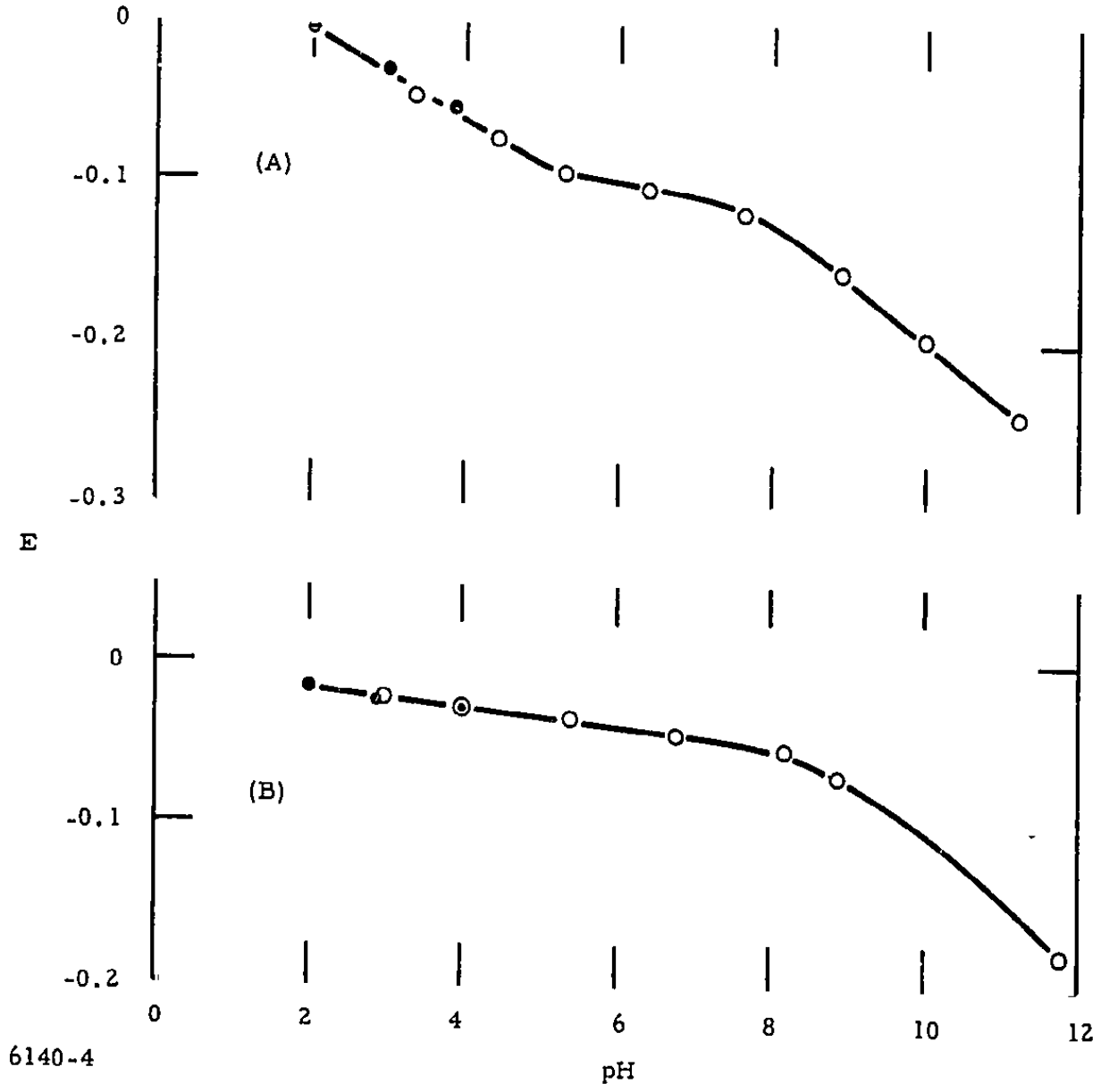

Figure 23 pH Response of the 8% CdSe-1173 Membrane. (a) 0.1 M KNO_3. (b) 10^{-2} M Cd^{+2} and 0.1 M KNO_3.

in the pH 2 to pH 6 range was ~ 25 mV, which suggested that the potential mechanism involved an exchange of a monovalent cation for a divalent cation.

Although ion exchange appeared to be probable with the 10% CdSe-1173 membrane, the lack of potential response to Mn^{+2}, Fe^{+2}, and Ca^{+2} indicated that no reversible exchange process existed between these divalent cations and the Cd^{+2} in the sensor.

Additional work on Cd^{+2} sensors appears warranted, particularly in view of their applications to the environmental monitoring of various waste water and natural streams.

C. Na^+ and K^+ Sensors

Several materials and sensors were prepared to measure the concentration of univalent ions, particularly Na^+ and K^+.[1,2] A number of commercial electrodes are available for these ions. The several sensors prepared and tested during this contract exhibited poorer performance than the commercially available electrodes. Although the commercially available electrodes did respond, additional work is required if these electrodes are to be used in routine applications. More information is presented on this point in the next section of this report.

Materials and sensors have been investigated for a number of ionic species in solution. The most successful sensors were discussed in Section II through V. In addition, some supporting evidence exists for sensors that are selectively responsive to Mn^{+3} and Cd^{+2}; further investigative work is required on these sensors. Additional, but unsuccessful, investigations were carried out in attempts to establish materials and sensors for Mn^{+2}, Na^+, and K^+. No direction for future investigation of these latter sensors is indicated by this work.

VII. APPLICATION OF SENSORS TO MONITORING OF DEMINERALIZATION PROCESSES

Laboratory applications were attempted for some of the sensors developed during this program to monitor various process streams encountered in the several different demineralization processes. Actual samples of raw well water were received from Mason-Rust in Webster, South Dakota; the Roswell Test Facility, Roswell, New Mexico; and the Desalting Demonstration Plant in Freeport, Texas. This section describes the various laboratory tests performed and the results of these tests. Although it is not a part of this contract, a description will also be presented of the application of the Fe^{+3} and Ca^{+2} sensors to monitoring samples of acid mine drainage water obtained from the Experimental Mine Drainage Treatment Facility, Hollywood, Pennsylvania.

A. Na^{+}, Ca^{+2}, and Fe^{+3} Applications

A system of sensors utilizing commercially available electrodes (Corning Monovalent Cation Electrode, Corning Ca^{+2} Electrode, and Orion Divalent Cation Electrode) and TI's Fe^{+3} sensor was used to analyze a sample of raw well water obtained from Mason-Rust in Webster, South Dakota. The Corning monovalent cation electrode detected 35 ppm univalent ions calculated as Na^{+} as opposed to the 106 ppm Na^{+} reported in the water analysis. This error, as discussed later in the evaluation of another sensor, was due to the large effect of ionic strength caused by the high concentration of divalent ions present in the sample. The results obtained for the Ca^{+2} concentration with the Corning Ca^{+2} electrode were more difficult to explain. The water analysis reported 192 ppm Ca^{+2}, but the sensor determination yielded 400 ppm Ca^{+2}. The high Ca^{+2} value cannot be explained by the ionic strength effect. The total divalent cation concentration (Ca^{+2} and Mg^{+2}) calculated as Ca^{+2} was found to be 105 ppm with the Orion divalent cation electrode. The low value for this determination is understandable when the ion strength effect is considered. TI's Fe^{+3} sensor (2% Fe^{0}-1173) indicated 0.56 ppm Fe, versus the 1.05 ppm Fe reported. It was necessary to adjust the pH of the test sample to 3.0 so that the potentials measured would be meaningful when compared with those of the working curve. Here again, the ionic strength of the test solution would make the results low. In addition, it is possible that a portion of the Fe was present as Fe^{+2} and therefore could not be detected with the Fe^{+3} sensor.

The Corning Na^+ electrode (NAS-11-18) was evaluated for its response to Na^+. This electrode has a working concentration range from saturated solutions to 10^{-6} M (Figure 24), but the lower limit increases as the ionic strength of the solution increases. The electrode was used to analyze the Na^+ content in water samples from the Roswell Test Facility and Webster, South Dakota. In the Roswell water sample, the Na^+ was a major constituent (largest contributor to ionic strength), and the determination using the working curve for the Corning Na^+ electrode was straightforward (reported, 4650 ppm Na^+; found, 4380 ppm Na^+). The accuracy of these results (~ 6% error) is as good as can be expected from this type of analysis. With the Webster water sample, however, the Na^+ is only a minor constituent; thus, the potential displayed is greatly influenced (with regard to ionic strength) by the large concentration of divalent ions, making analysis by the standard calibration curve useless (reported, 106 ppm Na^+; found, 38 ppm Na^+). A technique involving dilution of and standard addition of Na^+ to the water sample gave results with a relative error of ± 30%. A one-liter sample of the Webster water was concentrated to 330 milliliters in a rotor evaporator. Further evaporation caused precipitation of $CaSO_4$ from solution. This concentrated sample was then diluted with deionized water to 1/2, 1/3, 1/4, 1/5, 1/8, and 1/10 of its initial concentration. The relative Na^+ content of each of these solutions was measured with the Corning Na^+ electrode. A least-squares analysis of these data was made with a computer, and the plot shown in Figure 25 was drawn. The potential of the Corning Na^+ electrode was then measured in the Webster water sample and in a similar sample to which 39.3 ppm Na^+ had been added.

Using the slope of 48 mV from the plot in Figure 25, the following calculations were made:

$$E_+ - E = 0.048 \log \frac{C + X}{C} = 0.006 \text{ V}$$

$$\frac{0.006}{0.048} = \log \frac{C + X}{C} = 0.125$$

$$\frac{C + X}{C} = 1.33$$

$$C = \frac{X}{0.33} = \frac{39.3}{0.33} = 119 \text{ ppm Na.}$$

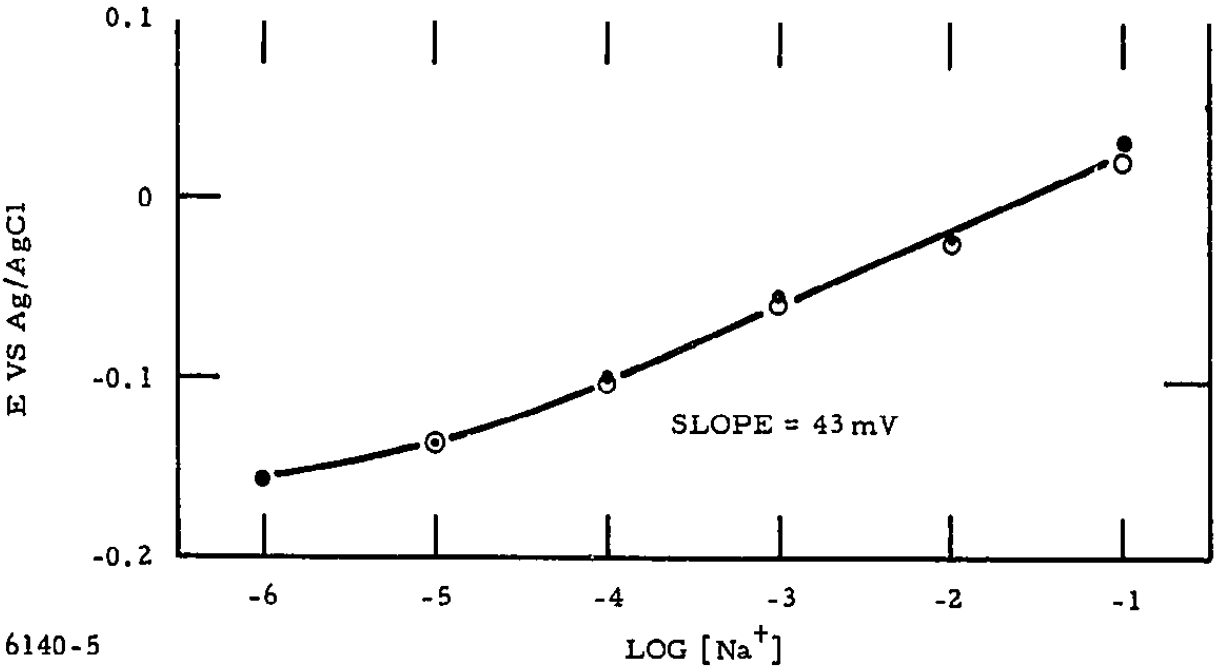

Figure 24 Potential Response of Corning Na^+ Electrode (NAS-11-18) to Na^+. Solutions of NaCl with no electrolyte added to keep the ionic strength constant.

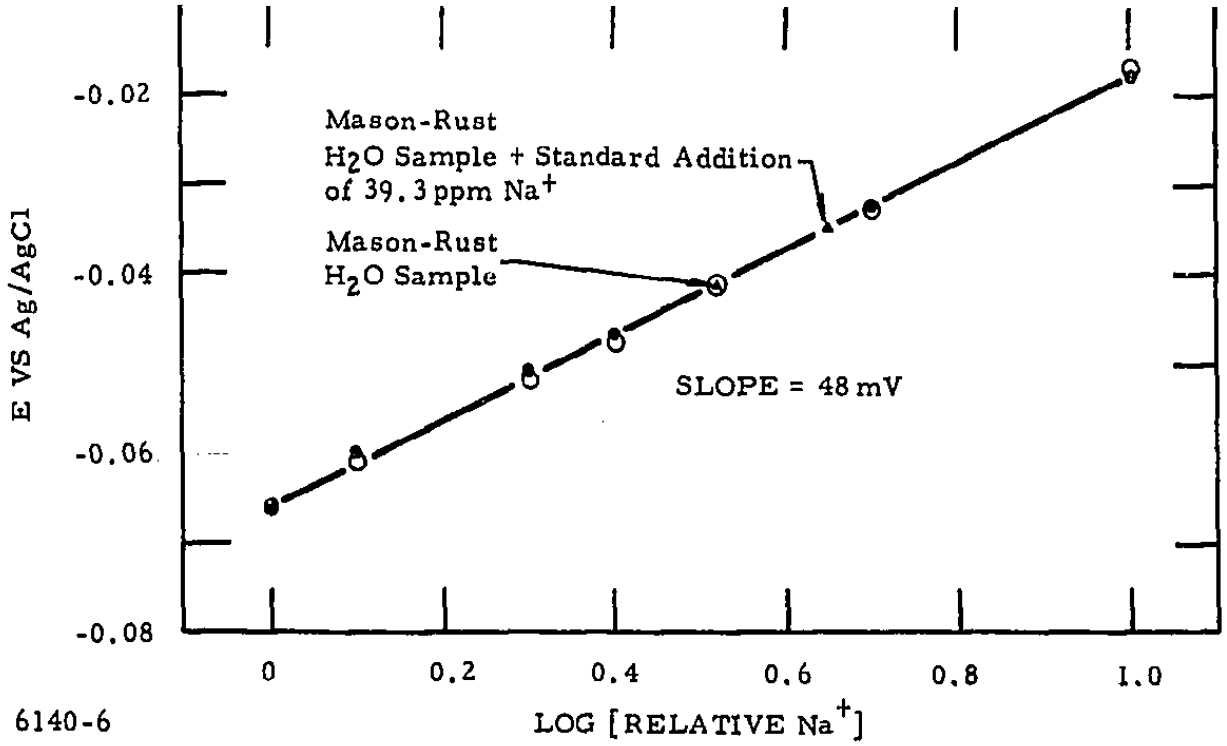

Figure 25 Calibration Curve for Corning Na^+ Electrode (NAS-11-18) Using Diluted Mason-Rust Water Samples and a Standard Addition of Na^+.

In these calculations,

E_+ = potential of electrode in solution containing standard addition of 39.3 ppm,

E = potential of electrode in Webster water sample,

C = Na^+ content in Webster sample, and

X = content of Na^+ added to Webster sample in standard addition.

The measurement of E_+ and E is very critical in this analysis. If the E_+ - E = 0.005 instead of 0.006, then C becomes 151 ppm Na^+. The relative error in the analysis due to the error in measuring E_+ and E can be reduced by making X large so that ± 1-2 mV will not be so significant in the value of E_+ - E.

Determination of Ca^{+2} in the Webster well water sample and the Roswell Test Facility well water sample with the 10% $NaF-CaF_2$, 10% YF_3-CaF_2, and 5% YF_3-CaF_2 membranes gave encouraging results, as shown in Table XIII.

TABLE XIII

Determination of Ca^{+2} Concentration in Raw Well Water Samples From Webster and Roswell Test Facility with the Doped CaF_2 Membrane Sensors

Sample	ppm Ca^{+2} Reported	ppm Ca^{+2} Found		
		10% $NaF-CaF_2$	10% YF_3-CaF_2	5% YF_3-CaF_2
Webster	192	68	159	63
Roswell	517	400	503	450

The calibration curve used in these analyses was prepared from potential responses to $CaCl_2$ test solutions. The low analysis data probably resulted because the ionic strength of the raw well water samples was higher than that of the calibrating solutions. Without consideration to the ionic strength of the solutions, the results of the 10% YF_3-CaF_2 membrane sensor must be considered either very good or fortuitous.

The results of the tests indicate that ion-selective electrodes can be used to monitor various ions in brackish waters; however, one must have some general knowledge about the water. It is not sufficient merely to place electrodes in unknown solutions, measure potential values, and determine concentrations from some standard calibration curves. It is important that calibration curves be obtained under conditions that are as nearly as possible identical to those for the unknown ions (i.e., ionic strength, interferences, etc.). Standard additions which yield changes of ~ 18 mV for electrodes with nominal 60 mV/decade slope yield the original concentration equal to the amount added. For 60 mV/decade electrode response, doubling the concentration should result in an 18 mV change.

B. $SO_4^=$ Sensor Applications

Section IV of this report describes the chemical and electrochemical basis of a simple and rapid potentiometric titration technique for the determination of sulfate ion in water. The pertinent concepts involved in the analysis were shown to be the following:

(1) Electrodes formed from an iron-doped chalcogenide glass, $Fe_2(Ge_{28}Sb_{12}Se_{60})$, respond selectively to uncomplexed ferric iron[4,5];

(2) Ferric iron forms stable soluble complexes with sulfate ion[7];

(3) Barium ion is added incrementally to break up the complex by precipitating barium sulfate;

(4) The electrode senses the liberated ferric ion;

(5) The end point is signalled by the onset of a constant potential.

The limit of detection of the method is approximately 100 mg sulfate/liter. Although this value is too high to be of interest in the analysis of many fresh and drinking waters, it is more than sufficient for the analysis of many brackish waters, brines, seawaters, and waste waters. Such aqueous solutions are, of course, considerably more complex than the simple sodium sulfate - sulfuric acid solutions used to develop the method, and, as with all methods based on barium sulfate precipitation, some interferences are to be expected from these other major ionic constituents. This application describes the evaluation of such interferences in the context of the subject method and provides some preliminary data on the application of the technique to the analysis of some natural waters high in sulfate content.

The experimental methods used in this study were essentially the same as described in Section IV. The sulfuric acid stock solution used for preparing synthetic brackish waters was standardized against a sodium hydroxide solution, which, in turn, was standardized against potassium acid phthalate. The barium chloride titrant was standardized with EDTA, which, in turn, was standardized against calcium carbonate.

The test solutions were prepared for titration: (1) by adding the proper amount of sulfuric acid and the specified concentration of the interfering ion under study, (2) by adjusting the pH to 2.1 ± 0.1 to avoid subsequent precipitation of ferric hydroxide, and (3) by adding sufficient ferric iron to produce a concentration of approximately 10^{-3} molar iron.

The actual titrations were carried out manually as described in Section IV; approximately 3 to 5 minutes were required to complete one titration. The sensor electrode was used in the membrane configuration. Potentials were read out on a Hewlett-Packard 3440A digital voltmeter; impedance matching was provided by a Keithley Model 610C electrometer.

Calcium is known to co-precipitate with barium sulfate.[23] Table XIV shows the results of applying the titration method to sulfate solutions containing various calcium ion concentrations. The range was chosen to approximate that found in sea water.[24]

TABLE XIV

Sulfate Recovery vs Ca^{+2} Concentration

(pH 2.1, 2380 ppm $SO_4^=$ added)

Ca^+ Concentration (M)	% Recovery
5×10^{-3}	96.5
10^{-2}	95
5×10^{-2}	91.5

Clearly, calcium ions do constitute an interference for the titration method. Based on replicate runs, these departures from stoichiometry were reproducible within the accuracy of the method so that a correction factor based on calcium concentration becomes possible. Since routine waste water analysis generally involves simultaneous calcium analysis, this correction factor is often available.

Potassium also coprecipitates with $BaSO_4$. As in gravimetric barium sulfate analysis, potentiometric analysis in KCl solutions routinely yield less than stoichiometric recovery of sulfate, e.g., 94% recovery was obtained in 10^{-1} M KCl for 2×10^{-2} M SO_4. Potassium is present in seawater at the 0.01 M level,[24] so coprecipitation should be less important for such samples. For more accurate results, however, potassium ions would have to be removed as, for example, via passage through a cation ion exchange resin.

Magnesium and calcium also form soluble complex ions with stability constants which approximate those of the ferric iron-sulfate complexes.[7] A series of titrations were made in a medium of 0.05 M $MgCl_2$; the magnesium content of seawater is a nominal 0.054 M.[24] Complete recovery was achieved in all cases, indicating little or no coprecipitation of magnesium sulfate at this concentration level. However, the break in the titration curve at the stoichiometric addition of barium ion was not as large as that observed with distilled water and sodium ion solutions. This is shown in Table XV, which presents the potential difference between the end point and a volume of titrant 0.3 ml before the end point. (Although these potential changes are small, they are well within the stability range of the electrode and the electronics.)

TABLE XV

Potential Change at the End Point vs Solution Composition

(2380 ppm $SO_4^{=}$, pH 2.1)

Solution	Potential Change (mV)
DI H_2O + 10^{-3} M Fe	1.8
0.05 M $MgCl_2$ + 10^{-3} M Fe	0.7
0.05 M $MgCl_2$ + 3×10^{-3} M Fe	0.4
0.05 M $MgCl_2$ + 2×10^{-4} M Fe	0.8
0.05 M $CaCl_2$ + 10^{-3} M Fe	1.0
0.01 M $CaCl_2$ + 10^{-3} M Fe	2.1

Also shown in the table are data for the titration of calcium chloride solutions of comparable concentrations. A somewhat less sensitive end point is also obtained in titrating the 0.05 M $CaCl_2$ solution besides the lower recovery discussed above. With natural seawater and other waters high in sulfate concentration this effect can be minimized by dilution of the sample prior to titration; salt concentrations at and below 10^{-2} M do not cause problems in determining the end point. Finally, the data in Table XV also indicate that there is little to be gained from manipulating the ferric ion concentration.

The method was then applied to a waste water, a brackish water, and seawater. The waste water (~ 950 ppm $SO_4^{=}$) was analyzed by the standard sulfate-turbidimetric method, as well as by the subject method. Both methods agreed within experimental error; the titrimetric end point was similar to that found in distilled water.

A seawater sample (taken near Galveston, Texas) was run following a 10:1 dilution. Recovery was 2950 ppm sulfate, which is well within the sulfate range expected for seawater (e.g., 2800 ppm given in Reference 24).

Brackish water from the Roswell Test Facility, Roswell, New Mexico, was titrated without dilution; 1360 ppm was found, compared to the 1490 ppm reported (Table XVI). However, this water also contained 0.05 M calcium, which can be expected to yield a lower sulfate recovery (Table XIV). Correcting this sulfate

result by the factor shown in Table XIV yields a value of 1490 ppm, which compares favorably with the value reported in Table XVI. The end point, although readily detectable, was not as sharp as in distilled water samples. A 5/1 dilution of the sample before titration improved the end point without altering the accuracy of the analysis. This is as predicted from the data in Tables XIV and XV.

Among the more ubiquitous ions to be found with sulfate ion are the alkalis and the alkaline earths. The resulting difficulties thereby introduced into the subject method are essentially the same as in all barium sulfate methods. Sodium ion and chloride ion at a hundredfold excess cause no problems. Potassium ion interferes at this concentration level via coprecipitation; 94% recovery was obtained for 2×10^{-2} M $SO_4^=$ in 10^{-1} M KCl. Magnesium and calcium distort the end point due to simultaneous complexation with sulfate ion, but this does not cause a major problem with the titration technique. Although calcium also coprecipitates, this effect is sufficiently reproducible to allow for correction if the Ca content is known. At high sulfate concentrations the sample can be diluted to minimize interference.

TABLE XVI

A Roswell Test Facility Well Water:

OSW Analytical Results

Item	Concentration (ppm)
Ca^{++}	517
Mg^{++}	163
Na^{++}	4,650
$SO_4^=$	1,490
Cl	7,340
HCO_3^-	206
$CO_3^=$	0
Fe	0.22
SiO_2	15
Total Dissolved Solids	14,400
Total Hardness (As $CaCO_3$)	1,980
pH 7.5	

C. Cu^{+2} Application

The $Cu\text{-}As_2S_3$ sensors for Cu^{+2} are described in Section III of this report. The application studied with these electrodes was limited to the monitoring of Cu in seawater and the various brines from a distillation desalination plant. To establish whether or not these electrodes could in fact respond to Cu^{+2} in seawater, a sample of seawater was obtained from the Gulf of Mexico at the beach in Galveston, Texas. Cu^{+2} was added to this water in varying amounts, and the total Cu in solution was independently determined by atomic absorption. The responses of two different sensors are shown in Figure 26. The pH of the seawater was found to be 6.8, indicating that as the Cu concentration increased, some of the Cu may have precipitated. This may account for the nonlinearity. However, if the solution is acidified to a pH in the range of 2.0 to 4.0, Cu^{+2} concentrations in the parts-per-billion (ppb) range can be readily measured.

Seawater samples of varying copper concentrations with pH adjusted to 2 were contacted with several $Cu\text{-}As_2S_3$ electrodes, and the potentials were measured. A Nernstian response of 60 mV/decade was obtained over the concentration range 6 ppb to 6 ppm. In simulated brine (1 M KCl, pH 2) a 60 mV/decade response was obtained from 6 ppb to 630 ppm. The best of the commercial copper ion-selective electrodes were shown not to function in brines above 1 ppm copper, in accord with the mode of operation recommended by the manufacturer in the "operation manual." The $Cu\text{-}As_2S_3$ electrode showed response to changing copper concentration down to 2 ppb, but the slope between 6 and 2 ppb was less than Nernstian.

The response time at these low concentrations was satisfactory, provided the changes were less than an order of magnitude. For example, steady state was achieved within two minutes after adding 6 ppb to the stock seawater sample ($\sim$ 2 ppb).

A one-gallon sample of final brine was obtained from the OSW test facility at Freeport, Texas. This sample, taken on 18 September 1972, contained a significant amount of sediment. Measurements were made after various treatments of the as-received sample.

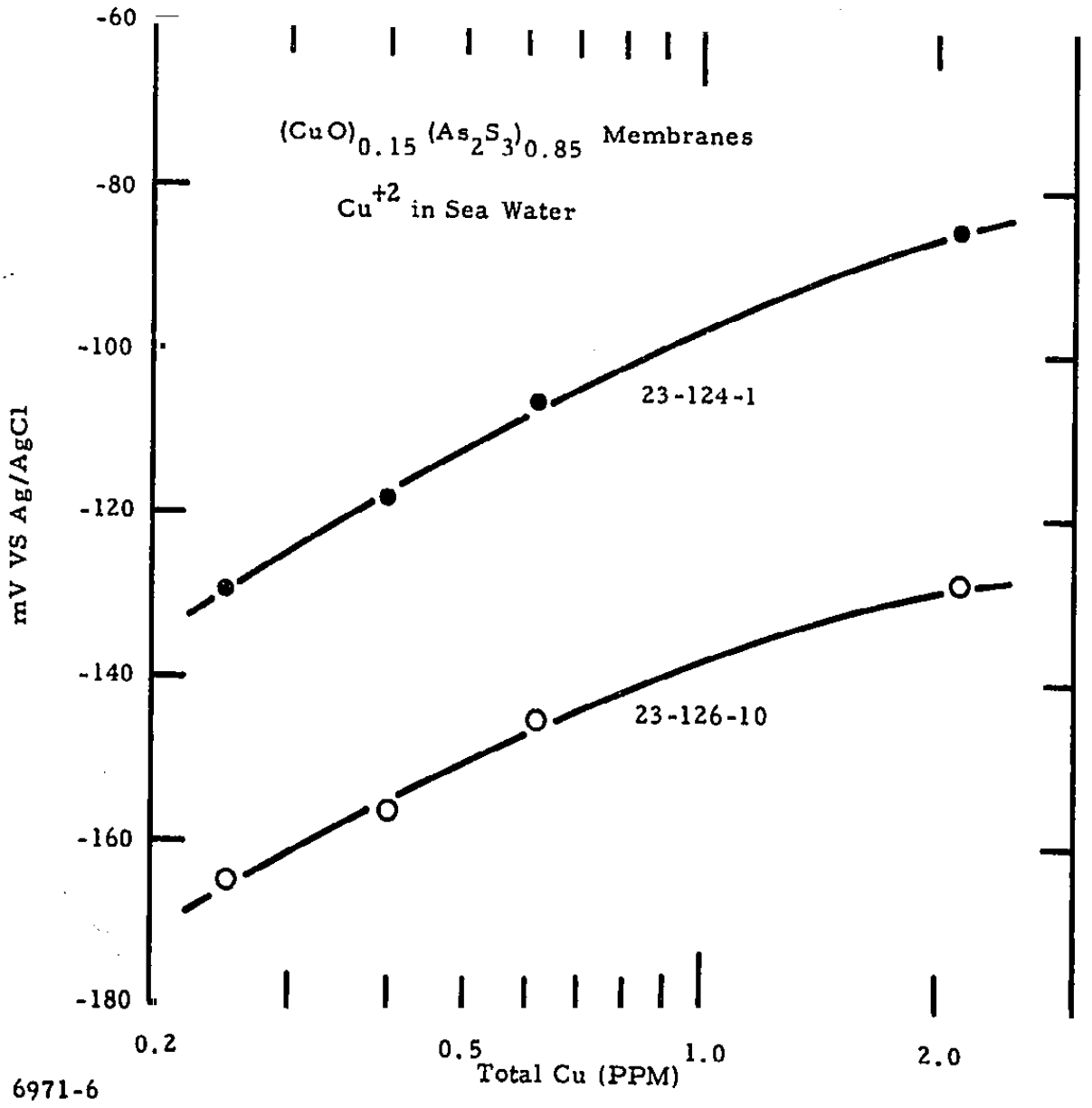

Figure 26 Response of Two Membrane Sensors to Cu^{+2} in Seawater. Total Cu determined by atomic absorption.

The sample as-received had a pH of 7.1. Before a sample was withdrawn for analysis, the original gallon was mixed well and the sample decanted with sediment. Analysis of the mixed pH 7.1 sample indicated only 6 to 8 ppb Cu^{+2}. The mixed sample was then acidified to pH 1.9 with perchloric acid. The average value of four different sensors was 2.15 ppm Cu^{+2}. The mixed sample was filtered and acidified to pH 1.9. It then yielded an average Cu^{+2} value of 0.44 ppm, indicating that some fine particulates of copper passed through the laboratory filter paper. An independent check of the total copper by atomic absorption yielded a value of 1.1 ppm. However, this latter value is probably low for several reasons; e.g., the high salt content of the sample prevented complete atomization of copper, and particulate copper may not have been aspirated into the flame.

The results obtained with the four Cu-As_2S_3 copper-selective electrodes are given in Table XVII. It appears that a simple monitoring system for both dissolved and particulate copper in the final brine can be demonstrated. In addition, it will be possible to monitor the difference between incoming and outgoing brine with little difficulty.

In order to prove this last point, additional samples were obtained from the O.S.W. Test Facility in Freeport. Sample #1 was raw incoming seawater. Sample #2 was taken after addition of H_2SO_4 and the deaerator-decarbonator. Sample #3 was the final brine. The results of these analyses are presented in Table XVIII.

The $SO_4^{=}$ determinations were made by titration with $BaCl_2$ using an Fe-1173 electrode to signal the end point. This procedure has been discussed previously in this report and further demonstrates the applicability of ion-selective sensors to the desalting process.

In analyzing the data for Cu^{+2} in Table XVIII, it is important to consider sources of error in each measurement. The electrode data obtained at a pH of 6.0 may be in error on the low side due to precipitation or complexation of the Cu as $Cu(OH)_2$ or $Cu(OH)^+$. At this pH, Fe^{+3} is not an interference. At pH 2.0, Fe^{+3} is an interference and can yield high results. The atomic absorption analyses

TABLE XVII

Analyses of Final Brine from Freeport Desalting Plant
(Sample Taken 9/18/72)

Cu^{+2} in ppm

Sample Treatment	Electrode Response				
	52-5	52B-12	58-5	58-21	Average
As-received, pH 7.1	< 0.006	< 0.006	0.006	0.007	0.006
Adjusted, pH 1.9	2.3	2.1	2.2	2.0	2.15
Filtered, adjusted, pH 1.9	0.34	0.46	0.53	0.44	0.44

TABLE XVIII

Analyses by Cu-As_2S_3 Electrodes of Brines From
OSW Desalting Plant, Freeport, Texas
(Samples taken 10/2/72)

	Sample # 1	Sample # 2	Sample # 3
pH (as received)	8.0	6.3	7.0
Cu^{+2} (ppm) pH 6.0	N.D.*	0.025	0.63
Cu^{+2} (ppm) pH 2.0	N.D.*	0.45	1.44
Cu^{+2} (ppm) pH 6.0 (AA†)	0.001	0.080	1.02
$SO_4^{=}$ (ppm)	2360	2550	5700

*N.D. = Not detectable

†AA = Extraction followed by atomic absorption analyses

were accomplished by extraction at pH 6.0. The results can only be low due to the inability to extract particulate Cu.

These results indicate at least that the total Cu content is between the values obtained by the ion-selective electrodes at pH 2 and pH 6. The AA results indicate that the values are more nearly between those obtained by AA and the ion-selective electrode at pH 2.

Free Fe^{+3} can cause a positive interference in the ion-selective electrode determination of Cu^{+2} by a Cu-As_2S_3 electrode, particularly when the Fe^{+3} concentration is ten times greater than Cu^{+2}. The brines obtained from the Freeport Desalting Plant contain suspended particulates which have some Fe^{+3}, Cu^{+2}, and silicates. The silicates are dissolved by adding 0.5 ml of concentrated HF per 100 ml of sample. The resulting solutions at pH 2.0 contain sufficient Fe^{+3} to pose a possible interference in the Cu^{+2} determination, and the effect of HF on the Cu-As_2S_3 electrode had not been determined.

Fe^{+3} forms stable complexes with F^- such that the large amount of F^- available after the addition of HF should decrease the free Fe^{+3} activity to an insignificant level and not be sensed by the Cu-As_2S_3 electrode. When 10^{-4} M Fe^{+3} was added to 10^{-6} M Cu^{+2} in 1 M KCl solutions containing 0.5 mole % HF, no increase in potential was observed on either an Fe-1173 or two Cu-As_2S_3 electrodes. The two Cu-As_2S_3 electrodes were then calibrated in solutions containing 0.5 vol % HF, 10^{-4} M Fe^{+3}, and varying Cu^{+2} concentrations from 1×10^{-6} to 5×10^{-5} M. The resulting curves were Nernstian, and the potentials obtained were almost identical to those obtained in the absence of the HF and Fe^{+3}. Thus, it can be stated that F^- and Fe^{+3} in the presence of F^- do not interfere with Cu^{+2} determination in 1 M KCl, even at concentrations as low as 0.06 ppm Cu^{+2}.

The procedure of adding a 0.5 vol % HF to the sample was next tried with seawater. It was hoped that the HF would dissolve the silicates, release the adsorbed Cu^{+2}, adjust pH to 2.0, and remove the Fe^{+3} interference by complexing the iron. This was attempted in both a batch and a simulated continuous flow system. The results were questionable. The brines from Freeport contain significant quantities of calcium and magnesium. The Ca^{+2} and Mg^{+2} react with F^- to precipitate CaF_2 and MgF_2. In the presence of this material Cu^{+2} tends to be both coprecipitated and

adsorbed on these suspended particles. Tests carried out at the Freeport plant indicated that in the presence of this precipate, when standard additions of Cu^{+2} were made, about two-thirds of the added Cu^{+2} was removed from solution. By repeating this test in the laboratory it was possible to observe an increase in Cu^{+2} for the first few minutes after the addition of the HF, followed by a slow decrease in Cu^{+2} as the precipitate formed and the Cu^{+2} was coprecipitated and adsorbed.

It appears likely that a system for continuous monitoring of Cu^{+2} in seawater brines can be worked out. The Fe^{+3} interference can be suppressed and the Cu^{+2} can be released from the various silicates and clays present. The problem is to prevent the precipitation of CaF_2 and MgF_2. Additional applications work is required to circumvent this difficulty. However, several suggestions come to mind. For instance, the electrodes have sufficient sensitivity so that by diluting the original brine, the concentration of calcium could be reduced and the Cu^{+2} concentration still maintained in a range that can be easily measured by the Cu-As_2S_3 electrode. In this instance semicontinuous monitors can easily be envisioned.

D. Fe^{+3} and Ca^{+2} Application to Acid Mine Drainage Water

Although not a part of this contract, an investigation was made of the application of the Fe-1173 and 10 % YF_3 - CaF_2 sensors to monitoring acid mine drainage water. Samples were provided by Dr. Harold L. Lovell, Director of the Experimental Mine Drainage Treatment Facility, Hollywood, Pennsylvania. These samples were taken from various points in the plant, preserved with acid, and shipped to Dallas. Analyses were performed as soon as possible; however, there was a time lapse of several days between sampling and analyzing.

The samples were preserved in three different ways. One set was preserved for total iron; a second was preserved for Fe^{+2}; and the third sample was the raw, unpreserved water. The very low pH (< 0.5 pH) of the two preserved samples made exact calibration difficult, but relative values could be obtained. The raw samples had some Fe^{+3} precipitates. The Fe-1173 sensor results yielded the correct relative values. For instance, the oxidation tank had by far the most Fe^{+3} concentration. Examination of samples from four different points in the treatment plant showed that the ratio of Fe^{+3} in each sample agreed with that obtained by the analytical laboratory in the plant.

In this particular acid mine drainage treatment process the acid is neutralized and the Fe^{+3} is precipitated by adding limestone ($CaCO_3$). The 10% YF_3 - CaF_2 sensor was used to measure the Ca^{+2} concentration in the water from this step of the process. These sensors yielded very stable readings, which indicated the Ca^{+2} concentration was 250 ppm, in good agreement with previous analytical results. This electrode functions well in this application because Ca^{+2} is the predominant cation at this point.

The results with the acid mine drainage water indicate that these sensors can be used to monitor such waters. These particular experiments were performed several years ago. With the added information obtained since then and the added application of the Fe-1173 to measure $SO_4^{=}$, it should be relatively straightforward to apply these ion-selective electrochemical sensors to continuous, or at least semi-continuous, monitoring of acid mine drainage waters and treatment processes for these waters.

VIII. SUMMARY AND RECOMMENDATIONS

A. Summary

The research performed on United State Department of the Interior, Office of Saline Water Contract No. 14-01-0001-1737 has demonstrated the feasibility and the initial development of new ion-selective electrochemical sensors. Specifically, highly selective sensors have been demonstrated for Fe^{+3} and Cu^{+2}. Proper use of the Fe^{+3} sensor can yield a system and/or procedure for rapidly monitoring and/or determining $SO_4^{=}$. A solid-state sensor was demonstrated for Ca^{+2} and Mg^{+2}. Although it is not as selective as the previous sensors, there are many applications and conditions in which this sensor will perform an adequate monitoring function. Some applications of these sensors to actual demineralization processes has been demonstrated.

1. Fe^{+3}

Sensors made of Fe-doped TI #1173 glass ($Ge_{28}Sb_{12}Se_{60}$) are selectively responsive to Fe^{+3}. The response is Nernstian over the range 10^{-2} to 10^{-5} M Fe^{+3}, with some response in some instances to as low as 5×10^{-7} M Fe^{+3}, (0.03 ppm). The sensor may be used to measure concentrations greater than 10^{-2} M Fe^{+3}; however, an additional activation procedure will be required to obtain linear response. The procedure for sensor material preparation and sensor activation, calibration, and operation has been established and shown to be reasonably reproducible. The average slope in the Nernstian range for 12 sensors from four different material runs was 56.7 mV/decade, with an average deviation of 2.1 mV/decade. The 1 σ level for this slope was 1.8 mV/decade. A limited number of these sensors has been made available in response to unsolicited requests. In addition, application of this sensor for monitoring acid mine drainage waters and other acid waste streams which contain iron is practical.

2. Cu^{+2}

Sensors made of $Cu\text{-}As_2S_3$ are selectively responsive to Cu^{+2}. The response of these sensors is dependent on the supporting electrolyte, particularly the anions.

In a pure NO_3^- electrolyte the response is Nernstian with a slope of 30 mV/decade. As the chloride concentration of the electrolyte is increased, the response still remains Nernstian, but increases and finally approaches a value of 59 mV/decade in 3 M chloride solutions. Intermediate chloride concentrations yield slopes between 30 and 59 mV/decade. Procedures have been established for material preparation and sensor activation, calibration, and operation.

Comparisons of commercially available Cu^{+2} selective electrodes and the Cu-As_2S_3 sensors were made. The Cu-As_2S_3 sensor appears to have superior response and range, particularly in a chloride medium. In fact, the manufacturers of the commercial Cu electrode warn against use of the electrode in high concentrations of chloride, since this results in corrosion of the electrode; therefore, the commercial electrode would not be useful in the concentrated brine solutions encountered in various desalination processes, particularly if the Cu^{+2} concentration approaches 1 ppm or greater.

It has been demonstrated that Cu-As_2S_3 sensors can be used to monitor the Cu^{+2} concentration brines involved in desalination processes.

3. $SO_4^=$

During the course of our investigation of the Fe-1173 sensor we observed an unusual response to Fe^{+3} in the presence of $SO_4^=$. Further investigations reestabished that the Fe sensor measured "free" Fe^{+3} and that the $FeSO_4^+$ was not sensed. With a knowledge of the equilibrium constants for the various complex species in solutions of Fe^{+3} and $SO_4^=$ and at a constant concentration of Fe^{+3} and a constant pH, the potential of an Fe-1173 sensor is relatable to the $SO_4^=$ concentration. This method is fully described in Section IV of this report. Manual monitoring of seawater and brackish water has been accomplished in this laboratory. The sensor can be used in a continuous monitoring mode by incorporating it in a process titrator system, or it can be used to indicate the end-point of a $BaCl_2$ titration. The latter method has good accuracy and reproducibility and can readily be applied to solutions containing more than 100 ppm $SO_4^=$.

4. Ca^{+2} and Mg^{+2}

Crystalline materials were used as sensors for Ca^{+2} and Mg^{+2}. For the most part, these materials were $NaF-CaF_2$, YF_3-CaF_2, and Nd_2O_3 doped $CaWO_4$ crystals. All materials appear to respond in the same way. These sensors do not distinguish between Ca^{+2} and Mg^{+2}, but respond to the sum of the two ions. Major interference is to be expected from all univalent ions unless the divalent ions predominate (make up greater than 50% of the total cation content). If the divalent ions are the major positive ionic constituents, then the sensor appears to have sensitivity down to at least 10^{-4} M (4 ppm Ca^{+2}), or possibly lower.

B. Recommendations for Future Investiqations

The relatively small amount of effort expended during this investigation on applications yielded most encouraging results. Certainly some additional effort should be devoted to exploiting the new sensors discussed in this report, as well as those that are commercially available. Ion-selective electrochemical sensors cannot simply be placed in an unknown process stream and be expected to yield the correct answer. However, this work has demonstrated that after a small amount of work and modification, ion-selective electrochemical sensors can be applied to monitoring a number of processes, including demineralization processes.

More specifically as a result of this work, additional research and development should be directed to instrumentation to automatically and continuously determine $SO_4^=$ using the Fe-1173 sensor. Many applications of this system to other waters for $SO_4^=$ monitoring requirements, including acid mine drainage, appear practical.

The use of As_2S_3 and other chalcogenide glasses as host materials still warrants further investigation in an attempt to produce a family of very similar ion-selective electrochemical sensors.

Since the doped chalcogenide glasses are good conductors, the steady-state current potential characteristic of these sensors should be investigated. The current response is a linear function of concentration, while the potential response

is logarithmic. Increased sensor accuracy could be obtained by having the option of measuring either current or potential.

Other characteristics of these sensors which should be investigated are temperature effects, long-term stability, lifetime between activations, and response time.

The goal of any future work in this area should include the construction of at least feasibility equipment and the application of this equipment to actual processes.

Ion-selective electrochemical sensors and systems can prove to be a useful aid in controlling, optimizing, and reducing the cost of the various demineralization processes.

REFERENCES

1. I. Trachtenberg and C. T. Baker, United States Department of Interior, Office of Saline Water Research and Development Report #496, December 1969.
2. I. Trachtenberg and C. T. Baker, United States Department of Interior, Office of Saline Water Research and Development Report #619, December 1970.
3. I. Trachtenberg, United States Department of Interior, Office of Saline Water Research and Development Report #761, March 1972.
4. C. T. Baker and I. Trachtenberg, J. Electrochem. Soc. 118, 571 (1971).
5. R. J. Jasinski and I. Trachtenberg, Anal. Chem. 44, 2373 (1972). (See also Section IV of this report.)
6. R. J. Jasinski and I. Trachtenberg, Anal. Chem. (in press).
7. L. Sillen and A. Martell, "Stability Constants of Metal-Ion Complexes," Special Publication #17, The Chemical Society, London (1964).
8. J. Jones and R. Eddy, Anal. Chim. Acta 43, 165 (1968).
9. F. Marumo and W. Nowacki, Schweiz. Min. Petrog. Mitt. 44, 439 (1964).
10. L. Cambi and M. Elli, Chim. Ind. (Milan) 49, 606 (1967).
11. J. Koryta, Anal. Chim. Acta 61, 329 (1972).
12. P. Ruetschi and R. Amlie, J. Electrochem. Soc. 112, 665 (1965).
13. W. Latimer, Oxidation States of the Elements and Their Potentials in Aqueous Solutions, second ed. (Prentice-Hall, New York, 1952).
14. H. McConnell and N. Davidson, J. Am. Chem. Soc. 77, 3168 (1950).
15. E. Pungor and J. Havas, Acta Chim. Hung. 50, 77 (1966).
16. R. Durst, "Ion-Selective Electrodes," National Bureau of Standards Publication No. 314 (U. S. Government Printing Office, Washington, D. C., 1969).
17. G. Rechnitz, Z. Lin, and S. Zamochnick, Anal. Lett. 1, 29 (1967).

18. J. Ross and M. Frant, Anal. Chem. 41, 967 (1969).

19. W. Hillebrand, G. Lundell, M. Bright, and J. Hoffman, Applied Inorganic Analysis (John Wiley & Sons, Inc., New York, 1953).

20. S. Preziosi, R. R. Soden, and L. G. Van Uitert, J. Appl. Phys. 33, 1893 (1962).

21. K. Nassau and L. G. Van Uitert, J. Appl. Phys. 31, 1508 (1960).

22. K. Nassau and A. M. Broyer, J. Appl. Phys. 33, 3064 (1962).

23. W. Hillebrand, G. Lundell, M. Bright, and J. Hoffman, Applied Inorganic Analysis, (John Wiley & Sons, Inc., New York, 1953).

24. J. Riley and G. Skirrow, Chemical Oceanography (Academic Press, New York, 1965).